ABSTRACT

Title of Document: CHARACTERIZATION OF THE N-ACETYLGLUTAMATE SYNTHASE KNOCKOUT MOUSE, A NOVEL MODEL OF HYPERAMMONEMIA.

Emilee Senkevitch, PhD, 2012

Directed By: Professor Mendel Tuchman, Department of Pediatrics, Children's National Medical Center, George Washington University
Professor David Mosser, Department of Cell Biology and Molecular Genetics

All knockout mouse models of urea cycle disorders die in the neonatal period or shortly thereafter. Since N-acetylglutamate synthase (NAGS) deficiency in humans can be effectively treated with N-carbamyl-L-glutamate (NCG), we sought to develop a mouse model of this disorder that could be rescued by biochemical intervention, reared to adulthood, reproduce, and become a novel animal model for hyperammonemia. NCG and L-citrulline (Cit) were used to rescue the NAGS knockout homozygous (*Nags*$^{-/-}$) pups and the rescued animals were characterized. This regimen has allowed for normal development, apparent health, and reproduction. Interruption of this rescue intervention resulted in the development of severe hyperammonemia and death within 48 hours. We have developed a home cage behavioral system that allows to monitor and analyze the chronology of animal

behaviors during healthy and hyperammonemic states. Data collected from this study reveals that mice decrease their normal activity around 12 hours and become severely lethargic by 20 hours following NCG withdrawal. Understanding the chronology of hyperammonemia will aid in future studies to discover neuro-protective drugs for treating hyperammonemia. This mouse model will also allow studies of the pharmacokinetics and pharmacodynamics of NCG, much of which is still unknown. Understanding how NCG is transported into cells and then cleared is clinically relevant and can potentially lead to more efficient administration of this drug. We conclude that a novel NAGS deprived mouse model has been developed which can be rescued by NCG and Cit and reared to reproduction and beyond. This biochemically salvageable mouse model recapitulates the clinical phenotype of proximal urea cycle disorders and can be used as a reliable model of induced hyperammonemia by manipulating the administration of the rescue compounds.

CHARACTERIZATION OF THE N-ACETYLGLUTAMATE SYNTHASE KNOCKOUT MOUSE, A NOVEL MODEL OF HYPERAMMONEMIA

By

Emilee Senkevitch

Dissertation submitted to the Faculty of the Graduate School of the
University of Maryland, College Park, in partial fulfillment
of the requirements for the degree of
Doctor of Philosophy
November 2012

Advisory Committee:
Professor David Mosser, Chair
Professor Mendel Tuchman, Co-chair
Associate Professor Brian Bequette
Associate Professor Ljubica Caldovic
Assistant Professor Kenneth Frauwirth
Associate Professor Wenxia Song

Acknowledgements

A very special thank you to the following:

Mendel Tuchman, Ljubica Caldovic and Hiroki Morizono -- I am forever grateful for all of your support, advice, and mentorship over the last two years.

My committee members Wenxia Song, David Mosser, Brian Bequette and Kenneth Frauwirth for all the guidance and advice given to me during my graduate school career.

Members of the lab -- Net Haskins, Amy Mumo, Elena Pumbo, Nick Ah Mew and Norma Allewell.

Juan Cabrera-Luque for all of the animal training, and Elena for all her help with genotyping.

The Research Animal Facilities at Children's National Medical Center and Veteran's Affairs, especially JanNean Williams and Maria Okolita for all the training and assistance with animal husbandry.

Kanniboyina Nagaraju and members of his lab for collaborations with animal behavior experiments.

The Knockout Mouse Project, KOMP, for the creation of the *Nags*$^{-/-}$ mouse, NIH NIDDK and ARRA for providing funding for this project.

The Biochemical and Genetics lab at CNMC, especially Mike Jones and Crystal Stroud for help with plasma analysis and assistance with LCMS work; Yale University Metabolic Phenotyping Core for assessment of liver damage in *Nags*$^{-/-}$ mice.

Leslie Pick, Ann C. Smith, and University of Maryland Graduate School for providing me with fellowships throughout my graduate school career.

Jennifer Staiger, for instilling in me a love of teaching and research, as well as my teaching mentors at University of Maryland, Patty Shields, Ann Smith, and Wenxia Song.

And finally, I would not have survived graduate school without the support of my friends and family. To my parents, my sisters Laura and Phoebe, Allison, Lauren, Shana, and Anthony- thank you for everything. You have been there for me through the good and the bad, and I am truly blessed to have you in my life.

Table of Contents

Acknowledgements ii
Table of Contents iv
List of Tables vi
List of Figures vii
Abbreviations ix
Chapter 1: Introduction 1
Urea Cycle 1
Urea Cycle in the Liver Protects the Brain from Hyperammonemia 5
Urea Cycle Enzymes in Arginine Production 7
N-Acetylglutamate Synthase Deficiency 10
N-Carbamylglutamate as treatment for NAGS deficiency 10
Using Cell Culture to Study the Urea Cycle 12
Mouse Models of Hyperammonemia 13
Mouse Models of Urea Cycle Disorders 13
Inducing Hyperammonemia in Rodents 15
Rationale for the Creation of the $Nags^{-/-}$ Mouse 16
Chapter 2: A Novel Biochemically Salvageable Animal Model of Hyperammonemia Devoid of N-Acetylglutamate Synthase 18
Publication 18
Introduction 18
Materials and Methods 20
Generation of the NAGS knockout mouse 20
Animal Care and Husbandry 22
Genotyping and Identification 22
Western Blots 25
Chemical Rescue of Nags-/- mice 26
Plasma Ammonia and Amino Acid Measurements 26
Liver Function 27
Statistical Analysis 27
Results 28
Breeding of Mice 28
Biochemical Rescue of $Nags^{-/-}$ Mice 32
Appearance of $Nags^{-/-}$ Mice 36
Metabolic Phenotype of $Nags^{-/-}$ Mice 41
Discussion 47
Chapter 3: Use of a Home Cage Monitoring System to Define the Chronology of Behavioral Change during Hyperammonemia 50
Introduction 50
Materials and Methods 51
Animal Husbandry 51
Voluntary Wheel 52
Home Cage Monitoring 52

Results and Discussion 56
Voluntary Wheel 56
Home Cage Behavioral System 59
Chapter 4: Determination of a liquid chromatography-mass spectrometry method for the determination of N-carbamyl-L-glutamate in biological samples 67
Introduction 67
Materials and Methods 68
Chemicals 68
Synthesis of Isotopic N-carmabyl-L-glutamate 68
Instrumentation 69
Chromatographic and Mass Spectrometer Conditions 69
Tissue Collection 69
Statistical Analysis 70
Results and Discussion 71
Chapter 5: Future Directions 83
Identifying drugs that have a neuroprotective effect against hyperammonemia 83
Testing known neuroprotective drugs in $Nags^{-/-}$ mouse 84
Identification of the N-carbamylglutamate transporter 85
Identification of the plasma membrane and mitochondrial transporters for NCG by affinity labeling 88
Using siRNA knockdown to identify the NCG transporters 88
Chapter 6: Conclusions 90
Appendix: Urea Cycle Enzyme expression in HepG2 and IEC-6 cell lines 93
Methods and Materials 93
Bibliography 96

List of Tables

Table 1. Progeny from heterozygote mating…….....31

Table 2. Home Cage System generated behaviors…….55

Table 3. Cease of activity following the removal of NCG/cit Supplementation……..64

Table 4. Primers for Urea Cycle enzyme genes in HepG2 and IEC-6 cell lines……94

List of Figures

Figure 1. Anatomy of the liver…….2

Figure 2. The urea cycle……..4

Figure 3. Arginine synthesis via the intestinal-renal axis…….8

Figure 4. Metabolic fates of arginine……....9

Figure 5. Strategy for deletion of the *Nags* gene…….21

Figure 6. Strategy for genotyping *Nags*$^{-/-}$ mice……...24

Figure 7. SW;B6 heterozygous females produce larger litters and maintain them better compared to inbred BL/6N mice……..29

Figure 8. Western blots of NAGS from liver and intestine…….33

Figure 9. Western blots of CPS1 and OTC in liver and intestine……...34

Figure 10. Biochemical rescue of *Nags*$^{-/-}$ pups…….37

Figure 11. Biochemical rescue of *Nags*$^{-/-}$ mice after weaning……..38

Figure 12. Phenotype of *Nags*$^{-/-}$ mice……...39

Figure 13. Growth of *Nags*$^{-/-}$ mice…….....40

Figure 14. Ammonia levels of *Nags*$^{-/-}$ mice…….....42

Figure 15. Plasma amino acid levels of *Nags*$^{-/-}$ mice……....43

Figure 16. Liver function tests in Wild Type and *Nags*$^{-/-}$ mice…….46

Figure 17. Running activity of wild type and *Nags*$^{-/-}$ mice..…….58

Figure 18. Behavior of Wild Type and *Nags*$^{-/-}$ mice with NCG + Cit supplementation and after withdrawal…….60

Figure 19. Activity plots of Wild Type and *Nags*$^{-/-}$ mice with NCG + Cit supplementation and after withdrawal…….62

Figure 20. Structure of N-carbamylglutamate and isotopic N-carbamylglutamate……...72

Figure 21. Representative LC-MS chromatogram of N-carbamylglutamate……73

Figure 22. Concentration of NCG in liver samples……...74

Figure 23. Glutamate + carbamylphosphate produce NCG in the presence of TCA…….76

Figure 24. Concentration of NCG in intestinal epithelial cells…….77

Figure 25. Concentration of NCG in plasma…….79

Figure 26. Concentration of NCG in urine……80

Figure 27. Concentration of NCG in feces……81

Figure 28. NCG uptake in HepG2 Cells……87

Figure 29. Expression of Urea Cycle enzymes in HepG2 and IEC-6 cell lines……...95

Abbreviations

ARGI	Arginase I
Arg	Arginine
ASL	Argininosuccinate lyase
ASS	Argininosuccinate synthase
Cit	Citrulline
CP	Carbamyl phosphate
CPS1	Carbamyl phosphate synthetase 1
MSO	Methionine Sulfoximine
NAG	N-acetylglutamate
NAGS	N-acetylglutamate synthase
NCG	N-carbamylglutamate
NMDA	N-methyl-D-aspartate
OAT	ornithine aminotransferase
ORNT1	Ornithine transporter 1
OTC	Ornithine Transcarbamylase
RT-PCR	Real Time Polymerase Chain Reaction

Chapter 1: Introduction

Urea Cycle

The urea cycle, discovered by Hans Krebs in 1932, is a biochemical process that converts toxic ammonia to urea [1,2]. Ammonia is a source of nitrogen waste from multiple biochemical processes: hydrolysis of urea and nitrogenous compounds by urease positive gut bacteria, catabolism of dietary proteins, and catabolism of cellular proteins, including skeletal muscle during exercise [3,4]. A healthy adult will produce an average of 0.3-1.2 moles of nitrogen a day; more than 90% of which is excreted in the form of urea to maintain plasma ammonia concentration of less than 35 μM [3]. Ammonia enters the liver via the portal vein (Figure 1) where concentrations of ammonia can be up to 350 μM (about 10-fold higher than in the systemic blood). The liver removes almost all the ammonia in one pass, utilizing two main pathways expressed in two different forms of hepatocytes; the urea cycle in the periportal hepatocytes and glutamine synthase in perivenous hepatocytes. Approximately two-thirds of the ammonia detoxification occurs via the urea cycle [3].

The urea cycle requires at least eight proteins for proper function. Ureagenesis is initiated in the mitochondria by the activation of carbamyl phosphate synthetase 1 (CPS1) by N-acetylglutamate (NAG). NAG is produced by N-acetylgutamate synthase (NAGS) from L-glutamate and acetyl-CoA [5,6]. CPS1 condenses ammonia (NH_3), bicarbonate (HCO_3^-), and 2 ATP molecules to form carbamyl phosphate (CP).

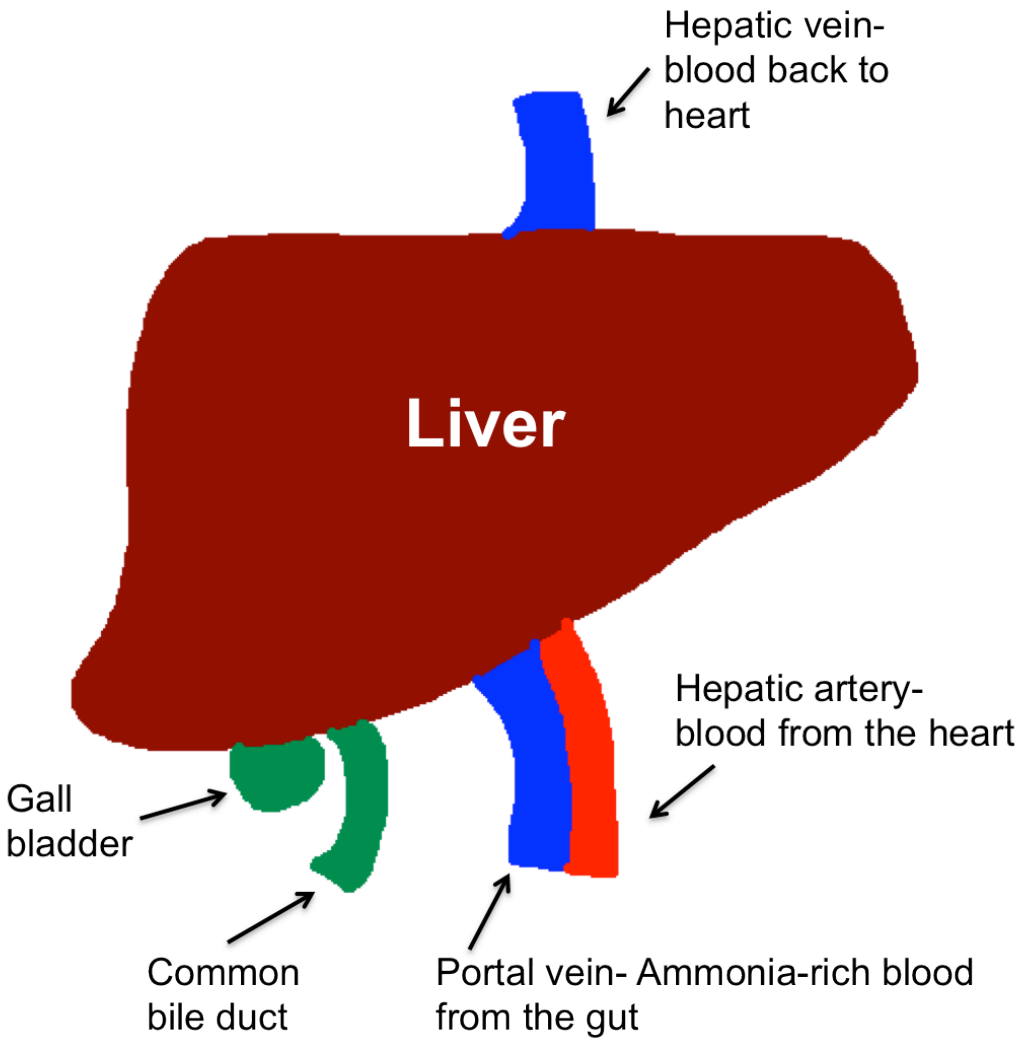

Figure 1. The liver detoxifies ammonia.
Ammonia produced mainly by the intestine enters the liver via the portal vein where it is taken up by hepatocytes and converted to urea.

Ornithine transcarbamylase (OTC) then condenses CP and ornithine to form citrulline [5]. Citrulline is then transported out of the mitochondria into the cytoplasm where it condenses with aspartate via the enzyme argininosuccinate synthase (ASS) to form argininosuccinate. The enzyme argininosuccinate lyase (ASL) then cleaves argininosuccinate into arginine and fumarate. Lastly, arginase I (ARG1) hydrolyzes arginine to form ornithine and urea. Urea produced in the liver is excreted from the body through the kidneys and ornithine is transported back into the mitochondria to re-enter the urea cycle. In addition to these six enzymes, there are two mitochondrial transporters in the urea cycle. The ornithine transporter (ORNT1) transports citrulline out of the mitochondria and ornithine in [7,8]. Citrin transports aspartate out and glutamate into mitochondria [7] (Figure 2).

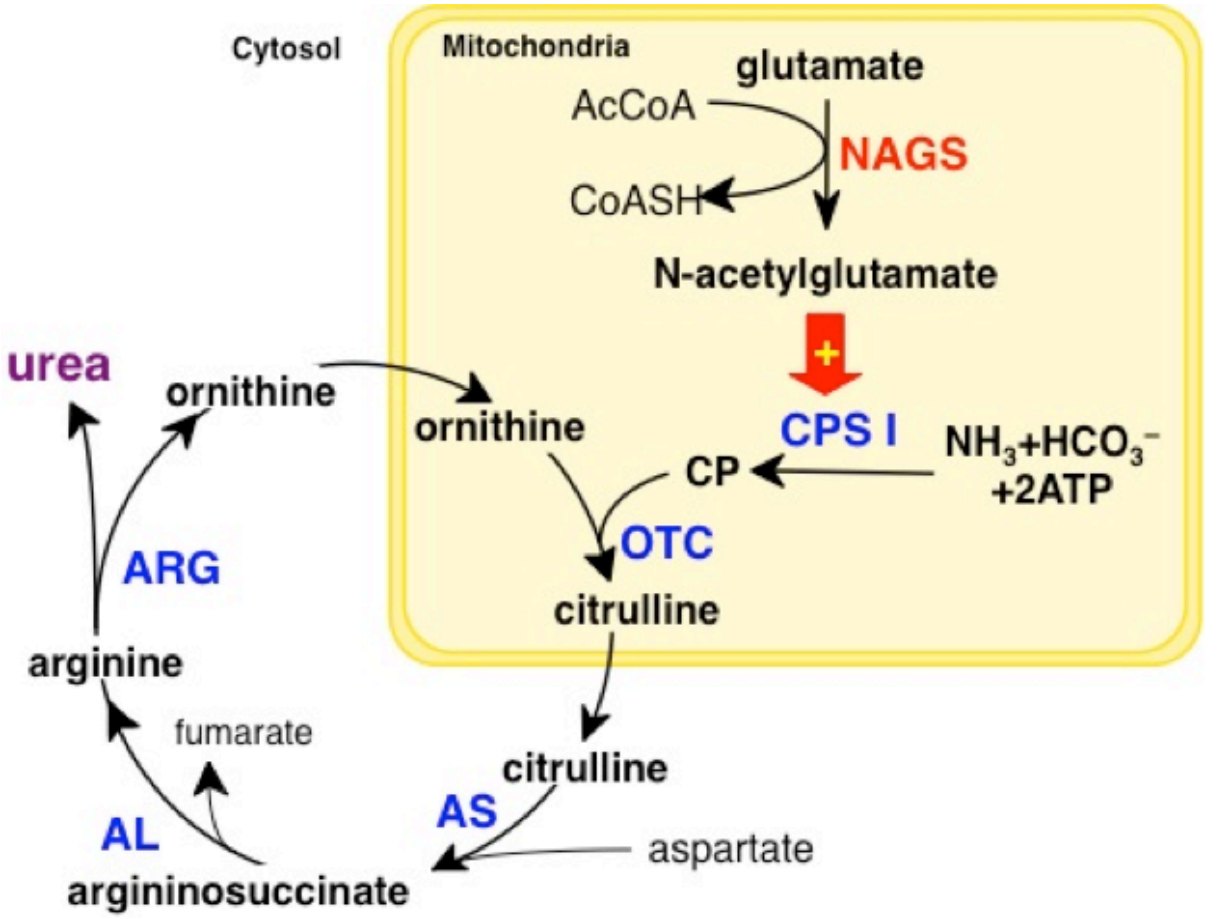

Figure 2. The Urea Cycle in Liver Cell.
The proximal urea cycle enzymes, NAGS, CPS1, and OTC are expressed in the mitochondria, and the distal urea cycle enzymes ASS, ASL, and ARGI are expressed in the cytosol. (Source: Caldovic et al [9])

Urea Cycle in the Liver Protects the Brain from Hyperammonemia

The urea cycle is essential for protecting the brain from the toxic effects of ammonia. In general, the ammonia level in the plasma remains low (less than 35 μmol/L). However, there are numerous conditions that can cause an accumulation of excess ammonia. Hyperammonemia is caused by urea cycle defects, defects in fatty acid oxidation, cirrhosis, acute liver failure, certain surgeries, Reye syndrome, and chemotherapy [1,4,10]. The accumulation of excess ammonia in the plasma, hyperammonemia, has negative consequences on the brain with resulting symptoms of vomiting, lethargy, slurred speech, weakness, ataxia, seizures, and if untreated, coma and death [4,10,11].

Ammonia rapidly enters the brain and rapidly combines with glutamate to generate glutamine via glutamine synthase, which is expressed in astrocytes [3,10-13]. Under physiological conditions, this enzyme functions at maximal capacity, and thus is not induced during hyperammonemia [3,4,10,12,13]. The autopsies of patients that have died from hyperammonemia show gross cerebral edema and astrocytic swelling [4,10,14]. Evidence suggests that the accumulation of glutamine is related to cerebral edema, first by osmotic action [14,15], then by increasing inner mitochondrial membrane permeability and lastly through free radical damage [11,15]. Studies using the glutamine synthase inhibitor methionine sulfoximine show reduced ammonia-induced brain edema both *in vivo* and *in vitro* [11,16,17].

Cerebral edema may also be caused by a change of Aquaporin 4 channels, which are involved in water homeostasis [13,16,17]. Additionally, ammonia can be transported through the astrocytic potassium channels Kir 4.1 and Kir 5.1; hyperammonemia blocks

potassium transport which results in extracellular potassium accumulation and neuronal depolarization [13,18,19].

Alterations in the neurotransmitter receptor N-methyl-D-aspartate (NMDA) have also been described in hyperammonemia. The NMDA receptor is both ligand gated and voltage dependent. Activation of the receptor by glutamate and glycine opens the ion channels, which cause influx of Na^+, Ca^{2+}, and efflux of K^+. Ammonia toxicity can result in excess extracellular glutamate, due to pH and Ca^{2+}-dependent release of glutamate and then inhibition of glutamine uptake by astrocytes. The increase of extracellular glutamate causes overstimulation of the NMDA receptor which results in excessive influx of Na^+, Ca^{2+}, and Cl^-, ultimately causing cell swelling and neurodegeneration [18,19]. Administration of the drug memantine, a noncompetitive NMDA receptor antagonist, to rats experiencing encephalopathy, resulted in improved electroencephalography (EEG) activity, less increase in glutamine, and decreased intracranial pressure and brain water compared to non-treated encephalopathic rats [19,20]. Administration of another NMDA receptor antagonist, MK-801, protected against acute liver failure induced death, increasing survival time two-fold [20].

These studies show that separately, astrocytes and NMDA receptors on neurons play a role in the neurological symptoms of hyperammonemia, and the administration of drugs that target these cells can attenuate hyperammonemia. It is unknown how these two mechanisms connect, and if a combination of drugs can lead to the maximal blocking of cerebral edema or reverse the neurological symptoms of hyperammonemia. Additionally, studies on the mechanisms underlying hyperammonemia have not yet explained the clinical symptoms presented in patients.

Urea Cycle Enzymes in Arginine Production

Though the urea cycle produces arginine, there is no net arginine production from the liver because the high levels of ARGI hydrolyze arginine to ornithine and urea. Instead, the small intestine and kidneys are tasked with producing endogenous arginine. First, intestinal epithelial cells convert glutamine to citrulline. Glutamine is the most abundant amino acid in the cells and the plasma, where it serves as both an ammonia scavenger and a nitrogen donor [21]. The intestine has access to glutamine from two sources: the intestinal lumen and the arterial supply. Within the mitochondria of the intestinal epithelial cells, glutamine is first converted to glutamate via glutaminase. Then, pyrroline-5-carboxylate synthase converts glutamate to pyrroline-5-carboxylate or glutamate semialdehyde [22-26]. Next, proline-5-carboxylate or glutamate semialdehyde is transaminated via ornithine aminotransferase to form ornithine. NAGS, CPS1, and OTC are also present in the mitochondria of intestinal epithelial cells where they perform the same role as in the hepatocytes [22,24,27,28]. CP produced from CPS1 activity condenses with ornithine via ornithine transcarbamylase to yield citrulline. The citrulline is then released into the blood where it bypasses the liver and enters the renal artery [27-29]. ASS and ASL are expressed in the proximal convoluted tubules where citrulline is converted to arginine [29] (Figure 3). Arginine is necessary for many physiological processes, including protein building, creatine production, NO production, and wound repair (Figure 4) [28].

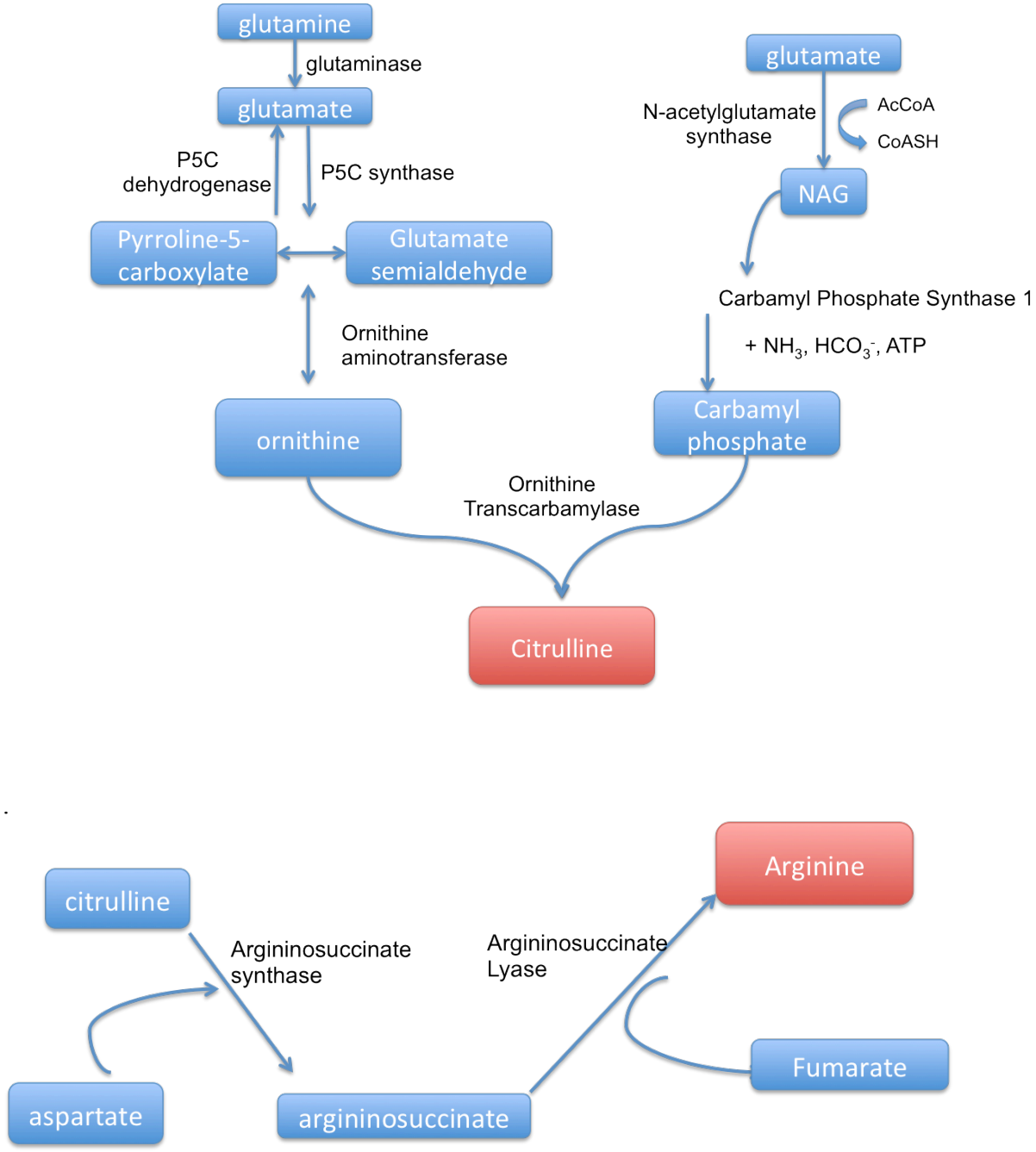

Figure 3. Arginine synthesis via the intestinal-renal axis.
Citrulline is produced in small intestinal epithelial cells, bypasses the liver, and is converted to arginine in the kidneys.

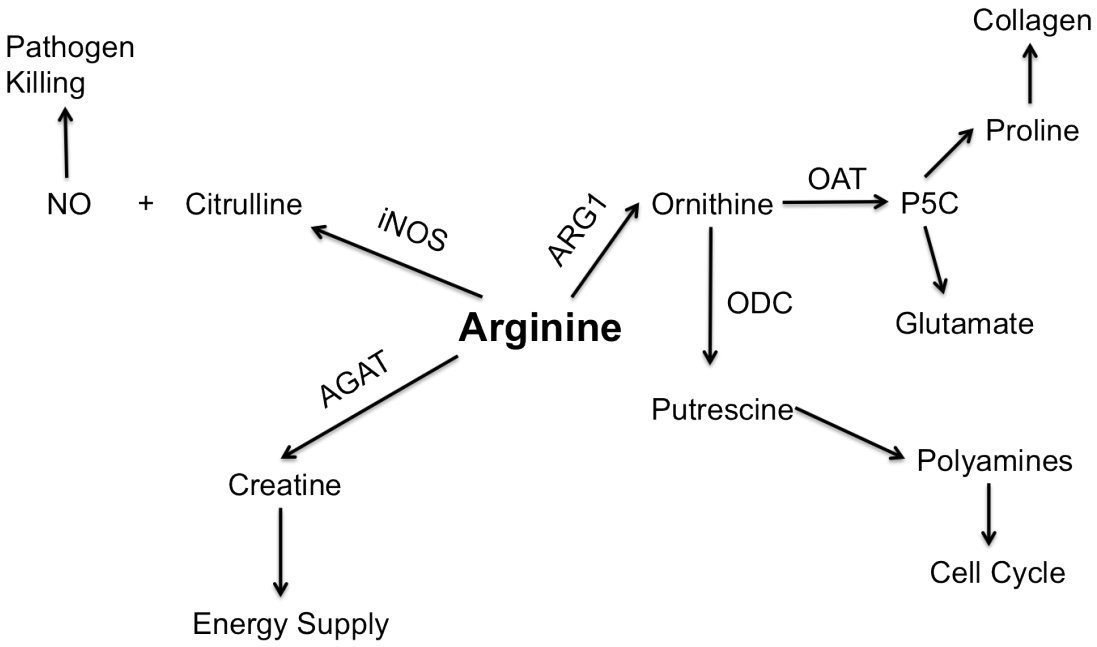

Figure 4. Metabolic Fates of Arginine.
Arginine is a precursor for multiple biochemical pathways, including the production of nitric oxide (NO), proline, glutamate, polyamines, and creatine. iNOS=inducible nitric oxide synthase, ARG1= arginase I, OAT= ornithine aminotransferase, AGAT=arginine glycine amidinotransferase, ODC= ornithine decarboxylase.

N-Acetylglutamate Synthase Deficiency

For all eight urea cycle associated proteins, there are documented cases of patients showing a genetic deficiency. NAGS deficiency is the rarest of the urea cycle disorders, with only 34 reported cases from 28 families [30-32]. The first case of NAGS deficiency was described in 1981 [30]. A deficiency in any of the urea cycle enzymes manifests as hyperammonemia, which results in vomiting, seizures, mental retardation, coma, and death if left untreated [14,31,32]. The biochemical symptoms of NAGS deficiency are identical to those of CPS1 deficiency and include elevated plasma ammonia and glutamine and reduced levels of urea cycle intermediates arginine, citrulline, and ornithine [32-35]. Due to the identification of the NAGS gene by our laboratory in 2002 [33-35], NAGS deficiency can now be definitively confirmed genetically. This autosomal recessive disease has varying degrees of severity. Patients presenting in the neonatal period tend to have nonsense or frameshift mutations that result in complete absence of the NAGS protein [36-41], while missense mutations may allow for some residual NAGS enzyme activity and present after the neonatal period [31,36,38,40,42]. There are also documented "late-onset" cases that have presented during adulthood [31,42,43].

N-Carbamylglutamate as treatment for NAGS deficiency

When a patient is first suspected as having a urea cycle disorder, the initial objective is to reduce plasma ammonia [43] by removing protein from the diet [44]. In extreme cases, clinicians will prescribe dialysis and/or scavenging agents sodium benzoate, sodium phenylacetate, or sodium phenylbutyrate [45]. These three drugs work by incorporating waste nitrogen into compounds that have high renal clearance [46,47]. While patients are taking these drugs, they also remain on low-protein diets.

N-carbamylglutamate (NCG) effectively restores ureagenesis and reverses hyperammonemia in NAGS deficient patients and is the only specific treatment available for any urea cycle disorder. NCG is a stable glutamic acid derivative that activates CPS1 in the absence of NAG [30]. NCG has a lower affinity for CPS1, but is more effective than NAG since administered NAG is inactivated by acylases and does not reach the mitochondria [48].

NCG was first described as a result of Grisolia and Cohen's experiments to uncover the mechanism for synthesis of citrulline from ornithine [5]. They showed that the combination of the enzyme system, ammonia, and NCG followed by addition of ornithine results in citrulline synthesis. As a result of these observations, they hypothesized that reaction involves two steps; the creation of NCG, and the fixation of ammonia [49,50]. However, further experiments failed to isolate any detectable amount of NCG from the liver. Instead, they isolated and characterized NAG from mammalian liver. The presence of NAG and high catalytic CPS1 activity indicated that it is the natural co-factor in CP synthesis [51]. Despite the failure to detect endogenous NCG, the fact that it is not degraded in the liver held promise as a treatment for hyperammonemia. A combination of NCG and arginine prior to giving rats a lethal dose of ammonia protected 100% of the rats, while NAG was relatively ineffective due to hydrolysis by acylaminoacid acylase. This was the first time showing rational basis for using NCG and a urea cycle intermediate in the treatment of hyperammonemia [52].

The first case of NAGS deficiency and successful treatment with NCG was documented in 1982 [30]. Since Bachmann's initial diagnosis and treatment, other cases of treating NAGS deficiency with NCG have been described [38,39,53-55]. NCG is sold

and marketed by Orphan Europe under the name Carbaglu, and is approved by the FDA for the treatment of NAGS deficiency. Additionally, NCG has been used off-label for the treatment of CPS1 deficiency [56], propionic acidemia [57,58], and isovaleric acidemia [59].

Using Cell Culture to Study the Urea Cycle

While cell lines are often useful in uncovering mechanisms involved in disease, they are not the best method to study urea cycle diseases. HepG2, a liver cell line derived from human hepatoblastoma, is a popular liver cell line. These cells continue to express genes related to cholesterol and triglyceride metabolism, which makes them a sufficient model to study some aspects of liver function [60]. However, these cells have lost other primary functions, including the ability to produce urea. HepG2 cells do not detoxify ammonia and produce urea when exposed to ammonium chloride and do not express detectable levels of urea cycle intermediates. This is due to the absence of OTC and ARGI expression [61,62]. These results were confirmed in our lab as well, demonstrating negligible levels of OTC and ARG1 in this cell line (see Appendix, Figure 29). One hypothesis to explain the lack of OTC and ARG1 is that this cell line is using excess carbamyl phosphate for pyrimidine synthesis [63] and excess arginine for polyamine production [64,65]. The synthesis of pyrimidines and polyamines would be beneficial to promote proliferation of these cancer cells. The lack of a complete urea cycle in this cell line shows that these cells are not adequate for the study of urea cycle function. A recent study showed that HepG2 cells could be stably transfected with OTC and ARG1, which results in an increase in ammonia detoxification [66]. Other hepatocellular carcinoma cell lines have shown a consistent down-regulation of CPS1 due to DNA methylation of the

promoter and first intron [67]. Therefore, the use of cell lines, especially those originating from cancer cells, is not suitable to study ureagenesis.

IEC-6, a rat intestinal epithelial cell line, was first established and cultured successfully in 1979 [68]. Small intestinal epithelial cells are mitotically active and can divide in culture without being transformed into tumor cells. IEC-6 cells were derived from undifferentiated small intestinal crypt cells, and have normal morphology and karyotype. Despite this, this cell line does not produce citrulline. Our experiments revealed that IEC-6 only expresses trace of NAGS (Appendix, Figure 29), and thus is not suitable as a model to study citrulline production in the intestine.

Mouse Models of Hyperammonemia

Mouse Models of Urea Cycle Disorders

The first mouse model for a urea cycle to be discovered and characterized was the model for OTC deficiency. There are two natural mouse models for OTC deficiency, which arose from spontaneous mutations in the X chromosome. The best characterized is the sparse fur (spf) mouse first reported in 1976 [69]. This mouse has a C→A mutation in exon 4 (H117N) which results in 10% normal enzyme activity associated with pH optimum shift[70]. The other OTC model, spf^{ash} (abnormal skin and hair) was reported in 1974 [71] and is the result of a G → A missense mutation in exon 4 (R129H) which causes abnormal splicing and 5% normal enzyme activity [72]. Both models display the characteristics of OTC deficiency including elevated plasma ammonia, glutamine and urinary orotic acid, and decreased arginine and citrulline. Hemizygote males have an average lifespan of 42 days [73]. Recently, focus has been on using the spf^{ash} model in pre-clinical gene therapy studies [74].

The mouse model for CPS1 deficiency was created by deleting a portion of exon 17 from the gene. The mutation in the gene abolishes all CPS1 activity in the liver of homozygotes. All *Cps1*$^{-/-}$ mice begin to experience hyperammonemia around 6 hours following birth, and die within 36 hours of birth. This model no longer exists [75].

There are also multiple models for ASS deficiency. The first, described in 1994, has an engineered mutation in exon 4 which abolishes all ASS activity [76]. Homozygous ASS mice develop hyperammonemia about 10 hours post-birth and most die within 24 hours. This model has also been used for gene therapy using an adenovirus vector that seems to be successful in restoring some ASS activity [77]. Two spontaneous mutations in the ASS gene have also been reported. These mice exhibit growth retardation, alopecia, lethargy, ataxia, and delayed cerebellar development associated with increased levels of citrulline and ammonia, similar to symptoms in patients. Treatment of these mice with sodium benzoate and arginine has been successful, resulting in normal brain development and survival to at least 6 weeks of age [78].

The mouse model for ASL deficiency was created by deleting exons 8 and 9 of the gene, which decreases enzyme activity to about 4% of wild type. All ASL homozygote mice die within 48 hours post-birth and exhibit elevated ammonia, glutamine, citrulline, and argininosuccinic acid, and low arginine [79].

Lastly, the ARG1 knockout mouse was created by replacing exon 4 with the gene encoding neomycin resistance, which completely abolishes all enzyme activity. Genotypic analysis revealed there is a non-Mendelian distribution of genotypes, with a significant deficit of ARG1 homozygotes. ARG1 homozygotes die within 10-14 days post-birth and exhibit hyperammonemia and increased arginine and decreased ornithine levels. The

authors of this study postulate that the ARG1 deficient mice survive for 10 days because during the neonatal stage, the enzyme ornithine aminotransferase (OAT) converts glutamate into ornithine. However, at approximately two weeks of age, intestinal OAT switches to produce glutamine, leaving ARG1 as the sole source of ornithine production. With no pathway to produce ornithine, the ARG1 mice are lacking a key metabolite in the urea cycle, resulting in hyperammonemia [80].

Though mouse models for all the urea cycle disorders have been created and characterized, these mice either do not survive beyond the neonatal period, or do not reproduce. Therefore, it is difficult if not impossible to conduct comprehensive studies of hyperammonemia using these models.

Inducing Hyperammonemia in Rodents

In order to study hyperammonemia in rodents, several models have been developed which result in increased plasma ammonia levels. The simplest model involves feeding the rodent a standard diet supplemented with 20% ammonium acetate for 100 days. This diet results in increased ammonia levels in the brain, liver, and muscle, a 2-fold increase in urea production, an increase in expression of glutamine synthase, glutamate dehydrogenase, and higher brain glutamine concentrations [81]. It appears as though the liver can adjust to this high-ammonia diet, as it increases urea production. This occurs without an increase of CPS1 or NAGS activity; however it is reported that the high-ammonia diet increases the mitochondrial content of NAG [82]. There were no neurobehavioral changes in these animals and levels of brain glutamate and aspartate were not significantly affected. Therefore, simply supplementing mice with high-ammonia

diets is not sufficient to significantly alter the brain chemistry in a way that mimics a hyperammonemic crisis.

There are two surgical methods to induce hyperammonemia in rodents. The first is by creating a portocaval shunt. In this case, portal blood carrying ammonia is no longer processed by the liver, instead this blood enters the systemic circulation, resulting in liver atrophy [83]. This model leads to chronic hyperammonemia, which results in neurological symptoms such as abnormal circadian rhythms and sleep patterns [84] and postural abnormalities [85] that are associated with increased brain ammonia/glutamine and neurotransmitter function and altered ratios of aromatic/branched chain amino acids [83], When rats with a portocaval shunt are given an ammonia challenge, they develop lethargy, myoclonic twitching, and coma, whereas normal rats given an ammonia challenge develop some mild neurological symptoms but eventually recover. [86-88].

Chronic liver injury can also be induced with bile duct ligation, which induces a reproducible model of biliary cirrhosis, an autoimmune disease that causes bile buildup in the liver [83]. Rodents with a bile duct ligation develop hyperammonemia but only low-grade encephalopathy with decreased locomotor function. These rodents only develop hepatic encephalopathy with neurological symptoms following the ingestion of ammonium salts [89-91].

Rationale for the Creation of the Nags$^{-/-}$ Mouse

As mentioned, the usefulness of mice with urea cycle defects has been rather limited due to neonatal lethality and difficulties in rescue by biochemical interventions for any significant length of time. Rodent models for inducible hyperammonemia involve extensive surgery, cause unnecessary stress to the rodent and are not reversible. The

availability of a mouse with a severe urea cycle defect that could be salvaged by a simple biochemical intervention would enhance research into various aspects of hyperammonemia and ureagenesis. Since NAGS deficiency is the only urea cycle disorder with a biochemical cure, we hypothesized that we could create a NAGS knockout mouse, and rescue the homozygous pups (*Nags*$^{-/-}$) with NCG, which would allow them to survive past the neonatal period into adulthood and reproduce. We reasoned that if such a murine model could be reared to reproductive age, a large number of homozygous mice could be produced and studied. Furthermore, hyperammonemia could be induced and suppressed as necessary by manipulating the biochemical rescue allowing studies during, and off treatment. The creation of this mouse represents the first "clean", inducible, salvageable model of hyperammonemia due to an inborn error of metabolism.

Chapter 2: A Novel Biochemically Salvageable Animal Model of Hyperammonemia Devoid of N-Acetylglutamate Synthase

Publication

Senkevitch E, Cabrera-Luque J, Morizono H, Caldovic L, Tuchman M. "A novel biochemically salvageable animal model of hyperammonemia devoid of N-acetylglutamate synthase." Mol Gen Metab. 2012 June; 106(2): 160-168

Introduction

In mammals, nitrogen waste in the form of neurotoxic ammonia is converted in the liver to urea, which is then excreted in the urine [14]. Ureagenesis requires at least eight proteins and is initiated in the mitochondria via the activation of carbamyl phosphate synthetase 1 (CPS1) by N-acetyl-L-glutamate (NAG) [9]. NAG is produced by NAG synthase (NAGS) from L-glutamate and acetyl-CoA [6]. Inherited or acquired deficiency of NAGS catalytic activity causes a functional block in ureagenesis, due to the corresponding reduction or abolishment of CPS1 activity, leading to the accumulation of ammonia in the blood [30,92]. The clinical presentation and biochemical features of NAGS deficiency are indistinguishable from those of CPS1 deficiency and include elevated plasma glutamine, reduced citrulline, and normal levels of urinary orotic acid and orotidine [43].

Mouse models of complete enzyme deficiency and hyperammonemia have been created for each of the urea cycle enzymes with the exception of NAGS [43,69,75,79,80,93-95]. However, their usefulness for research has been rather limited due to neonatal lethality and difficulties in rescue by biochemical interventions for any significant length of time. Among these models, the one produced by Schofield et al. [75]

for complete CPS1 deficiency (homozygous knockout) proved to be lethal within one day after birth. The availability of a mouse with a severe urea cycle defect that could be salvaged by a biochemical intervention would enhance research into various aspects of hyperammonemia and ureagenesis. We reasoned that if such a murine model could be reared to reproductive age, a large number of homozygous mice could be produced and studied. Furthermore, hyperammonemia could be induced and suppressed at will by manipulating the biochemical rescue allowing studies during, and off acute disease.

Unlike all other urea cycle disorders, NAGS deficiency in humans is amenable to effective treatment with N-carbamyl-L-glutamate (NCG) [54], a functional analog of NAG that has been shown to be resistant to *in vivo* degradation. There is good evidence that this molecule reaches the liver, enters the mitochondria and activates CPS1 *in vitro* and *in vivo* [9,52]. We therefore surmised, that if a NAGS knockout mouse could be created, the homozygous pups (*Nags*$^{-/-}$) could potentially be rescued by treatment with NCG allowing them to survive beyond the neonatal period and perhaps even to adulthood.

We document herein, the successful creation of the first salvageable mouse model of a urea cycle enzyme deficiency. We demonstrate that the *Nags*$^{-/-}$ mouse, which shows neonatal lethality similar to *Cps1*$^{-/-}$ mice, can be rescued by combinational therapy of NCG and L-citrulline (Cit), and consequently reach adulthood and reproduce to create litters of exclusive *Nags*$^{-/-}$ animals. We describe the procedure for rescue of *Nags*$^{-/-}$ mice, characterization of this new hyperammonemia mouse model, and show that the animal wellbeing depends on continued supplementation of NCG with the addition of Cit.

Materials and Methods

Generation of the NAGS knockout mouse

The trans-NIH Knock-Out Mouse Project (KOMP, www.komp.org), an NIH supported strain repository at the University of California Davis, was successful in transferring null alleles for *Nags* in two C57BL/6 embryonic stem cell lines and cryo-achieving germ line transfer embryos (C57BL/6N-Nags$^{tm1(KOMP)Vlcg}$). The strategy used for generating the ES cell clones with deletion of the entire gene is illustrated in Figure 5. Homologous recombination allows the entire *Nags* gene to be replaced with the ZEN-UB1 cassette within the bacterial vector, containing the coding sequences for lacZ and neomycin resistance genes. NIH grants to Velocigene at Regeneron Inc. (U01HG004085) and the CSD Consortium (U01HG004080) funded the generation of gene-targeted ES cells for 8500 genes in the KOMP Program which are archived and distributed by the KOMP Repository at UC Davis and CHORI (U42RR024244)[96]. The KOMP Repository provided us four C57BL/6N-Nags$^{tm1(KOMP)Vlcg}$ heterozygous mice from the cryo-archive.

These mice (*Nags*$^{+/-}$) were crossed with wild type Swiss Webster (Charles River Laboratories). The resulting first generation of heterozygous was crossed to obtain homozygous mice (*Nags*$^{-/-}$). Of these homozygous animals, those that were reared to reproductive age were crossed to obtain the homozygous mice used for the described experiments.

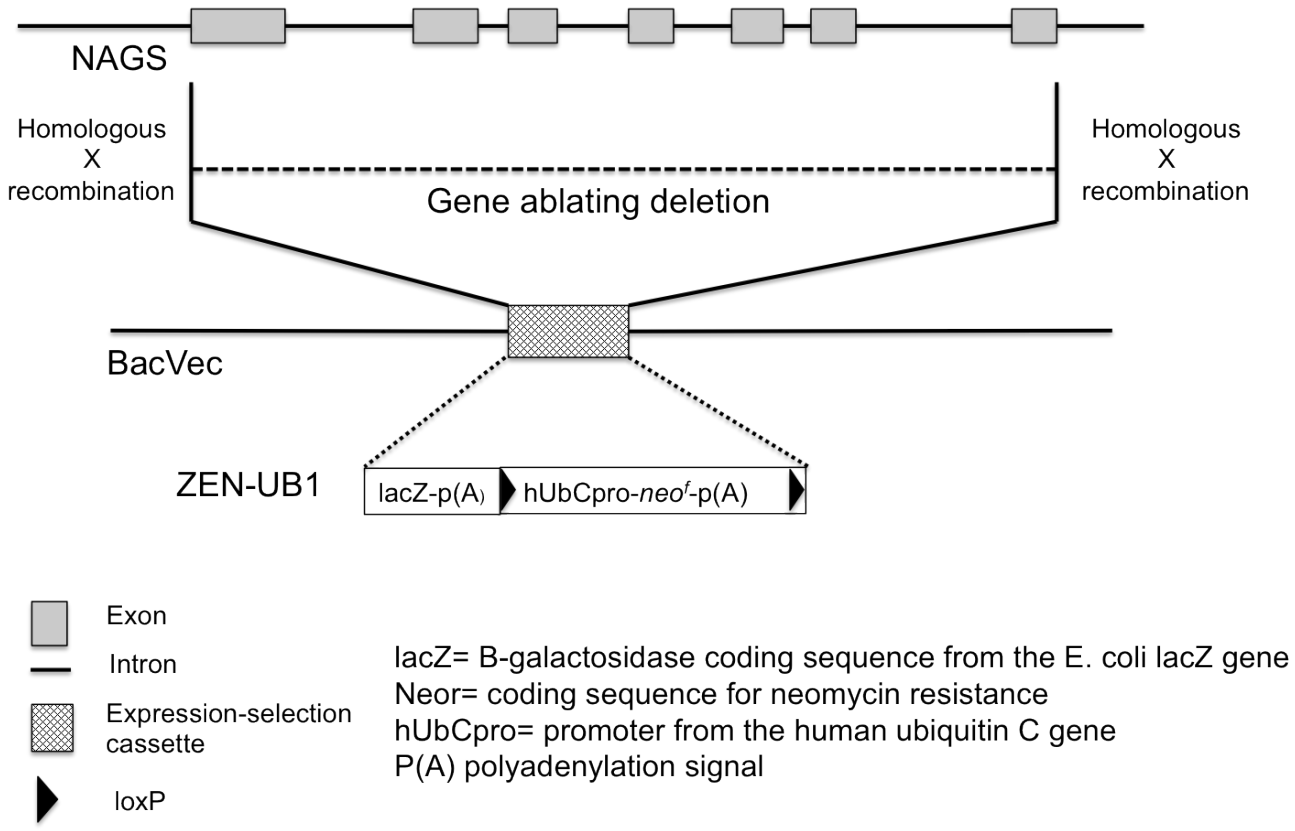

Figure 5. Strategy for deletion of the *Nags* gene.
Diagram of the *Nags* gene (top) and the large BAC-based targeting vector (bottom). Homologous recombination allows the entire *Nags* gene to be replaced with the ZEN-UB1 cassette, which contains the coding sequences for LacZ and neomycin resistance genes.

Animal Care and Husbandry

Mice were cared for in accordance with the guidelines set forth by the American Association for Accreditation of Laboratory Animal Care and all the studies were approved and supervised by the Children's National Medical Center Institutional Animal Care and Use Committee (protocol number 247-09-11). Mice were cared and bred in the Research Animal Facility (barrier facility) under controlled temperature (68°F) and a 12 hours light/dark period. They were fed Harlan Tecklad irradiated chow (2018) and sterilized water.

Genotyping and Identification

Newborn pups were identified using tattoo patterns (Ketchum Manufacturing Inc.). Genomic DNA was isolated from tail biopsies with the Puregene Core Kit A (Qiagen). Figure 6A illustrates the strategy used to genotype the pups using the PromegaGoTaq system. The strategy involves a three-primer PCR assay. Primer A (5'-ACTGTCAGAGAAAAGCGCTCAGGA-3') corresponds to a region in the 5' end of the *Nags* gene. Primer B (5'-ACATACACTTCATTCTCAGTATTGTTTTGCC-3') corresponds to a region within the neomycin selection cassette in the knockout allele. Primer C (5'- CTGTTTTTCAGACACATCAGATCCCG-3') is a "common" primer corresponding to a region downstream of the *Nags* gene. The product of Primer A and Primer C is a 1707 bp amplicon, which corresponds to the wild type allele. The combination of Primer B and Primer C produces a 1082 bp amplicon and corresponds to the knockout allele. Following one cycle of denaturation at 95 °C for 5 min, a total of 33 cycles were performed each consisting of 95 °C for 15 sec, 60 °C for 20 sec, and 72 °C for 1 minute. Both alleles were separated by electrophoresis in a 1% agarose gel, and a

depiction of this gel with patterns for wild type, heterozygous, and knockout alleles is show in Figure 6B, with a 1 Kb+ ladder as a reference (Invitrogen). Wild type and heterozygote control DNA were derived from tissue collected from original stock mice with known genotype.

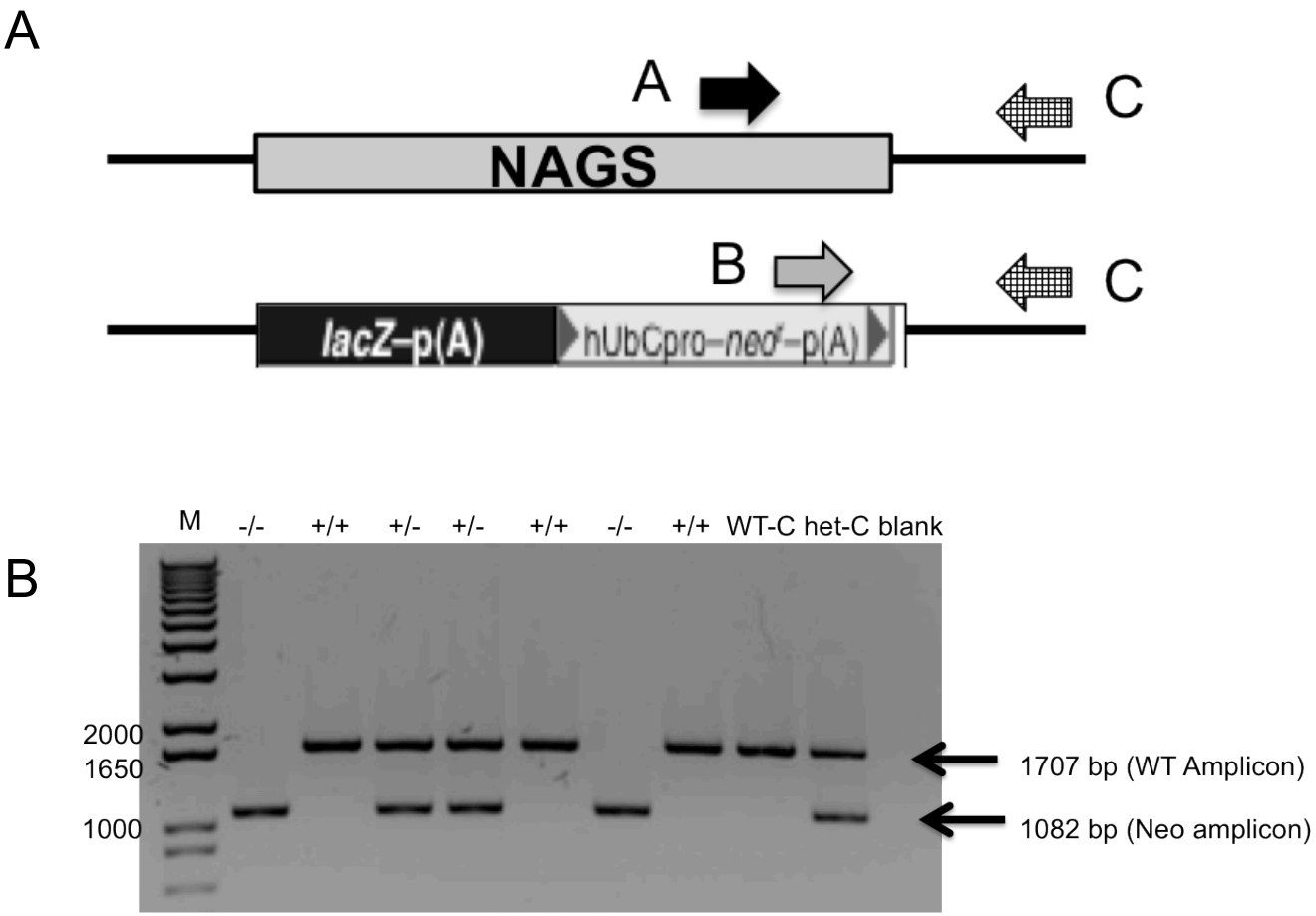

Figure 6. Strategy for genotyping.
(A) The combination of primers A and B and A and C amplifies a 1707 bp fragment from the normal *Nags* allele and a 1082 bp fragment from the targeted *Nags* allele respectively. (B) PCR products that indicate the animals' genotype. Genotype of each sample is shown at the top of each lane (WT-C: wild type control; het-C: heterozygote control sample; M: marker)

Western Blots

Frozen mouse liver was pulverized in liquid nitrogen. Small intestine epithelial cells were isolated according to Evans et al.[97]. Cells were lysed in RIPA buffer (Sigma) containing PhosSTOP protease inhibitor tablets (Roche). Protein concentrations were quantified using Protein Assay dye reagent (Bio-Rad) according to manufacturer's instructions. Proteins in cell lysate were resolved on 10% SDS-polyacrylamide gel, transferred to a nitrocellulose membrane, and blocked in Starting Block (Thermo Scientific) with 0.5% Surfact-Amps 20 (Thermo Scientific). Ten micrograms of total liver protein and 60 μg of small intestinal epithelial protein were used to probe with NAGS antibody (1:5000 dilution of primary rabbit anti-NAGS antibody raised against recombinant mouse NAGS) and HRP-conjugated donkey anti-rabbit secondary antibody (1:50,000) (Pierce). CPS1 was probed in 1 μg of total liver protein and 10 μg small intestinal epithelial protein using rabbit anti-CPS1 primary antibody (AbCam 1:5000) and HRP-conjugated donkey anti-rabbit secondary antibody (Pierce 1:10,000). OTC was probed in 1 μg of total liver protein and 10 μg small intestinal epithelial protein using rabbit primary antibody raised against recombinant ornithine transcarbamylase (OTC) (1:5000) and HRP-conjugated donkey anti-rabbit secondary antibody (Pierce 1:10,000). Protein bands were visualized using Super Signal West Pico kit (Pierce). Tubulin, probed with the anti-tubulin primary antibody (Abcam) at 1:200 dilution followed by goat-anti-rabbit (1:5,000) (Abcam), was used as a loading control. The density of NAGS, CPS1, OTC, and tubulin bands were quantified using a GS-800 calibrated densitometer (Bio-rad) and analyzed with Quantity One software, version 4.5.2 (Bio-rad). NAGS, CPS1, and

OTC bands were normalized against tubulin density and then expressed as a percentage of Wild type control.

Chemical Rescue of Nags-/- mice

Heterozygote breeding pairs were given water supplemented with NCG (1.0 g/L) (Orphan Europe, Paris) and L-citrulline (1.0 g/L) (VWR). *Nags*$^{-/-}$ pups were given daily intraperitoneal injections of NCG and citrulline dissolved in Lactated Ringer's solution starting at birth and continuing until weaning. The initial dose was 250 mg/kg/day for NCG and 1000 mg/kg/day for Cit, and as the animals grew, the dose was tapered to approximately 130 mg/kg/day NCG and 525 mg/kg/day Cit. After weaning (typically 21 days), *Nags*$^{-/-}$ mice were maintained on water supplemented with NCG and Cit (1.0 g/l each).

Plasma Ammonia and Amino Acid Measurements

Plasma was collected into a pre-chilled heparinized syringe from anesthetized mice via heart puncture. The sample was transferred immediately to a pre-chilled heparinized tube and centrifuged at 4^{o}C for 10 min to separate the plasma. The plasma was transferred to cryogenic tubes and immediately frozen in dry ice and stored at -80^{o}C until analysis within 48 hr. Plasma ammonia measurements were performed on a Dade Behring Dimension RXL clinical chemistry system (Dade Behring, Newark, DE), using an adaptation of the glutamate dehydrogenase enzymatic method of van Anken and Shiphorst [98] which substitutes NADPH for NADH, eliminating interference from other NADH-consuming reactions. The reaction was carried out in a Dimension® Ammonia (AMON) Flex reagent cartridge (K863840; Dade Behring, Newark, DE). The disappearance of

NADPH was measured by spectrophotometry.

Amino acid concentrations in plasma were measured by ion-exchange chromatography on a Biochrom amino acid analyzer. Plasma proteins were first precipitated with an equal volume of 7% sulfosalicylic acid and centrifuged for 10 minutes at 13200 rpm. Next, 5 μL of 2.5 N LiOH and 10 μL stock internal standard (S-2-aminoethyl-L-cysteine hydrochloride) were added to 100 μL of plasma supernatant before injection into the analyzer.

Liver Function

Plasma was collected as described above and sent to the Mouse Metabolic Phenotyping Core at Yale University. Plasma levels of alanine aminotransferase (ALT), aspartate aminotransferase (AST), alkaline phosphatase (ALP), and blood urea nitrogen (BUN) were conducted on the Roche COBAS Mira Plus automated chemistry analyzer.

Statistical Analysis

All statistical analyses were performed using Prism software, version 5 (GraphPad, San Diego, CA). The minimal level of confidence at which experimental results were considered significant was $p<0.05$. Statistical significance of differences in weight gain among the strains and between their amino acid levels was determined by a two-way ANOVA with Bonferroni posttest analysis. Statistical significance of differences in ammonia concentrations was determined by one-way ANOVA with Bonferroni posttest analysis. Analysis of genotype segregation from heterozygous matings was performed using a Chi-squared test. In all cases, data is presented as the mean ± SEM. In all figures, $p<0.05$,*; $p<0.01$,**; $p<0.001$,***; $p<0.0001$,****.

Results

Breeding of Mice

C57Bl/6N mice, heterozygous for the disrupted *Nags* allele (*Nags*$^{+/-}$) were crossed to obtain homozygote animals. After several litters, we observed that the average litter size was 6.5 pups, but overall survival rate of the pups was only 45% in these crossings, as mothers were not taking care of their pups. We also observed an increased incidence of birth defects due, possibly, to the inbreeding of the strain used to develop these mice. Therefore, *Nags*$^{+/-}$C57BL/6N mice were subsequently crossed with wild-type mice of the Swiss-Webster strain to increase the genetic heterogeneity. SW;B6-Nags$^{tm1(KOMP)Vlcg}$ heterozygous females were able to produce larger litters and maintain them, with an average litter size of 7.9 pups and overall survival rate of 87%, thus markedly reducing confounding factors with respect to survival and health of the pups (Figure 7A and 7B). No birth defects were observed using SW;B6-Nags$^{tm1(KOMP)Vlcg}$ heterozygous mice for crossing. Pups were genotyped within 48 hours of birth by PCR (Figure 6A and 6B).

NAGS deficiency is the most rare urea cycle disorder, with only 34 reported patients from 28 families worldwide. Our initial hypothesis was that NAGS deficiency could lead to *in utero* lethality, resulting in a lower number of children born with this disease. In order to determine if NAGS deficiency causes *in utero* lethality, the genotypes of offspring from 11 liters (127 pups) of heterozygote crosses were analyzed. This revealed that the genotypes of offspring were consistent with the

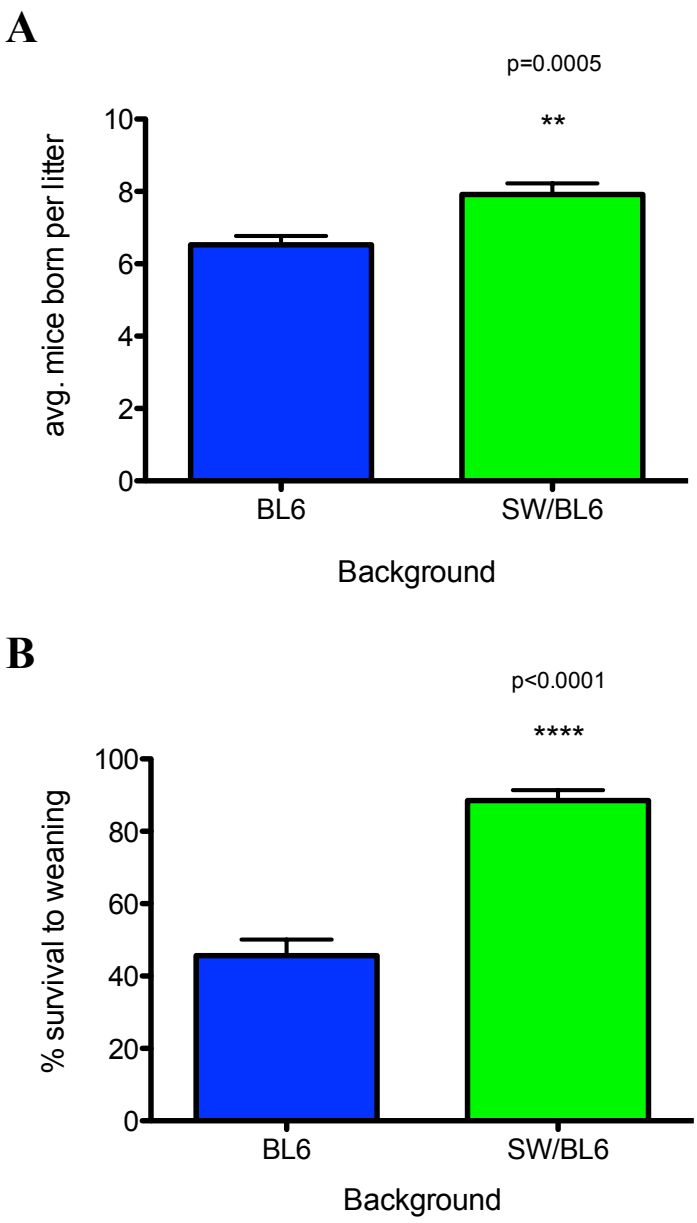

Figure 7. SW;B6-Nags$^{tm1(KOMP)Vlcg}$ heterozygous females produce larger litters (A) and successfully maintain them better (B) compared to inbred *Nags*$^{+/-}$C57BL/6N mice.

Nags$^{+/-}$C57BL/6N were mated with Wild Type Swiss Webster mice to produce a hybrid strain. *Nags*$^{+/-}$C57BL/6N n= 82 litters; SW;B6-Nags n= 60 litters. Statistical significance was calculated via t-test comparing BL6 vs. SW/BL6.

expected Mendelian inheritance (1:2:1) (X^2= 0.890, df=2, p=0.6409) indicating improbable *in utero* lethality of *Nags*$^{-/-}$ mice when the mothers are maintained on NCG and Cit supplementation in the drinking water (Table 1A). Based on this observation, it was hypothesized that the NCG/cit supplementation during the pregnancy benefits the *Nags*$^{-/-}$ fetuses, resulting in normal *in utero* health and development. In order to test this hypothesis, heterozygotes were mated without NCG/cit supplementation to the pregnant females. Collection of pups was performed prior to birth (E14) to prevent the loss of pups following birth. Analysis of the offspring from 4 litters (29 pups) from these crosses revealed that the genotypes were still consistent with the expected Mendelian inheritance pattern of 1:2:1 (X^2= 3.897, df=2 p=0.1425) (Table 1B). Therefore, we can conclude that *Nags*$^{-/-}$ mice remain healthy *in utero*, due to the mother's circulatory system detoxifying excess ammonia produced by the fetuses. It is only after birth that the *Nags*$^{-/-}$ mice require supplementation to promote ureagenesis. Additionally, *in utero* lethality is not a contributing factor in the extreme rarity of this disease.

A

Genotype	Observed	Expected	P value
Nags$^{+/+}$	32	31.75	0.6409
Nags$^{+/-}$	59	63.5	
Nags$^{-/-}$	36	31.75	
Total	127	127	

B

Genotype	Observed	Expected	P value
Nags$^{+/+}$	3	7.25	0.1425
Nags$^{+/-}$	19	14.5	
Nags$^{-/-}$	7	7.25	
Total	29	29	

Table 1. Progeny from heterozygous mating.
(A) Progeny of *Nags*$^{+/-}$ mice where mother was supplemented with NCG during pregnancy. Analysis was done on 127 mice from 11 litters (χ^2= 0.890 df=2 p=0.6409). (B) Progeny of *Nags*$^{+/-}$ mice were mother was not supplemented with NCG during pregnancy. Analysis was done on 29 pups from 4 litters (χ^2= 3.897, df=2 p=0.1425).

Analysis of the NAGS protein in the liver and small intestine was performed by Western blotting. The analysis confirmed the genotypes, showing absence of NAGS in these organs in *Nags*$^{-/-}$ mice. The abundance of NAGS protein in the liver and small intestine of *Nags*$^{+/-}$ mice ranged between 50-70% and 15-25% respectively, of *Nags*$^{+/+}$ littermates (Figure 8). This confirms that *Nags* disruption abolishes its expression in both the liver and small intestine. Expression of the remaining mitochondrial urea cycle enzymes, CPS1 and OTC, in both the liver and small intestine were similar in *Nags*$^{-/-}$, *Nags*$^{+/-}$ and *Nags*$^{+/+}$ littermates (Figure 9).

Biochemical Rescue of Nags$^{-/-}$ *Mice*

Heterozygote breeding pairs were supplemented with NCG (1.0 g/l) and Cit (1.0 g/l) in the drinking water. This ensured that *Nags*$^{-/-}$ fetuses received NCG and Cit during *in utero* development. However, supplementation of heterozygous pregnant females with NCG and cit proved to be insufficient to rescue the newborn *Nags*$^{-/-}$ pups and they died within 24-48 hours of birth if no other intervention was initiated (Figure 9). This suggested that insufficient NCG and/or Cit was transferred to the pups via the mother's milk to mitigate the enzyme deficiency and resulting hyperammonemia. To improve delivery of the rescue chemicals, homozygous pups were administered by intra-peritoneal injection of NCG and Cit dissolved in Lactated Ringer's solution within a few hours following birth and continuing once every day until weaning. The initial dose was 250 mg/kg/day NCG and 1000 mg/kg/day Cit, and as the animals grew, the dose was tapered to approximately 130 mg/kg/day NCG and 525 mg/kg/day Cit. The dosage for mice was determined based based on dose per weight recommendation for NAGS deficient patients [32].

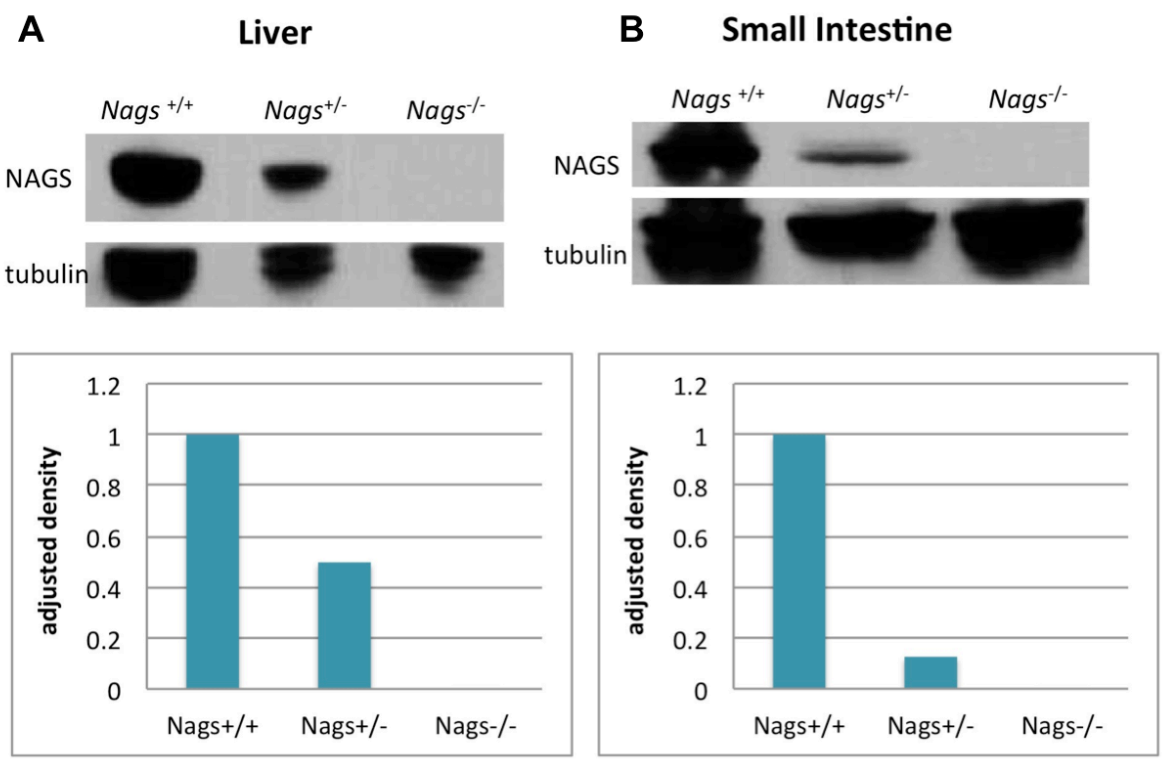

Figure 8. NAGS is absent in the liver (A) and small intestine (B) of *Nags*$^{-/-}$ mice. 10 µg of liver protein and 60 µg of small intestine protein were loaded in each lane to detect expression of NAGS protein in *Nags*$^{+/+}$, *Nags*$^{+/-}$, and *Nags*$^{-/-}$ mice. Densitometry analyses of the blots are shown. Data were normalized to the tubulin protein and then expressed as a fraction of the respective protein in the wild type (*Nags*$^{+/+}$) mice. Immunoblots represent one blot that is representative of the results obtained by three separate experiments.

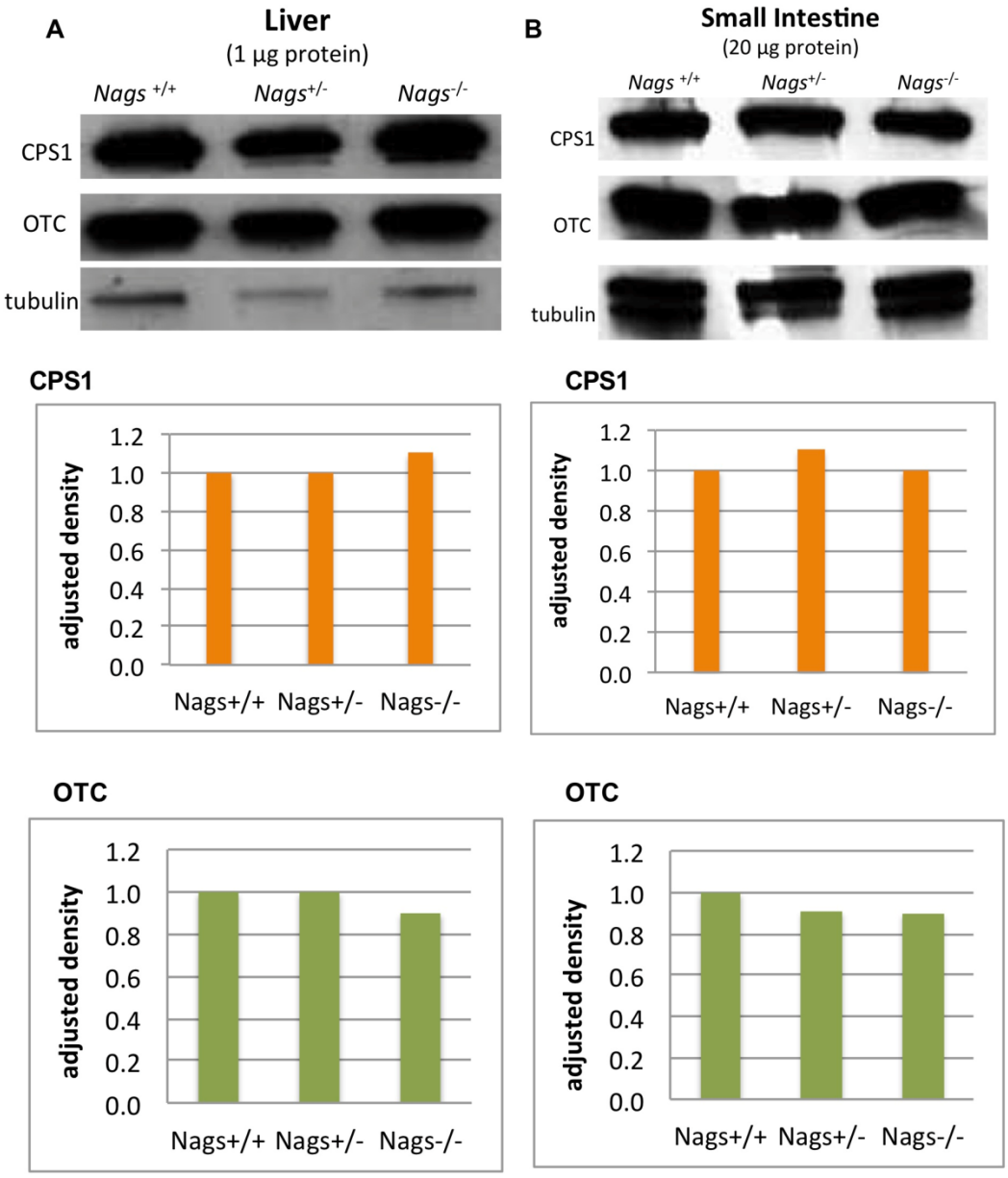

Figure 9. Western blots of CPS1 and OTC in liver (A) and small intestine (B). 1 µg of liver protein and (B) 20 µg of small intestine protein were loaded in each lane to detect expression of CPS1 and OTC proteins in *Nags* $^{+/+}$, *Nags*$^{+/-}$, and *Nags*$^{-/-}$ mice. Corresponding densitometry analyses of the blots are shown. Data were normalized to the tubulin protein and then expressed as a fraction of the respective protein in the wild type (*Nags*$^{+/+}$) mice. Immunoblots represent one blot that is representative of the results obtained by three separate experiments.

The addition of Cit to the treatment regimen enhanced survival of the mice. Without Cit, approximately 50% of the *Nags*$^{-/-}$ pups died before weaning, while the NCG plus Cit supplement increased survival to 85% (Figure 10). After weaning (typically 21 days), homozygous pups were switched to supplementation with NCG plus Cit in the drinking water, which had proved sufficient for survival to adulthood and reproduction. Our decision to supplement with citrulline was based on studies describing the ornithine aminotransferase (OAT) knockout mouse [99]. In neonatal mice, OAT is responsible for producing ornithine from glutamate. The deletion of OAT results in hypoornithinaemia and lethality, which is rescuable by arginine supplementation. Since urea cycle patients often display low plasma arginine, we decided to supplement these mice with citrulline, as it is an immediate precursor for arginine.

In order to investigate the dependency on NCG plus Cit in the adult period, 6-week-old male and female mice were given water with various combinations of supplements. Mice on water alone died within 24 hours, and mice drinking water with only Cit supplementation died within 24-48 hours (Figure 11). Mice given water with NCG only or NCG/Cit were monitored for survival over a 30-day period. At the end of 14 days, 50% of the mice on NCG alone were alive, whereas 89% of the mice on NCG/Cit supplementation were alive (Figure 11). These results indicate that while Cit is not absolutely required in the adult period, it does serve a beneficial role in overall health and survival of the *Nags*$^{-/-}$ mice. Based on the concentration of NCG and Cit that was provided, a 25 g mouse would consume approximately 150 mg/kg/day of NCG and Cit. This dosage is within the range of the standard dosage recommended for patients.

Appearance of Nags$^{-/-}$ Mice

At birth, *Nags*$^{-/-}$ mice are indistinguishable from their heterozygous and wild type littermates. As *Nags*$^{-/-}$ neonates age, a subtle phenotype arises. *Nags*$^{-/-}$ mice have less fur compared to their *Nags*$^{+/-}$ littermates (Figure 12). However, this phenotype is not present in every homozygote, and is more obvious in mice with white fur. Some homozygotes may develop a full coat of fur as they age. As a result, distinguishing homozygotes by fur pattern is not reliable. Fur abnormalities are also seen in the two partial OTC deficiency mouse models, OTC^{spf} and OTC$^{spf\text{-}ash}$ [69,71] suggesting perhaps that this phenotype is related to Cit or arginine deficiency as proposed previously [100]. In order to determine if *Nags*$^{-/-}$ mice have growth defects, litters were weighed daily until weaning. Overall, the weight of rescued *Nags*$^{-/-}$ mice was lower ($p<0.01$) during the pre-weaning period compared to their *Nags*$^{+/-}$ and *Nags*$^{+/+}$littermates (Figure 13).

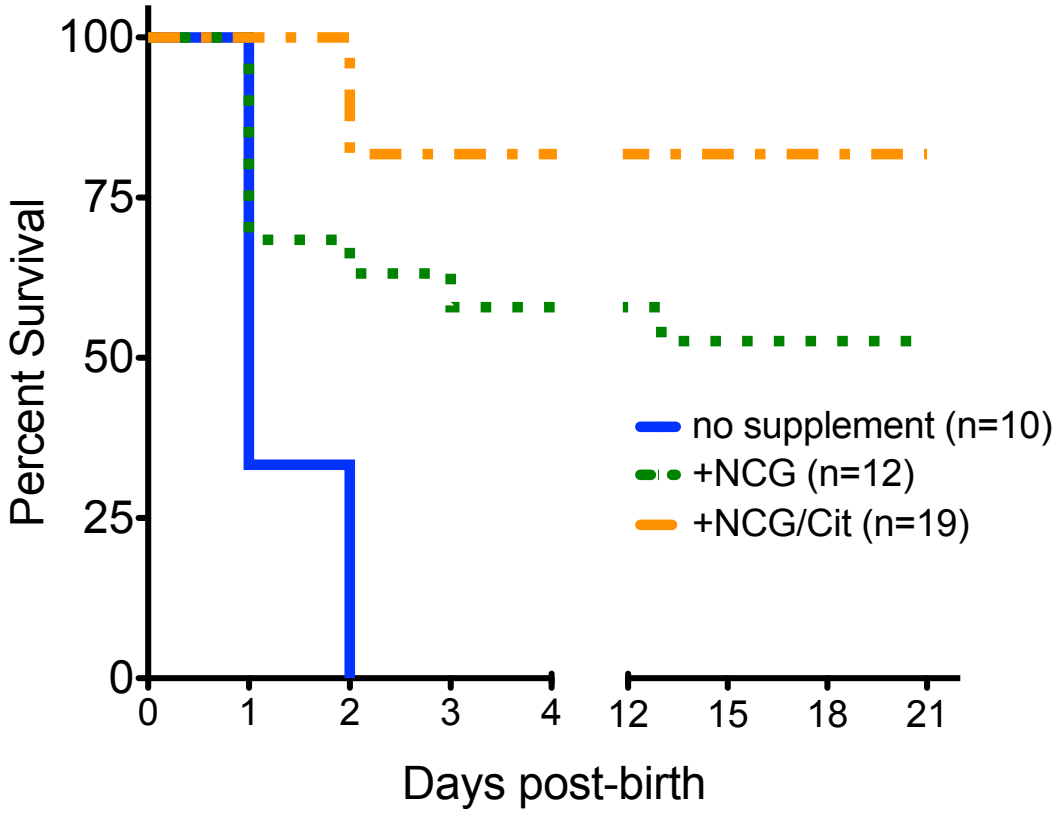

Figure 10. Biochemical rescue of *Nags*$^{-/-}$ pups.
(A) Kaplan-Meier survival curves of pups on and off NCG ± Cit treatment. *Nags*$^{-/-}$ pups were given either no supplementation or intra-peritoneal injections of NCG or NCG/cit daily starting at birth and assessed for survival.

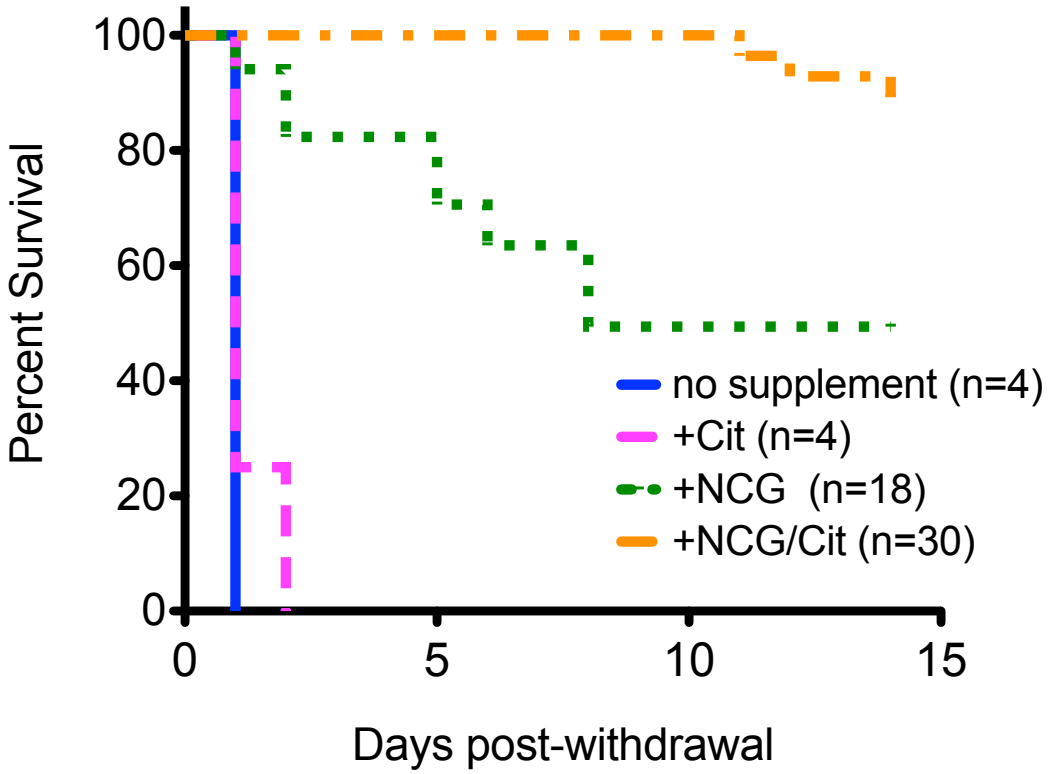

Figure 11. Biochemical rescue of *Nags*$^{-/-}$ mice after weaning.
Kaplan-Meier survival curves of six-week-old mice were given different supplements in water (NCG, Cit, or NCG/Cit).

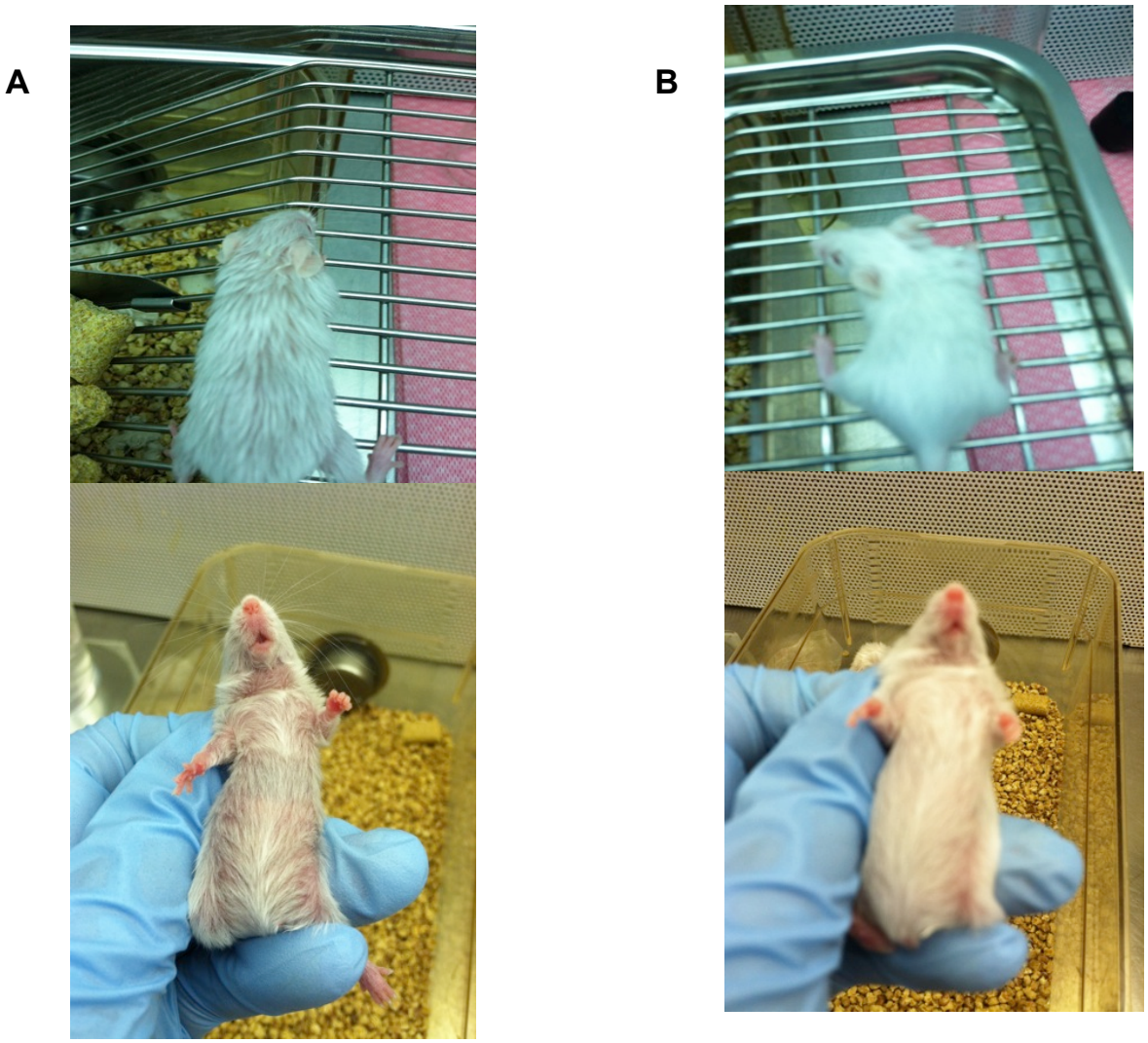

Figure 12. Phenotype of *Nags*$^{-/-}$ mice.
Outward phenotype of 6-week-old *Nags*$^{-/-}$ (A) and its *Nags*$^{+/-}$ (B) littermate.

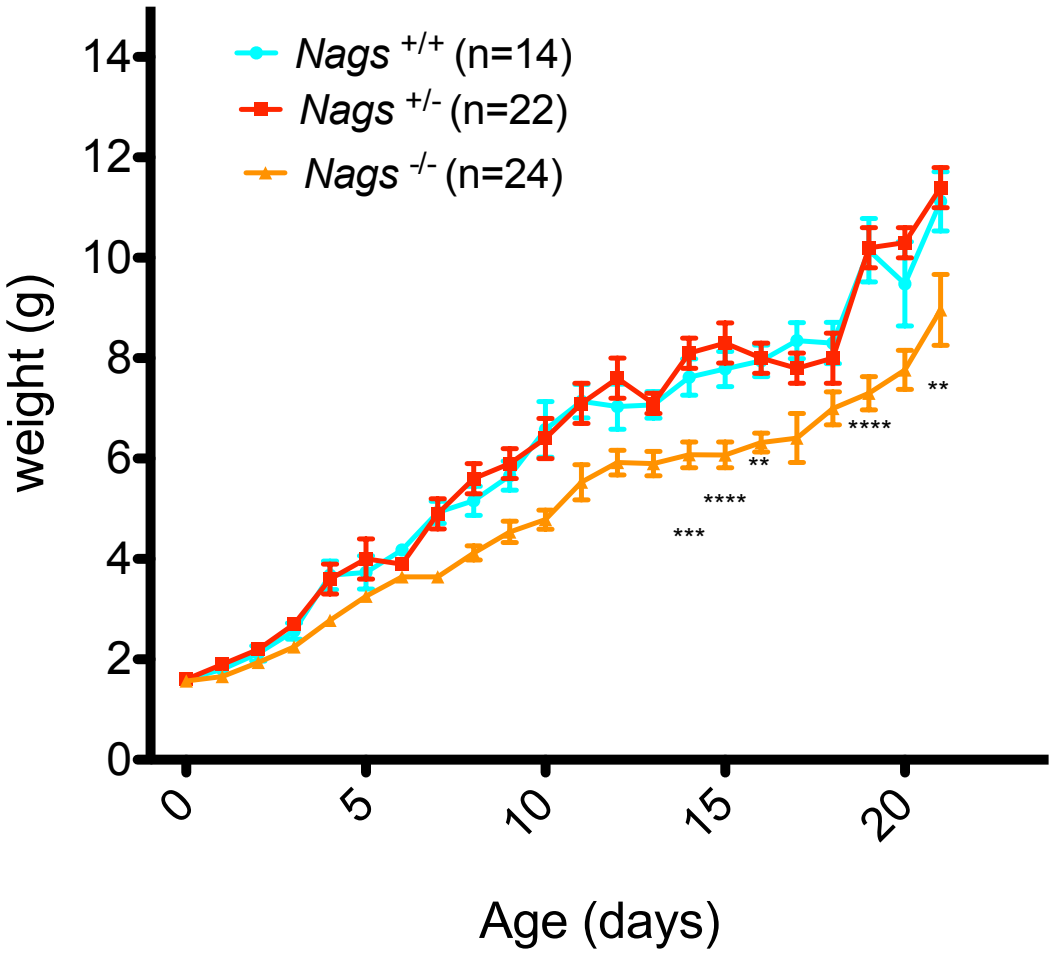

Figure 13. Growth of *Nags*$^{-/-}$ mice.
Nags$^{+/+}$, *Nags*$^{+/-}$, and *Nags*$^{-/-}$ mice were weighed daily during the pre-weaning period. Weight differences were analyzed using a two-way ANOVA followed by a Bonferroni post-test.

Metabolic Phenotype of Nags$^{-/-}$ Mice

NCG and Cit were withdrawn from 2-month-old *Nags*$^{-/-}$ mice in the evening prior to the dark period. Behavior related to hyperammonemia was assessed according to the scoring system outlined in Ye, X et al [101]. Mice were sacrificed when they showed symptoms of severe hyperammonemia (lethargy, seizures, lying on side, decerebrate posture). All *Nags*$^{-/-}$ mice deprived of NCG and Cit supplements developed signs of severe hyperammonemia, however time of onset of symptoms was variable ranging from 10 to 28 hours. Plasma ammonia levels did not differ between *Nags*$^{+/+}$, *Nags*$^{+/-}$, and *Nags*$^{-/-}$ littermates when NCG and NCG/Cit treatments were given. However, *Nags*$^{-/-}$ mice deprived of NCG/Cit supplements displayed plasma ammonia levels in the range of 1000-3000 μmol/L (approximately 10-fold higher than their littermates, $p<0.0001$), confirming that the development of severe hyperammonemia following treatment withdrawal is a characteristic of these mice and can be measured using methods similar to human subjects (Figure 14).

Plasma was also analyzed to determine the effect of NCG plus Cit supplementation on amino acid concentrations. *Nags*$^{+/+}$, *Nags*$^{+/-}$, and *Nags*$^{-/-}$ mice given NCG/Cit supplementation had similar plasma amino acid levels, except for higher plasma glutamate in the *Nags*$^{-/-}$ mice ($p<0.0001$) (Figure 15A). Hyperammonemic (NCG/Cit deprived) *Nags*$^{-/-}$ mice exhibited lower concentrations of plasma arginine, citrulline, ornithine, proline (Figure 15A) and alanine ($p<0.0001$) (Figure 15C), and elevated glutamine ($p <0.0001$), glutamate (Figure 15A), and lysine ($p <0.0001$), compared to healthy controls. (Figure 15C). All other amino acids (Figure 15C), including branched chain amino acids (Figure 15B), remained unchanged compared to healthy controls.

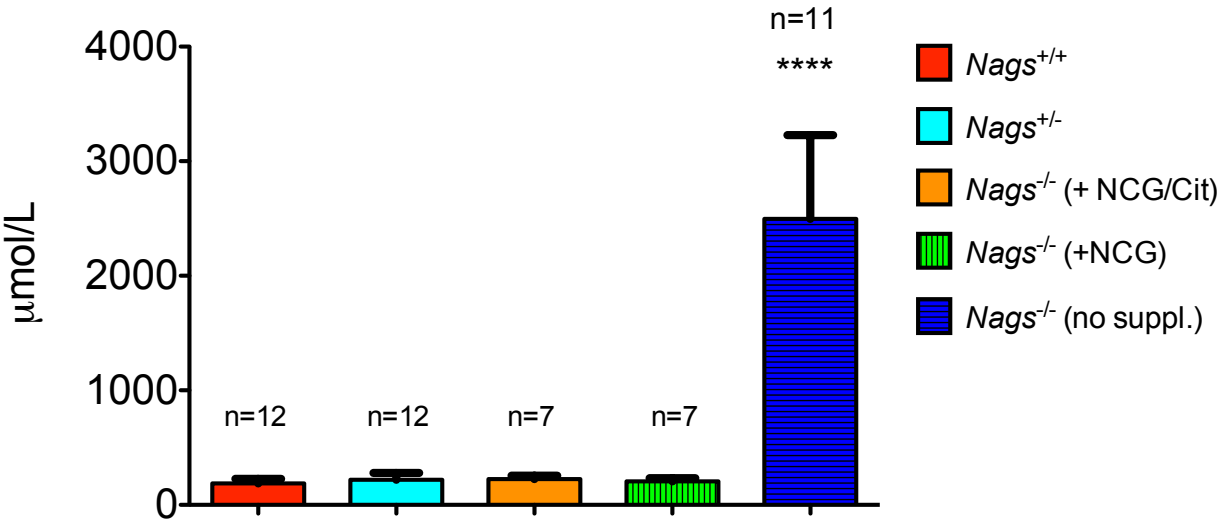

Figure 14. Ammonia levels of *Nags*$^{-/-}$ mice.
(A) Plasma ammonia levels in *Nags* mice were measured following withdrawal of NCG and citrulline from *Nags*$^{-/-}$ mice. Plasma was collected when *Nags*$^{-/-}$ mice showed symptoms of severe hyperammonemia (lethargy, seizures, lying on side, decerebrate posture). *Nags*$^{+/+}$, *Nags*$^{+/-}$, and supplemented *Nags*$^{-/-}$ mice were used as controls. Data were analyzed using a one-way ANOVA with Bonferroni post-test, ($p<0.0001$,****).

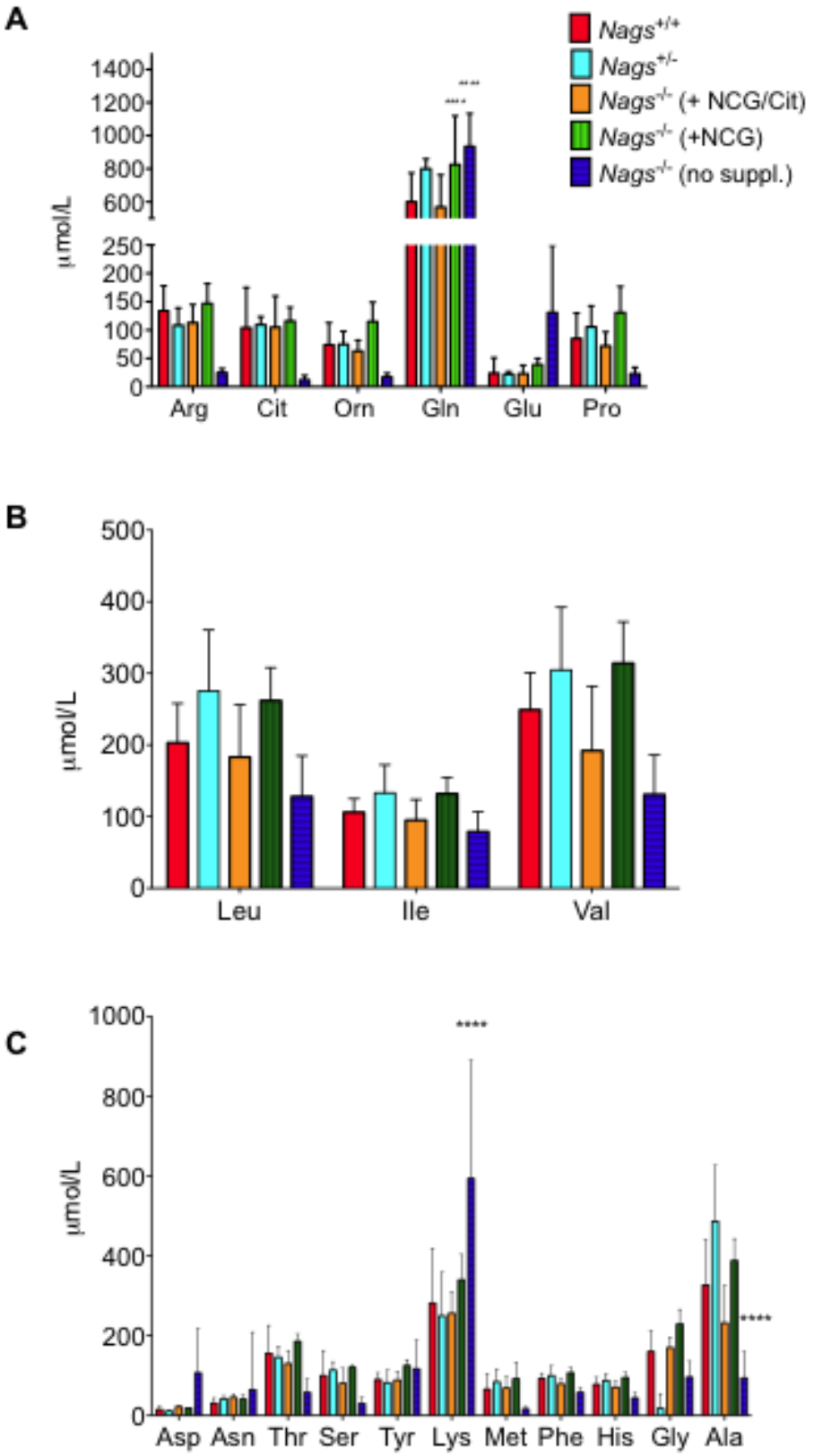
A
Nags+/+
Nags+/-
Nags-/- (+ NCG/Cit)
Nags-/- (+NCG)
Nags-/- (no suppl.)
µmol/L
1400
1200
1000
800
600
250
200
150
100
50
0
****
***
Arg
Cit
Orn
Gln
Glu
Pro
B
µmol/L
500
400
300
200
100
0
Leu
Ile
Val
C
µmol/L
1000
800
600
400
200
0
****
****
Asp
Asn
Thr
Ser
Tyr
Lys
Met
Phe
His
Gly
Ala

Figure 15. Amino acid panel of *Nags*$^{-/-}$ mice.
Plasma concentrations of (A) urea cycle related amino acids, (B) branched chain amino acids, (C) other amino acids. Plasma was collected when *Nags*$^{-/-}$ mice showed symptoms of severe hyperammonemia (lethargy, seizures, lying on side, decerebrate posture). *Nags*$^{+/+}$, *Nags*$^{+/-}$, and supplemented *Nags*$^{-/-}$ mice were used as controls. Graphs show mean ± SEM. Statistical significance was analyzed using a two-way ANOVA followed with Bonferroni post-test ($p<0.0001$,****), comparing to wild type mice. *Nags*$^{+/+}$ n=12, *Nags*$^{+/-}$ n=12, *Nags*$^{-/-}$ (NCG/cit) n=7, *Nags*$^{-/-}$ (+NCG) n=7, *Nags*$^{-/-}$ (no supplement) n=11.

Lastly, it was of interest to establish whether NAGS deficiency contributes to liver damage since liver damage has been reported in urea cycle disorders, including liver necrosis and abnormal mitochondria in ASS deficiency [102], mitochondrial abnormalities in OTC and CPS1 deficiency [103, 104], and fibrosis in females with partial OTC deficiency. As an indicator of liver damage, plasma aspartate aminotransferase (AST), alanine aminotransferase (ALT), alkaline phosphatase (ALP), and blood urea nitrogen (BUN) were measured. AST, ALT, and ALP are liver enzymes and their presence in the plasma is an indication of hepatocellular damage. BUN is a measurement of nitrogen levels in the blood; an elevated BUN can indicate kidney damage if the kidney is not excreting urea, while a decreased BUN may indicate liver damage or a block in the urea cycle (not producing urea). We compared the levels of these four indicators in healthy, 6-week-old *Nags*$^{-/-}$ mice to that of wild type litter mates. For all four, levels are identical suggesting that *Nags*$^{-/-}$ deficiency is likely not contributing to liver damage in mice (Figure 16).

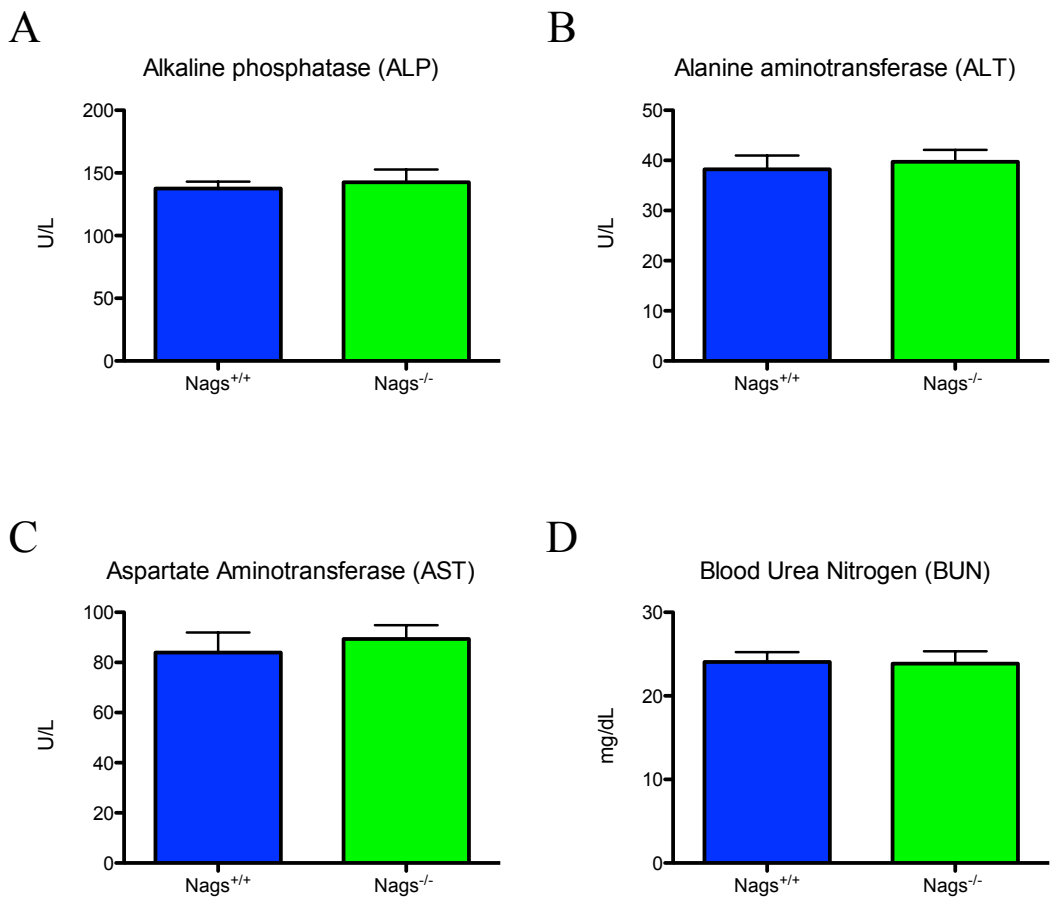

Figure 16. Liver function tests in Wild Type and *Nags*$^{-/-}$ mice.
Plasma levels of alanine aminotransferase (A), aspartate aminotransferase (B), alkaline phosphatase (C), and blood urea nitrogen (D) were analyzed on a Roche COBAS Mira Plus automated chemistry analyzer. (*Nags*$^{+/+}$, n=14, *Nags*$^{-/-}$, n=14)

Discussion

Using gene transfer techniques of null alleles available through KOMP, we produced a knockout mouse model of hyperammonemia due to complete NAGS deficiency. Genotypic analysis of the progeny from mating between *Nags*$^{+/-}$ mice revealed Mendelian segregation of the *Nags* null allele, thus excluding increased embryonic lethality in this model. Therefore, a potential role of NAGS in fetal development [32] seems unlikely to explain the extreme rarity of the NAGS deficiency in humans. *Nags*$^{-/-}$ mice lack NAGS protein in both the liver and small intestine (Figure 8). Thus, when this gene is absent, ureagenesis and *de novo* citrulline and arginine production do not occur resulting in neonatal death of *Nags*$^{-/-}$ pups unless they are rescued (Figure 10). Fortunately, *Nags*$^{-/-}$ mice could be rescued with a combination of NCG and Cit administration, where we obtained an 85% success rate in rearing homozygous pups to weaning and subsequently to reproduction. Since *Nags*$^{+/+}$ and *Nags*$^{+/-}$ pups did not die following injections with NCG/Cit, we believe that the 15% loss in the neonatal period for *Nags*$^{-/-}$ pups relates to NAGS deficiency in spite of rescue therapy. It is possible, that the stress of daily intra-peritoneal injections could have contributed to this loss. A portion of this 15% loss includes smaller newborn mice that died within 10-15 days after birth. Whether larger dosages of NCG and citrulline mitigates this low early lethality in all or a portion of these mice requires further testing.

The requirement for NCG/Cit supplementation for survival of *Nags*$^{-/-}$ mice continues into adulthood, since they become hyperammonemic within hours following withdrawal of NCG/Cit from the drinking water. If not supplemented with NCG/Cit, the *Nags*$^{-/-}$ mice experience a 10-fold increase in ammonia levels within one to two days

(Figure 14) similar to the phenotype reported in other mouse models with complete deficiency of other urea cycle genes that cannot be salvaged [75,78-80,105], as well as the ornithine aminotransferase (OAT) knockout mouse when not supplemented with arginine during the neonatal period [99]. Although the addition of Cit does not seem to be absolutely essential for survival of the *Nags*$^{-/-}$ mice, it appears to serve a beneficial role, as 50% of adult *Nags*$^{-/-}$ mice treated with only NCG in drinking water die within 14 days (Figure 11), compared to only 11% death if treated with NCG/Cit. Among the tests that were performed, the only significant difference found between *Nags*$^{-/-}$ mice on NCG vs. NCG/Cit is elevated plasma glutamine level in mice supplemented with NCG only (Figure 15A), suggesting some increase in nitrogen load in these animals [106,107]. However, these mice did not display reduced plasma arginine or Cit, nor did they manifest hyperammonemia when tested randomly (Figure 14). Although arginine is a semi-essential amino acid, it is required for biosynthesis of creatine, ornithine, glutamine, proline, and polyamines [108]. Arginine also serves a role in signaling functions, acting as the substrate for nitric oxide production [108] and in wound healing [109,110] and thus supplementation is recommended after physical stress such as post-surgery or trauma [111,112].

In humans, NCG is the standard treatment for NAGS deficient patients [38,55,69,75,79,80,93-95,113]. We chose a regimen of NCG and Cit based on a study by Kim et al. [52,75], where an intra-peritoneal injection of NCG and arginine protected rats against lethal doses of ammonia. We adapted the dosage plan based on information on patient dosages [32,54]. Additionally, in a mouse model of OAT deficiency, arginine injections every 12 hours over the newborn period were necessary to compensate for a

neonatal arginine deficiency [99]. We believed that Cit would be more efficient in this regard since arginine is rapidly degraded in the liver as a result of a high arginase activity [96,108] while citrulline bypasses the liver and is converted to arginine by the kidneys [27].

We have evidence suggesting that adult *Nags*$^{-/-}$ mice exhibiting early signs of hyperammonemia can be rescued with an intra-peritoneal injection of NCG/Cit (data not shown). This observation suggests that their hyperammonemia could be reversed upon early intervention, which should allow for more controlled studies of the recovery of the brain from hyperammonemia. The *Nags*$^{-/-}$ mouse represents the first mouse model in which hyperammonemia can be prevented by chemical intervention and induced with the removal of the chemical. The creation of this mouse will allow for the study of global effects of hyperammonemia, in particular the effects on the central nervous system. It should also prove useful as a model for the study of liver gene therapy in complete urea cycle disorders, which would be challenging in animals with complete enzyme deficiency that die during the neonatal period.

Chapter 3: Use of a Home Cage Monitoring System to Define the Chronology of Behavioral Change during Hyperammonemia

Introduction

Hyperammonemia is a metabolic disease state characterized by the excess of ammonia in blood. Ammonia is a source of nitrogenous waste that results from the catabolism of dietary and body proteins. Hyperammonemia occurs when there is an impaired capacity to detoxify ammonia; for example, in the case of urea cycle disorders, organic acidemias, cirrhosis, certain surgeries, Reye syndrome, drug overdose, or chemotherapy [1,114]. Hyperammonemia leads to clinical symptoms such as loss of appetite, vomiting, lethargy, seizures, neurological damage, coma, and potentially death if untreated [32,115]. Current treatments for hyperammonemia include dialysis [116], ammonia scavenging drugs, and complete removal of protein from the diet [10].

Recently we described the creation of a NAGS deficient mouse (*Nags*$^{-/-}$) a novel model of hyperammonemia [117]. Until the creation of this mouse, all other mouse models of urea cycle disorders have been unsuccessful in studying hyperammonemia due to neonatal lethality [43]. However, NAGS deficiency symptoms can be eliminated with the administration of the FDA approved compound, N-carbamyl-L-glutamate (NCG), a functional analog of NAG. Thus, the *Nags*$^{-/-}$ mouse is treated with NCG starting at birth where it survives to adulthood and reproduces. The availability of this mouse model with a severe urea cycle defect capable of being salvaged by a biochemical intervention has the potential to enhance research into various aspects of hyperammonemia and ureagenesis.

Early detection and therapy of hyperammonemia is important, as it decreases the risk of permanent brain damage. However, the earliest symptoms in mice are difficult to detect. In our previous study [117], we used a scoring system developed by Ye, et al [101], and sacrificed mice when they showed signs of severe hyperammonemia including lethargy, decerebrate posture, lying on their side, and seizures. The ability to define a behavioral biomarker indicative of early hyperammonemia would make possible the investigation of early neurological effects of hyperammonemia, and how the neurological effects relate to clinical symptoms observed in patients. Moreover, early detection of clinical hyperammonemia in this mouse model would allow for testing of interventions to treat hyperammonemia without resorting to death as an endpoint. In this current study, two activity-monitoring systems were employed to analyze the behavior of *Nags-/-* mice during a healthy, treated state, and during hyperammonemia following the removal of the rescue chemicals, NCG and Cit.

Materials and Methods

Animal Husbandry

Animals were housed at Children's National Medical Center and the Veterans Affairs Animal Research Facility and all protocols were approved by The Children's National Medical Center and V.A. IACUC, Washington, DC. Mice were checked daily for signs of distress and were maintained on a 12:12-h light–dark cycle in a low-stress environment (22 °C, 50 % humidity and low noise) and given food and water ad libitum.

The creation of the *Nags*$^{-/-}$ has been previously described[117]. *Nags*$^{-/-}$ pups were given daily intraperitoneal injections of NCG and Cit dissolved in Ringer's lactate solution starting at birth and continuing until weaning. The initial dose was 250

mg/kg/day for NCG and 1000 mg/kg/day for Cit, and as the animals grew, the dose was tapered to approximately 130 mg/kg/day NCG and 525 mg/kg/day Cit. After weaning (typically 21 days), *Nags*$^{-/-}$ mice were maintained on water supplemented with NCG and Cit (1.0 g/l each). For the purposes of these studies, wild type mice were given NCG/cit supplementation for a 2-week period before the experiments were conducted.

Voluntary Wheel

Seven *Nags*$^{-/-}$ and 8 wild type littermate mice of 6 weeks of age were housed individually in cages equipped with a running wheel. Wheel running activity was monitored by an on-line PC connected to the Minimitter Running Wheel activity system via a magnetic switch on the wheels. This system consists of QA-4 activity input modules, DP-24 dataports and Vital View data acquisition system (MiniMitter Company, Inc. Sunriver OR vers. 4.1) [118-120]. Wheel revolutions were collected continuously and binned into 60-minute intervals. Mice were allowed to acclimate to the system for 24 hours prior to data collection. Data was collected for 24 hours beginning at 10:00 AM, while mice were supplemented with NCG/Cit; after the initial 24-hour period, NCG/Cit supplementation was removed (at 10:00 AM) and data was collected for another 24 hours. Based on a wheel with a 14.13-inch circumference, one wheel revolution is equal to 0.36 meters. The number of wheel turns per hour was multiplied by 0.36 to determine distance in meters run per hour.

Home Cage Monitoring

We used the Home Cage Scan system from CleverSys [121-125] consisting of 4 cameras simultaneously monitoring 4 mice individually housed in separate cages on a

12:12 light: dark cycle. The cage environment was lit by white lights from 6 AM to 6 PM and infrared lights from 6 PM to 6 AM. The computer software allows the researcher to calibrate the cage, providing software with information about the cage environment such as the top/bottom of cage, height of bedding, placement of drinking spout, and food bin areas. The software then uses this information to recognize the animal and behavior in durations greater than 6 frames (30 frames/sec).

Eight 6-week-old *Nags*$^{-/-}$ and eight aged-matched wild-type controls were used for this study. Mice were housed with minimal bedding to minimize mounding, which can obscure the mouse during recording. Mice were acclimated to their cages and the environment for 48 hours prior to the study and were recorded for 23 hours beginning at 10:00 AM. Mice remained on NCG/Cit supplemented water for the first 23 hours. After the first 23 hours, the NCG/Cit supplemented water was replaced with regular water before the next 23 hours of recording. Recording of behavior lasted for 23 hours in order to give the researcher time to change the water and recalibrate the cages so that day 2 recording could also start at 10:00 AM. Random bouts of movies were inspected after the experiment to determine the accuracy of the behaviors called by the recognition software. Incorrect behaviors were manually changed by the researcher. Results are presented as the average percent of time where a given behavior was observed.

The information provided by the software provides the researchers with approximately 20 different behaviors. We chose to group some of these behaviors into seven categories for data analysis. The software recognizes and distinguishes the behaviors rear up, come down from partially reared, come down to partially reared, rear up from partially reared, rear up to partially reared, remain reared up, and remain partially

reared, which we grouped as “Rear up”. “Hanging” regroups the behaviors hang cuddled, hang vertical from hang cuddled, remain hang vertical, and remain hang cuddled as defined by the software. “Eat” regroups the software distinguished behaviors eat and chew. “Walk” regroups the software distinguished behaviors walk left, walk right, and walk slowly. “Sleep/no activity” regroups the software distinguished behaviors sleep and remain low (Table 2).

Mouse behaviors defined by Home Cage Scan program:	**Grouped by researcher for analysis as:**
Rear Up	Rear Up
Come down from partially reared	
Come down to partially reared	
Rear up to partially reared	
Remain reared up	
Remain partially reared	
Hang cuddled	Hanging
Hang vertical from hang cuddled	
Remain hang vertical	
Remain hang cuddled	
Eat	Eating
Chew	
Drink	Drinking
Walk left	Walking
Walk right	
Walk slowly	
Groom	Grooming
Sleep	Sleeping/no activity
Remain low	

Table 2. Home Cage System generated behaviors were grouped into seven categories for behavioral analysis.
The Home Cage System software can distinguish over 20 different mouse behaviors. Nineteen of these specific behaviors were grouped into seven general categories: rear up, hanging, eating, drinking, walking, grooming, and sleep/no activity for behavioral analysis as shown in Figures 19 and 20.

Results and Discussion

Voluntary Wheel

We first measured running activity in mice placed in cages with voluntary wheels. The voluntary wheel is a popular assessment of activity measurement in mice, as rodents are known to run a considerable distance, up to 5-6 km per day when placed in cages with a running wheel[126]. In this experiment, mice were introduced to the running wheel for 24 hours prior to the beginning of data collection. On day 1, both wild type and *Nags-/-* mice were monitored for 24 hours while on NCG/Cit supplement. There is no significant difference in the running wheel activity of these two genotypes. In both cases, they exhibited high activity at the beginning of the experiment, decreased their running activity approximately 7-8 hours into the study, and then increased their running activity again 17-18 hours into the study (Figure 17). This experimental set up does not provide other behavioral data, such as when they were hanging from the cage, eating, or grooming. Therefore, there is no way to determine what behaviors the mice were performing when not running. For example, mice are known to do the majority of their eating in the early evening hours.

Following NCG/Cit withdrawal, the WT mice did not exhibit any changes in running patterns compared to day 1. *Nags*$^{-/-}$ mice however, decrease their running activity around 6 hours post-withdrawal and did not appear to perform any running past 12 hours after the withdrawal (Figure 17). During high-intensity exercise, ammonia production is increased in skeletal muscle[127]. Once NCG/Cit was withdrawn from the water, the mice continued to run, which would have likely resulted in a buildup of ammonia and no

mechanism to remove it. Although this method does not account for other behaviors, we can hypothesize that high-intensity activity decreases and stops within 12 hours of NCG/Cit removal in *Nags-/-* mice.

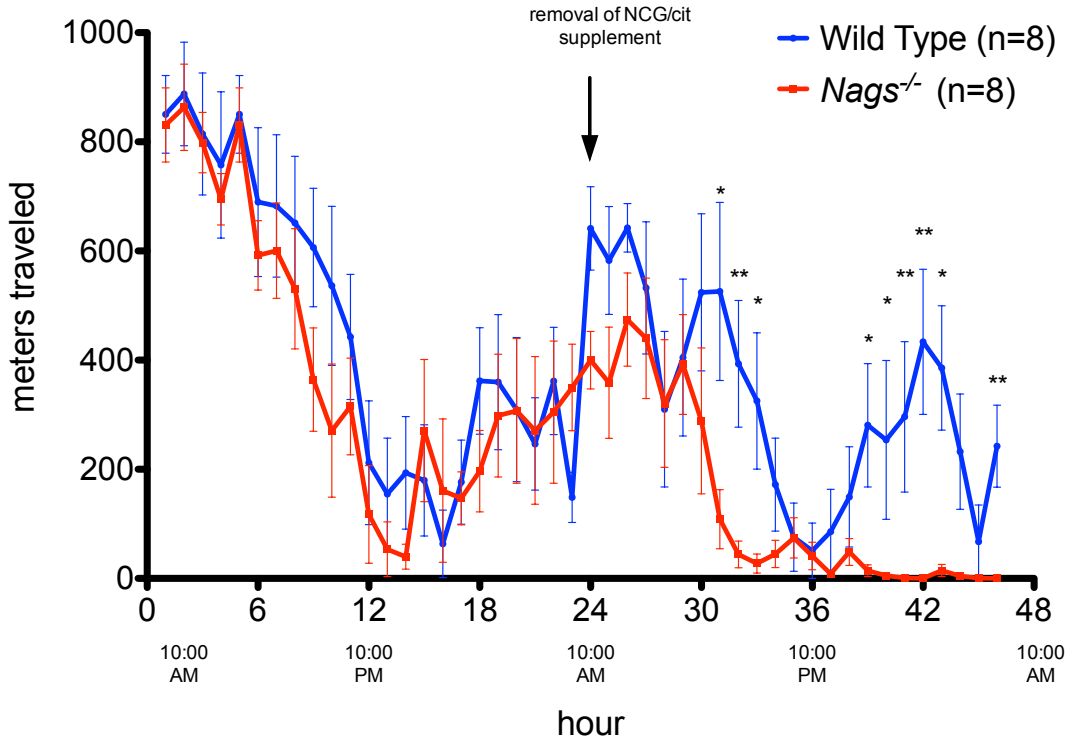

Figure 17. Running activity of wild type and *Nags*$^{-/-}$ mice.
Wild type and *Nags*-/- mice were placed in cages with running wheels, and running activity (in meters traveled/hour) were recorded for 24 hours on NCG/Cit supplement, and then for additional 24 hours after the supplement was removed. Data for each time point is presented as mean ± SEM. Statistical significance was performed using a one-way ANOVA. $p<0.05$,*; $p<0.01$,**; $p<0.001$,***; $p<0.0001$,****.

Home Cage Behavioral System

In order to comprehensively assess behavioral changes that occur during the development of hyperammonemia in mice, we used the Home Cage Scan behavioral monitoring system, which recorded mouse activity for 48 hours. We considered eight behaviors of interest: eating, drinking, hanging, walking, grooming, remaining low, sleeping, and rearing up.

During the first 24-hour period (on NCG/Cit), there is no significant difference in rearing up, hanging, eating, walking, and sleeping behavior (Figures 18 and 19). Wild type and *Nags*$^{-/-}$ mice were most active during the first half of the dark phase as demonstrated by decreased rest (Figure 19F) and increased hanging (Figure 19A) behaviors. In the second half of the dark phase, resting increased, and hanging vertical behaviors decreased. This is considered "normal" behavior for mice. Wild type mice increase their grooming, a comforting, low-stress activity, as they transition to their active period in the evening [123]. *Nags*$^{-/-}$mice seem to drink more while on NCG/Cit supplementation (Figure 19D), which may indicate that the mice are self-medicating as a learned behavior that makes them feel better. Additionally, *Nags*$^{-/-}$ mice groom less in the dark period compared to their WT littermates (Figure 19G).

After the withdrawal of NCG/Cit, wild type mice appeared to exhibit the same activity levels compared to the first 24-hour period (Figure 18). This seems to indicate that NCG/Cit has no effect on the activity in healthy mice. However, *Nags*$^{-/-}$mice decreased all activities nine hours following NCG/Cit withdrawal (Figures 18 and 19). Drinking and hanging were the first two activities to cease, approximately 12-13 hours following withdrawal, followed by eating at 14 hours post-withdrawal.

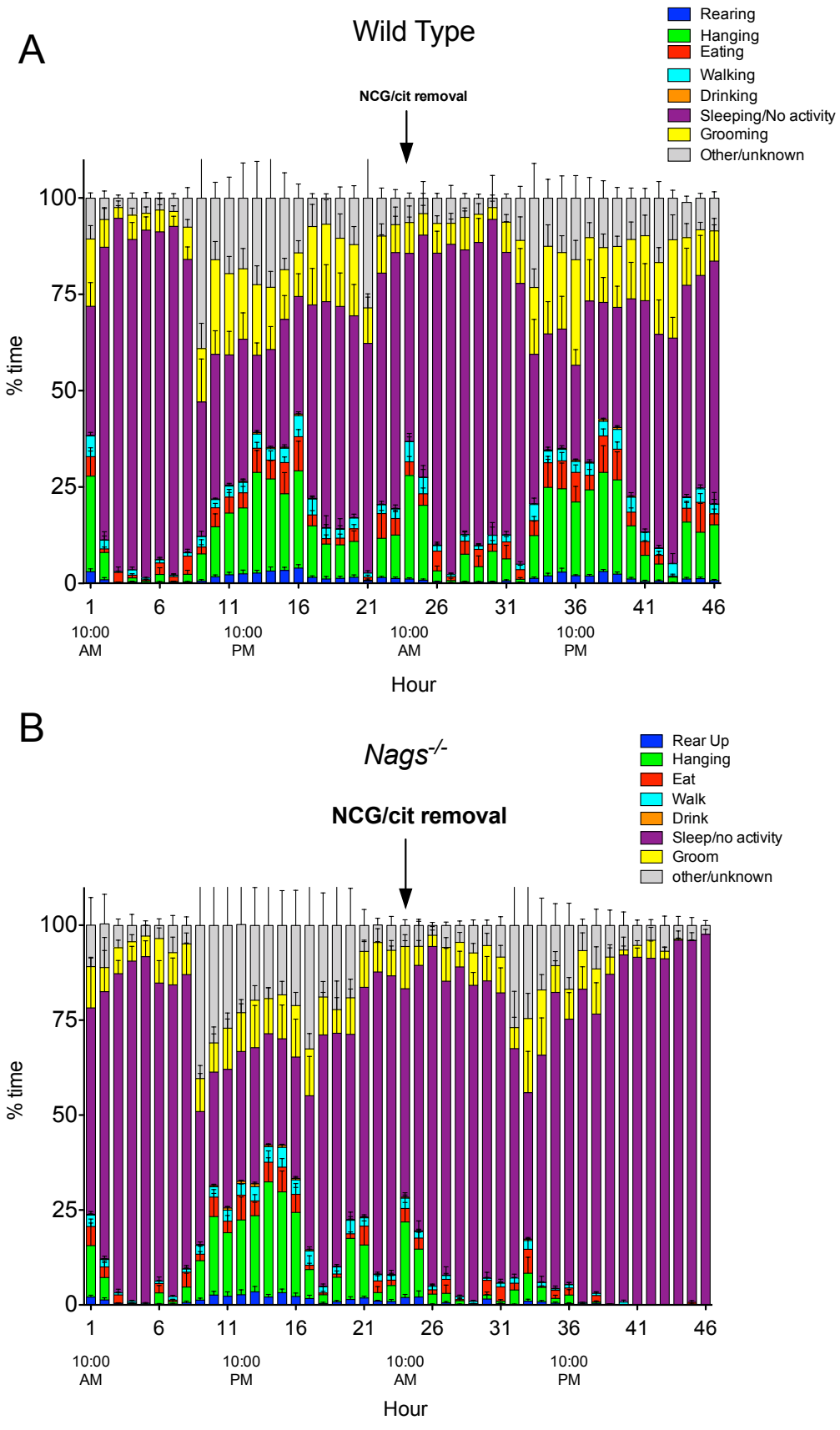
A
Wild Type
Rearing
Hanging
Eating
Walking
Drinking
Sleeping/No activity
Grooming
Other/unknown
NCG/cit removal
% time
100
75
50
25
0
1
6
11
16
21
26
31
36
41
46
10:00 AM
10:00 PM
10:00 AM
10:00 PM
Hour
B
Nags-/-
Rear Up
Hanging
Eat
Walk
Drink
Sleep/no activity
Groom
other/unknown
NCG/cit removal
% time
100
75
50
25
0
1
6
11
16
21
26
31
36
41
46
10:00 AM
10:00 PM
10:00 AM
10:00 PM
Hour

Figure 18. Behavior of Wild Type (A) and *Nags*$^{-/-}$ (B) mice during NCG/cit supplementation and following withdrawal.
Each bar represents one hour of the study. Behaviors are broken down into percentage of time each behavior was performed per hour, adding up to 100%. "Unknown" represents behaviors that were undefined by the analysis program. (Wild type n=8, *Nags*$^{-/-}$ n=8)

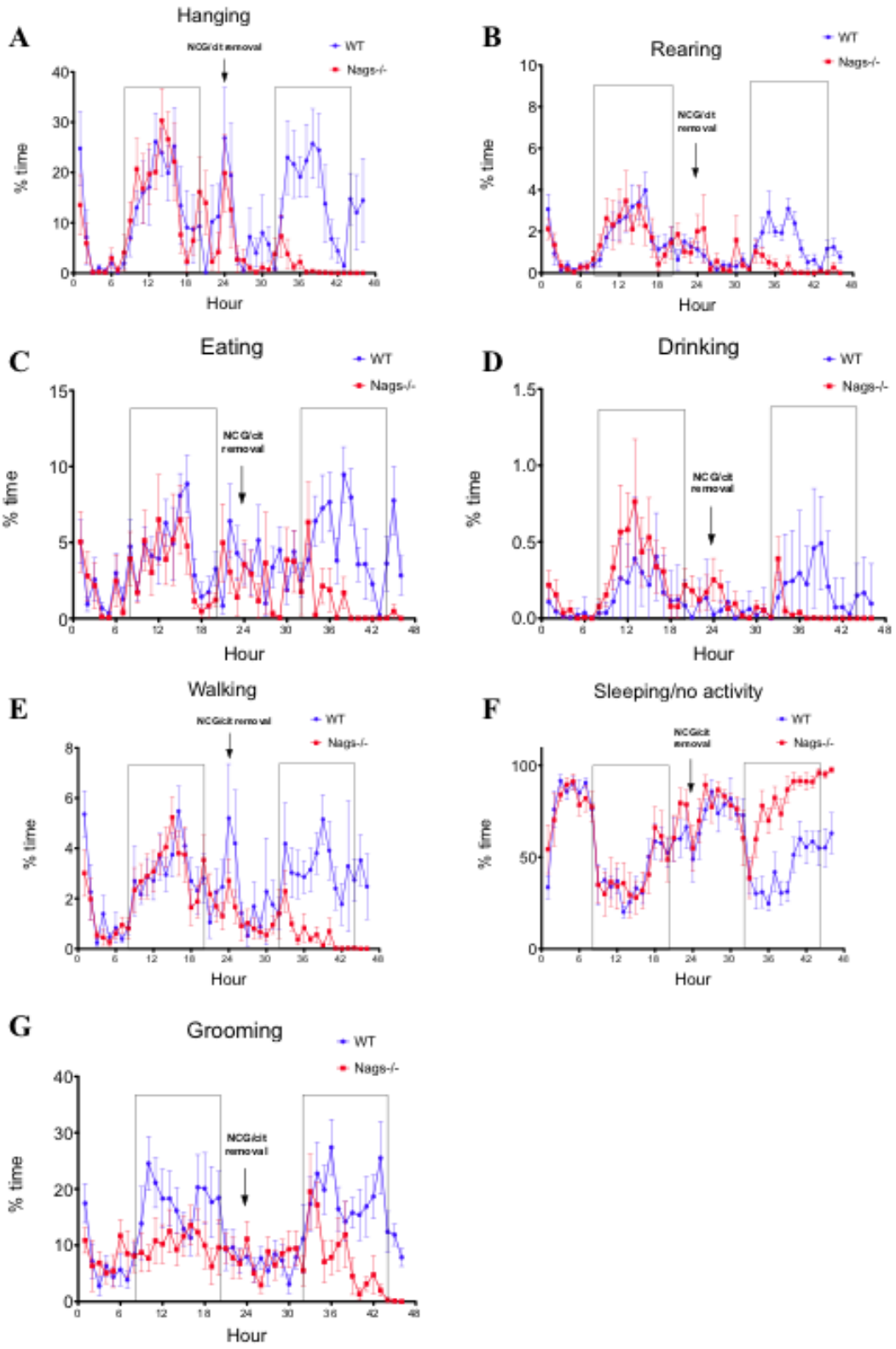
A
Hanging
NOGIdt removal
WT
Nags-/-
% time
Hour
B
Rearing
NOGIdt removal
WT
Nags-/-
% time
Hour
C
Eating
NOGIdt removal
WT
Nags-/-
% time
Hour
D
Drinking
NOGIdt removal
WT
Nags-/-
% time
Hour
E
Walking
NOGIdt removal
WT
Nags-/-
% time
Hour
F
Sleeping/no activity
NOGIdt removal
WT
Nags-/-
% time
Hour
G
Grooming
NOGIdt removal
WT
Nags-/-
% time
Hour

Figure 19. Activity plots of wild type and *Nags*$^{-/-}$ mice with NCG/cit supplementation and after withdrawal.
Hanging (A), rearing (B), eating (C), drinking (D), walking (E), sleep/no activity (F), and grooming (G) behaviors were analyzed for 24 hours while both wild type and *Nags*$^{-/-}$ mice received NCG/Cit supplement, and then for another 24 hours after NCG/Cit withdrawal. Boxed areas represent nighttime and thus the "active period" for rodents. Data is presented as an average of the percentage of time the mice were performing each activity per hour. (Wild type n=8, *Nags*$^{-/-}$ n=8)

Activity	Hour Where Activity was 0% following NCG withdrawal
Drinking	12.25 ± 3.01
Hanging	13.75 ± 3.96
Eating	14.75 ± 4.92
Rearing Up	18.5 ± 6.09
Grooming	19.5 ± 2.62
Walking	20.13 ± 1.26
	Hour Where All Activity Stops
Sleep/no activity	19.25 ± 2.66

Table 3. Cease of activity following the removal of NCG/Cit supplementation.

Other activities such as walking, rearing, and grooming may continue with some frequency through 18-19 hours following withdrawal. Table 2 summarizes when *Nags*$^{-/-}$ mice stop performing each activity following the withdrawal of NCG/Cit. Attempts to rescue the mice with injections of NCG/Cit at 23 hours were unsuccessful, indicating that in mice severe hyperammonemia beyond a certain stage cannot be cured with the rescue drug (Data not shown).

The timing of NCG/cit withdrawal is something that must be taken into account for future studies. To maintain consistency, NCG/cit supplement was removed at 10:00 AM for both the voluntary wheel and home cage studies. However, mice are not active during the day time, and possibly do not drink a significant amount of water during the day compared to nighttime. Therefore, experiments will be repeated with the NCG/cit withdrawal just prior to their active period to assess if the timing of the withdrawal affects the chronology of hyperammonemia.

Even though the *Nags*$^{-/-}$ mouse recapitulates the biochemical symptoms of hyperammonemia in humans, there are some limitations to this model. Poor feeding and vomiting is seen in patients experiencing hyperammonemia [32]. Rodents do not vomit due to the lack of neural connections and muscle strength required to open the barrier between the stomach and esophagus. Therefore, objectively measuring activity using a home cage behavioral system provides us with the best available method to assess early signs of hyperammonemia in the mice. In the *Nags*$^{-/-}$ mouse, it is the increase of lethargy that is indicative of developing hyperammonemia. The decrease of activity following removal of NCG/Cit is not surprising given that the symptoms of hepatic encephalopathy in patients includes lethargy, altered level of consciousness, and coma.

At the cellular level, hyperammonemia is known to have at least two effects on the brain; first, astrocytic swelling due to increased glutamine synthesis via glutamine synthase [15,128], and secondly, neuronal damage due to over-activation of the NMDA receptor [129,130]. Both contribute to cerebral edema. It is unknown how these cellular mechanisms contribute to the behavioral symptoms seen in hyperammonemic patients and rodents. Understanding the behavioral chronology of hyperammonemia in rodents will help determine the changes occurring on the cellular level. Additionally, identifying the cellular changes during hyperammonemia may aid in the discovery of drugs that could block or reverse the effect of hyperammonemia on the brain. NAGS deficiency is the only cause of hyperammonemia that can be prevented, using NCG. In the case of other hyperammonemia causing diseases, the only treatments are a strict no-protein diet, ammonia scavenging drugs, or hemodialysis during a hyperammonemic crisis. There are no drug-based therapies for neuroprotection from hyperammonemia to date. Drugs such as methionine sulfoximine [131], memantine, and MK-801 [20] have some success in protecting the brain in rodents, but their effectiveness and toxicity has not been tested in humans. The identification of behavioral biomarkers in the *Nags*$^{-/-}$ mouse should prove useful in future hyperammonemia drug discovery experiments.

Chapter 4: Determination of a liquid chromatography-mass spectrometry method for the determination of N-carbamyl-L-glutamate in biological samples

Introduction

NAGS patients lack the enzyme N-acetylglutamate synthase (NAGS), which produces N-acetylglutamate (NAG) from L-glutamate and acetyl-CoA [6]. NAG, in turn, is an essential activator of the urea cycle enzyme, carbamyl phosphate synthetase I (CPS1), the first step in the urea cycle [51]. Thus, the absence of NAG results in a reduction or abolishment of CPS1 activity, leading to a block in ureagenesis and accumulation of ammonia in the blood [30,92]. NAGS is also present in the small intestine, and deficiency in the enzyme will also result in citrulline and arginine deficiency [21,132].

N-carbamyl-L-glutamate (NCG) is a functional analog of NAG that has been shown to be resistant to *in vivo* degradation, which allows the molecule to reach the liver, enter the mitochondria, activate CPS1 [9,52] restore ureagenesis [54] and reduce plasma ammonia and glutamine levels [57] in patients. NCG (Carbaglu, Orphan Europe) has been approved by the FDA in 2010 for the treatment of NAGS deficiency. There is some evidence that NCG could be beneficial in other disorders where ammonia flux is reduced, such as CPS1 deficiency, organic acidemias, fatty acid oxidation disorders, and hepatic encephalopathy [57].

Currently, there are no established methods to measure NCG in biological samples or tissues. Such methods would allow one to measure how much NCG enters tissues given a certain dosage. Measuring NCG in samples such as plasma, urine, and feces would

allow one to determine absorption efficacy of the drug and compliance in taking the drug. Our goal was to develop a method using LC-MS to quantify NCG in the plasma, urine, and feces as well as liver and small intestine, Since NCG is not endogenously synthesized, any NCG detected with this method comes directly from treatment.

Biological samples were obtained from a newly characterized mouse model (*Nags*$^{-/-}$) for NAGS deficiency [117]. As previously described, this mouse model represents the first reversible animal model of hyperammonemia. *Nags-/-* mice develop hyperammonemia within 12 hours following the removal of NCG and Cit. As such, these mice receive daily supplementation of NCG and Cit starting from birth, thus, NCG should be measureable in their liver, intestine, urine, feces, and plasma. The method described herein was adapted from previously described experiments from this lab to measure NAG via GC-MS and LC-MS [133,134].

Materials and Methods

Chemicals

N-carbamyl-L-glutamate, trifluoroacetic acid (TFA), trichloroacetic acid (TCA), and acetonitrile were purchased from Sigma-Aldrich.

Synthesis of Isotopic N-carmabyl-L-glutamate

To be used as the internal standard, isotopic NCG (^{13}C-NCG) was synthesized at American University by Dr. Monika Konaklieva and Mr. Tim Beck. 500 mg [$^{13}C_5$]-glutamate (Sigma Life Science BioUltra) and 350 mg urea (Fisher) were combined with potassium hydroxide and water and incubated in a Discover LabMate IntelliVent Pressure Control System microwave for 30 min at 105°C and 300W. The mixture was then cooled

for 10 min at room temperature prior to placing in an ice bath and neutralized to pH 7 with 6M HCl. The mixture was then transferred to a beaker and exposed to continuous airflow under a fume hood for 3 days. The presence of isotopic carbamoylated glutamate was identified via ^{1}H NMR (400 MHz, D_2O) via Bruker 400 spectrometer and MS (Applied Biosystems 3200QTrap LC/MS/MS).

Instrumentation

LC-MS analysis was conducted using an Agilent 1200 series LC system consisting of a G1311A quaternary pump, a G1322A degasser, and an ALSG1329A refrigerated autosampler interfaced to an APO 150EX mass spectrometer. The turboionspray source (TIS) was operated in positive ion mode. Instrument control and data analysis were performed using ChemStation software (Agilent Technology).

Chromatographic and Mass Spectrometer Conditions

The mobile phase consisted of 92% Buffer A (0.1% TFA, 99.9% H_2O), and 8% Buffer B (90% acetonitrile, 0.1% TFA, 10% H_2O). Elution of analytes was carried out under the following setting: flow rate 0.6 mL/min, drying gas flow rate 13 L/min, nebulizer pressure 0.5 psig, drying temperature of 350^{o}C, capillary voltage of 3500 positive and negative. Mass spectrometric data were collected between 0 and 4 min, under selective ion monitoring for ions 191.1 (native NCG) and 195.7 (isotopic NCG).

Tissue Collection

All procedures for mice care were in accordance with the guidelines set forth by the American Association for Accreditation of Laboratory Animal Care and all the studies

were approved and supervised by the Children's National Medical Center Institutional Animal Care and Use Committee (protocol number 247-09-11). Mice were housed and bred in the Research Animal Facility (barrier facility) under controlled temperature (68°F) and a 12-hour light/dark period. Mice were fed Harlan Tecklad irradiated chow (2018) and sterilized water. The creation of the *Nags*$^{-/-}$ has been previously described [117]. After weaning (typically 21 days), *Nags*$^{-/-}$ mice were maintained on water supplemented with NCG and Cit (each 1.0 g/L).

Plasma was collected by cardiac puncture, as previously described [117]. Livers were frozen in liquid nitrogen, and then homozgenized. Intestines were collected and intestinal epithelial cells were isolated as previously described [117]. Urine was collected onto filter paper from mouse at the time of sacrifice. The urine was then extracted in water and shaken vigorously. Feces was collected from the mouse at the time of sacrifice and homogenized. ^{13}C-NCG was added to all the samples prior to analysis.

Statistical Analysis

All statistical analyses were performed using Prism software, version 5 (GraphPad, San Diego, CA). The minimal level of confidence at which experimental results were considered significant was $p<0.05$. Statistical significance was determined with a t-test comparing NCG-treated mice to non-supplemented, wild type mice. In all cases, data is presented as the mean ± SEM. In all figures, $p<0.05$,*; $p<0.01$,**; $p<0.001$,***; $p<0.0001$,****.

Results and Discussion

In order to measure NCG in clinically relevant samples, we developed a stable isotope dilution method using LC-MS, derived from a similar method for measurement of NAG [134]. Isotopic NCG was prepared from glutamate and urea, which has a mass-to-charge ratio (m/z) of 196 due to the universal 13-C label of carbons in the glutamate (Figure 20). NCG and ^{13}C-NCG are detected and quantified by selected ion monitoring mass spectrometry. ^{13}C-NCG and NCG have the same retention time (Figure 21). Thus, ^{13}C-NCG acts as an ideal standard in order to identify native NCG in the sample. This method allows the detection of as little as 0.001 mM NCG in a sample.

NCG is not endogenously synthesized in mammals. Though Grisolia and Cohen believed that NCG was the natural intermediate in the synthesis of citrulline [49,50], in 1958 NAG was isolated from liver preparations, suggesting that NAG is indeed the natural cofactor in carbamyl phosphate synthesis [51]. As a result, we expected that wild type mice, never given NCG supplementation, would have no detectable amount of NCG in any of their tissues. Additionally, wild type mice given NCG supplementation over a period of a few days, as well as *Nags*$^{-/-}$ mice, should have detectable amounts of NCG in all relevant tissues and body fluids.

We were surprised to find a detectable amount of NCG in liver tissue of wild type, non-supplemented mice (Figure 22). We hypothesized that the presence of NCG in untreated liver was due to a reaction artifact caused by the addition of the TCA to the homogenized liver. To test this hypothesis, we combined glutamate and urea, urea and carbamyl phosphate, and glutamate and carbamyl phosphate with 30% TCA. Analysis of chromatograms from these three combinations revealed that the combination of carbamyl

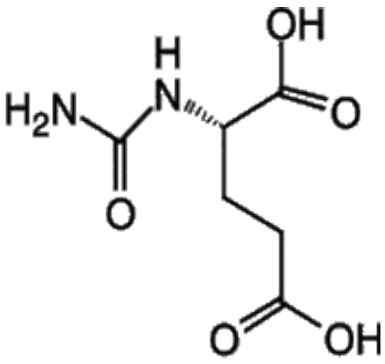

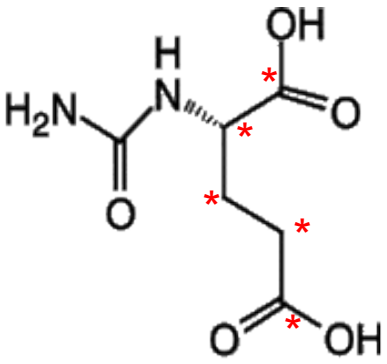

Unlabeled NCG mwt= 191

Isotopic NCG mwt= 196

Figure 20. Structure of N-carbamylglutamate and isotopic N-carbamylglutamate.
Red stars indicate ^{13}C carbon atoms.

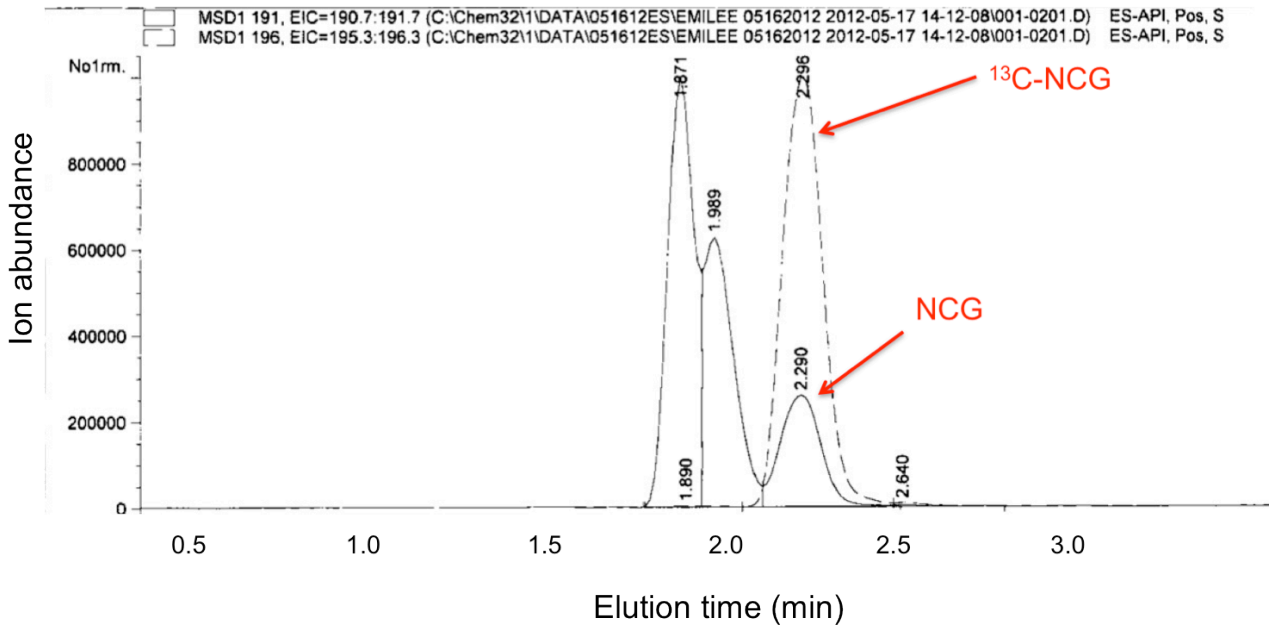

Figure 21. Representative chromatogram of N-carbamylglutamate.
Isotopic NCG with a molecular weight of 196 is represented by dashed lines, while the native NCG with a molecular weight of 191 is represented by a solid line. In this chromatogram both NCG and ^{13}C-NCG elute at 2.29 minutes.

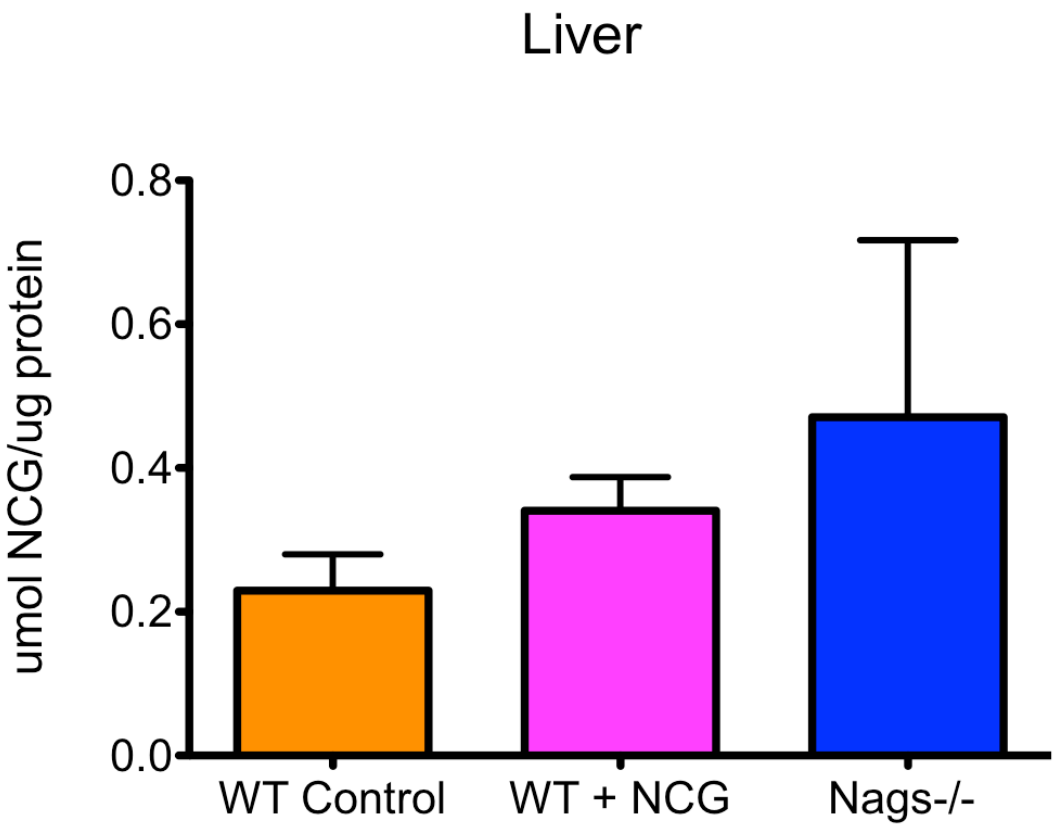

Figure 22. Concentration of NCG in liver samples.
Livers were collected from untreated wild type mice, wild type mice treated with NCG for 3 days, and 6-week-old *Nags*$^{-/-}$ mice. Livers were homogenized and analyzed for NCG content. NCG concentration (in μmol) was normalized to μg protein used. Liver NCG concentrations in treated mice are not statistically significant from WT control. (WT control n=10, WT+NCG n=5, *Nags*$^{-/-}$ n=5)

phosphate and glutamate in the presence of TCA produces a peak that corresponds to NCG (Figure 23). From the structures of glutamate (Top, Figure 23) and carbamyl phosphate (Bottom, Figure 23), one can deduce that NCG can be synthesized by spontaneous reaction. We believe that the appearance of NCG in wild type control samples is an artifact due to the addition of TCA. Thus, we need to explore other methods of precipitating protein from samples that do not involve the addition of acid. Such methods may include filtering the sample through columns to remove the protein.

The *Nags*$^{-/-}$ mice have a larger concentration of NCG in their intestines compared the wild type mice treated with NCG (Figure 24). This may be due to competition between NAG and NCG for CPS1 in the wild type mice. Since NAG has a stronger affinity for CPS1 than NCG, the latter may not bind as efficiently to CPS1 when NAG is present, and thus may not stay in the cell. NCG was not detected in the intestinal epithelium of non-supplemented mice (Figure 24). If sufficient amounts of NCG are transported into intestinal epithelial cells, it should activate CPS1 in the absence of NAG, which would result in citrulline production. However, previous experiments have shown that supplementation with NCG but not Cit results in 50% fatality after two weeks, suggesting that the *Nags*$^{-/-}$ mice supplemented with NCG are citrulline/arginine deficient. One hypothesis is that the *Nags*$^{-/-}$ mice may undergo stresses that lead to arginine deficiency that cannot be compensated by the amount of citrulline produced via the NCG activation of CPS1 in the intestine. Arginine is a precursor for cellular pathways involved in wound healing [109,135-137] and immunity [138-140]. For example, arginine is a precursor for nitric oxide, an anti-inflammatory agent and a promoter of vascular health [141]. Another study showed that in young mice (3 months or younger), arginine

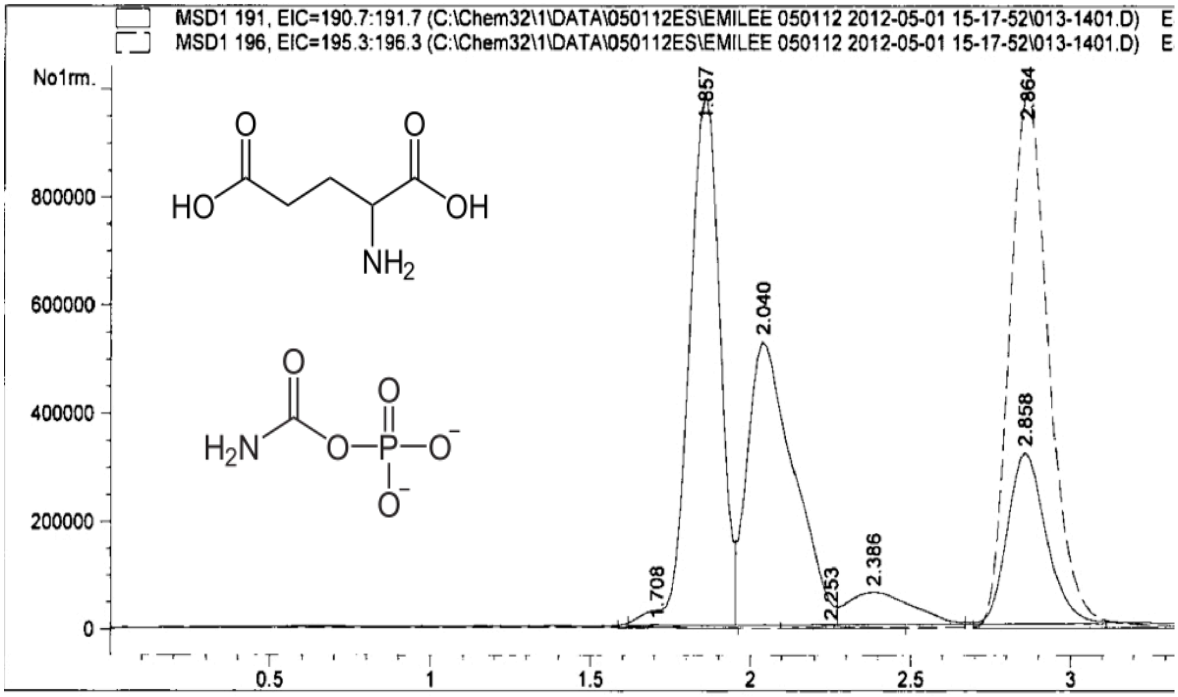

Figure 23. Combination of glutamate and carbamyl phosphate in the presence of TCA produces a product that corresponds to NCG.
Solutions of glutamate and carbamyl phosphate were combined and treated with 30% TCA before LCMS analysis. Top structure= glutamate; lower structure=carbamyl phosphate. Both NCG and isotopic NCG are eluting at 2.8 minutes in this chromatogram. Native NCG is indicated with a solid line, isotope with a dashed line.

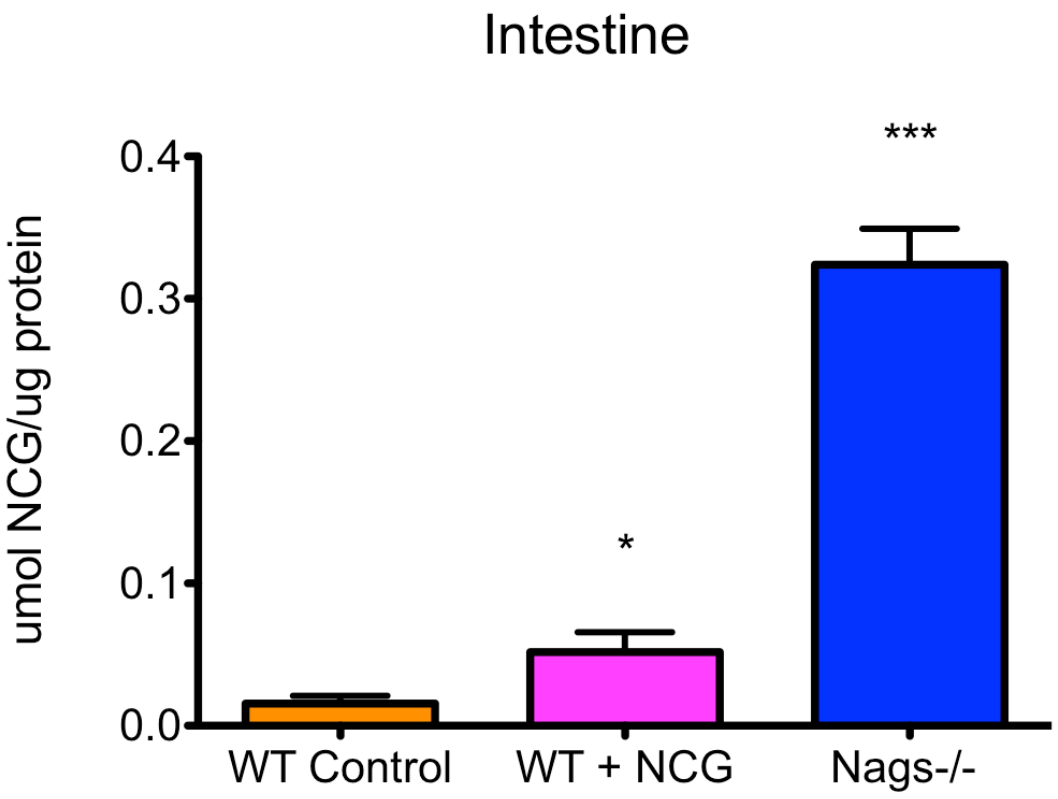

Figure 24. Concentration of NCG in intestinal epithelial cells.
Small intestine was collected from untreated wild type mice, wild type mice treated with NCG for 3 days, and 6-week-old *Nags*$^{-/-}$ mice. Intestinal epithelial cells were isolated as described, homogenized and analyzed for NCG content. NCG concentration (in μmol) was normalized to μg protein. (WT control n=10, WT+NCG n=10, *Nags*$^{-/-}$ n=5)

production decreased 30 minutes after a stressful period and remained low 3 days thereafter [142]. Circumstances that involve arginine deficiency, such as a wound or stress, can result in a decline in immune function and vascular health. If the concentration of NCG in intestinal cells is not promoting a sufficient amount of citrulline production to overcome this deficiency, it could potentially lead to a fast decline in health.

As expected, NCG is detected in the plasma and urine of supplemented mice, and is undetectable in non-supplemented control mice (Figures 25-26). The presence of NCG in the plasma and urine of supplemented mice is clinically relevant. A study in which radioactive NCG was given to healthy subjects showed that NCG could be measured in the plasma within 3 hours of administration, and by 12 hours, 40% of the dose was eliminated in urine and 22% eliminated in feces [143]. Currently, there are no clinical methods to detect NCG in patient samples. The ability to do so can help clinicians determine if patients are being compliant in taking medication. Additionally, there is an increasing use of NCG by athletes apparently to increase performance. If NCG eventually gets classified as a performance-enhancing drug, the presence of this drug could be measured easily in a blood or urine sample.

The presence of NCG in fecal samples of non-supplemented wild type mice was surprising (Figure 27). One possible explanation for this unexpected observation is gut bacteria that produce NCG. This hypothesis would also explain the presence of NCG in wild type liver since metabolites produced in the gut can eventually enter the liver through the portal vein. If a NAGS deficient person has gut bacteria producing NCG, then it is possible that the amount of NCG is sufficient to sustain a residual level of ureagenesis

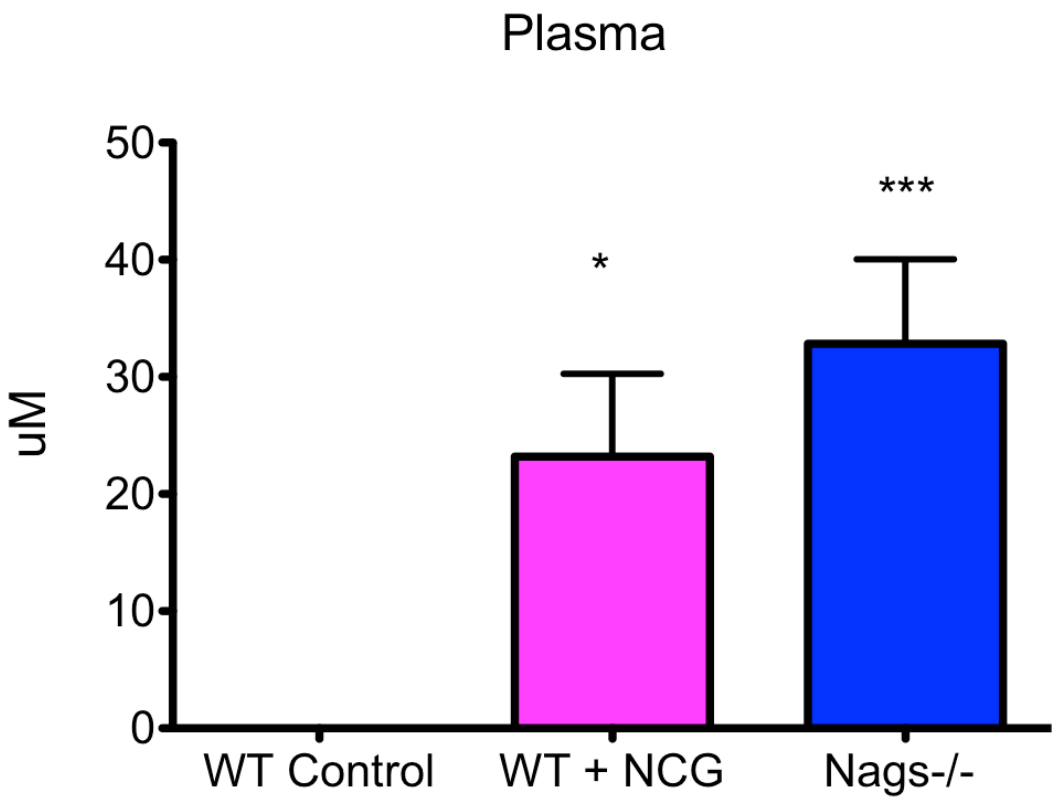

Figure 25. Concentration of NCG in plasma.
Plasma was collected from untreated wild type mice, wild type mice treated with NCG for 3 days, and 6-week-old *Nags*$^{-/-}$ mice. NCG concentration is expressed in μM. (WT control n=5, WT+NCG n=5, *Nags*$^{-/-}$ n=5)

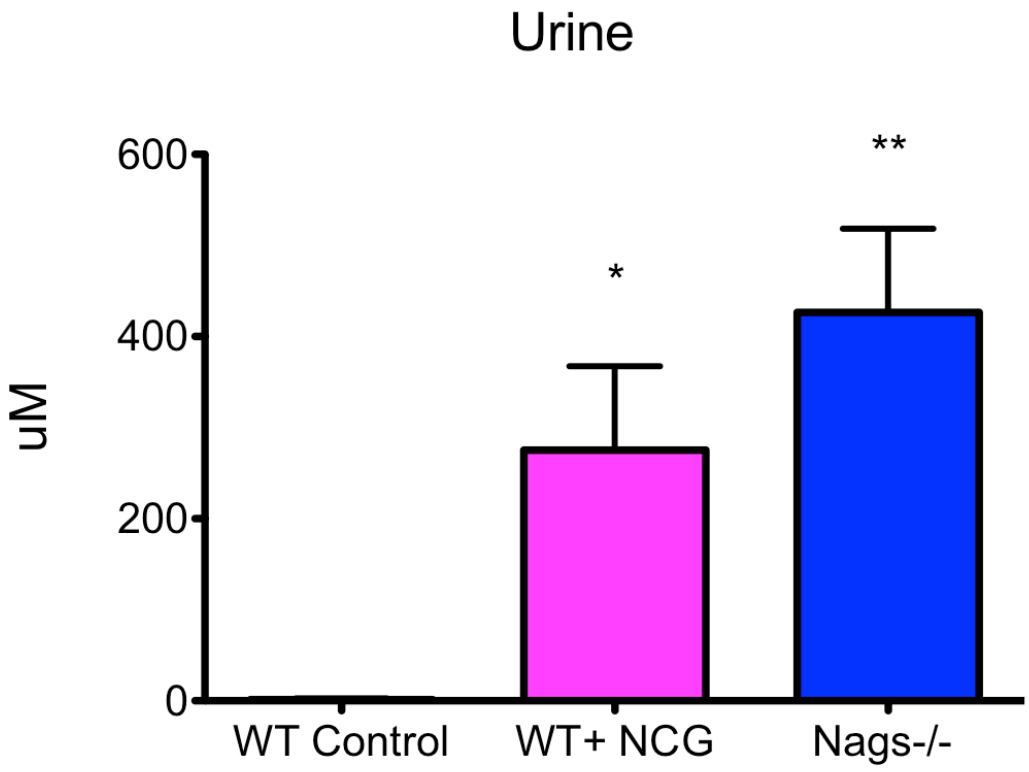

Figure 26. Concentration of NCG in urine.
Urine was collected on filter paper from untreated wild type mice, wild type mice treated with NCG for 3 days, and 6-week-old *Nags*$^{-/-}$ mice. Urine spots were then eluted in water and analyzed for NCG content. NCG concentration is expressed in μM. (WT control n=5, WT+NCG n=5, *Nags*$^{-/-}$ n=5)

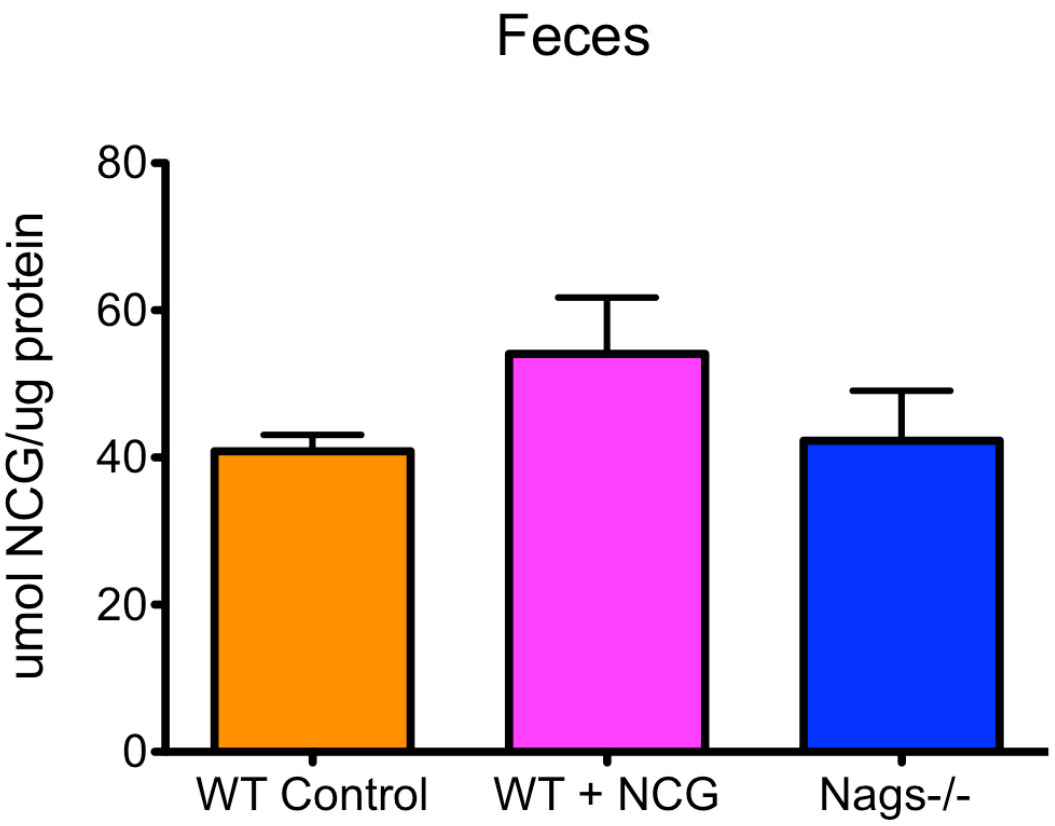

Figure 27. Concentration of NCG in feces.
Feces were collected from untreated wild type mice, wild type mice treated with NCG for 3 days, and 6-week-old *Nags-/-* mice. Samples were homogenized and analyzed for NCG content. NCG concentration (in μmol) was normalized to μg protein. Fecal NCG concentrations in treated mice are not statistically significant from WT control. (WT control n=5, WT+NCG n=5, *Nags*$^{-/-}$ n=5)

masking the disorder that could go undetected for life. This may also account for late-onset cases, where a deficiency is discovered after the affected individual experiences a stress-inducing hyperammonemic crisis brought on by disease, surgery, or pregnancy and/or delivery. Clearly, this hypothesis will need to be explored further. One approach would be to treat wild type mice with antibiotics, which would destroy gut bacteria, and then analyze their NCG content.

In conclusion, we have developed a method for the detection of NCG in biological samples. This method is clinically relevant and can be used to measure NCG concentrations in patient samples to confirm patient compliance or toxicity. Methods to measure NCG in liver and fecal samples will need to be refined, as NCG appears in non-supplemented control mice. We believe this could be an artifact of the method of sample preparation. Another hypothesis that warrants further exploration is the possibility of NCG-producing gut bacteria. Much needs to be learned about the intestinal flora, and the identification of a strain that produces NCG may explain the rarity of NAGS deficiency. Our hope is to use this method to explore the unknowns concerning NCG pharmacology, such as uptake and clearance kinetics. As the transport mechanism of NCG is unknown understanding it can help determine if there are drugs that would compete for transport, or potentially how clinicians can enhance the transport of this poorly-absorbed drug.

Chapter 5: Future Directions

Identifying drugs that have a neuroprotective effect against hyperammonemia

The use of the NAGS deficient mouse model provides opportunities that extend far beyond urea cycle disorders. Hyperammonemia is a result of many disease states, including organic acidemias, fatty acid oxidation diseases, acute and chronic liver failure, certain surgeries, and chemotherapy. Though the deficient or insufficient urea cycle occurs in the liver, the long-term damage of hyperammonemia occurs in the brain. Ammonia quickly crosses the blood brain barrier and has deleterious consequences on astrocytes and neurons. Patients affected with hyperammonemia develop a wide range of neuro-cognitive disorders, and if untreated, coma and possibly death. Currently, the treatment for hyperammonemia includes dietary manipulation, sterilization of the bowel, alternate pathway therapy for ammonia removal or liver transplantation. There are no specific treatments to directly protect the brain from hyperammonemia. We plan to use this mouse model to further understand the molecular mechanisms underlying hyperammonemia, as well as potentially identify drugs that may protect the brain from ammonia toxicity.

We have established the behavioral chronology of hyperammonemia in the *Nags*$^{-/-}$ mice following NCG withdrawal, with the earliest symptoms developing within 12 hours. With this model, we can begin to explore methods to block and/or reverse the effects of hyperammonemia.

Testing known neuroprotective drugs in Nags$^{-/-}$ mouse

We have chosen three drugs that have been reported to protect the brain against hyperammonemia in rodents. The first, methionine sulfoximine (MSO), is a glutamate synthase inhibitor that blocks the condensation of ammonia and glutamate into glutamine. Ammonia entering the brain is rapidly incorporated into glutamine via glutamine synthase expressed in astrocytes. Glutamine is increased in hyperammonemic individuals. MSO works by producing MSO-phosphate, which binds to the active site and inhibits glutamine synthase [144]. In cultured astrocytes and hyperammonemic rodents, inhibition of glutamine synthetase by pre-treatment with methionine sulfoximine prevents an increase in cortical glutamine, cortical water content (edema), and intracranial pressure [145]. Another study showed that MSO reduces glutamine synthase activity by 57% and glutamine accumulation by 71% compared to control groups [146]. In a model of induced liver failure, administration of MSO drastically increased animal survival and reduced glutamine synthase activity [144].

Increased activity of the NMDA receptor has also been implicated in hyperammonemia-induced neurological damage. Elevated ammonia concentrations lead to a down-regulation in astrocyte glutamate transporters glial glutamate transporter 1 (GLT1) and glutamate aspartate transporter (GLAST), resulting in a buildup of extracellular glutamate [147-149]. This extraceullar glutamate causes overstimulation of the NMDA receptor and excessive influx of ions, resulting in cell swelling and neurodegeneration [18,19]. Hyperammonemia induced by acute liver failure leads to activation of the NMDA receptors and subsequently oxidative stress and neuronal damage, leading to death. Both MK801 and memantine function to block the NMDA

receptor, doubling survival time of rodents subjected to chemical-induced liver injury [20].

We plan to test all three drugs using *Nags-/-* mice. Drugs will be administered prior to NCG/Cit withdrawal. Survival time as well as behavior will be assessed and compared to a control group of untreated, non-NCG supplemented *Nags-/-* mice. Alzet osmotic pumps will need to be inserted subcutaneously for the MK801 and memantine studies. This is necessary because MK801 and memantine are cleared quickly. These pumps provide a convenient and reliable method for the controlled delivery of drugs. MSO remains in the body for three days after administration, and will be injected intraperitoneally 3 hours prior to NCG withdrawal. We expect these drugs to act as neuroprotective agents and thus prolong the life of the mouse, which will be measured using the Home Cage Behavioral System. Additionally, we will also collect brain, liver, and plasma of these mice to assess transcriptional and proteomic changes that occur in these tissues during the time course of hyperammonemia. Analysis of these data will hopefully uncover molecular and cellular mechanisms underlying hyperammonemia in the brain. Again, we believe our mouse model is of hyperammonemia is unique because other confounding factors (such as exogenous toxins or surgery) are not involved.

Identification of the N-carbamylglutamate transporter

NCG is an FDA approved drug for the treatment of NAGS deficiency, with the potential for treatment of hyperammonemia from other causes. Despite this, little is known about its pharmacology, for example transport across plasma membrane and mitochondria of liver and small intestine, how efficiently it binds to CPS1, and how it is eliminated. Understanding the transport mechanisms of NCG is important for two reasons.

First, in the cases of NAGS deficiency and possibly other inborn errors of metabolism[58], activation of CPS1 by NCG is crucial for maintaining ureagenesis. Decreasing or blocking transport could potentially lead to hyperammonemia. Therefore, it is important to know which transporters are involved and whether there could be competition for these transporters by various drugs. Secondly, use of NCG is promoted as a muscle-building dietary supplement, which could potentially lead to wide spread use or abuse of this drug. Identifying any adverse drug interactions due to competition for transporters is therefore significant. Ultimately, we will use our previously described LC-MS assay, which was adapted from an LC-MS assay for detection of NAG [133,134], to determine if cells and tissues have successfully taken up NCG.

In order to determine which transporters are involved, we will use affinity labeling with activated NCG, proteomic analysis of liver and intestinal mitochondria and siRNA knockdown of candidate transporters in liver cells. NCG is anionic at neutral pH, therefore we hypothesize that likely candidates will include anionic amino acid transporters. We have shown that HepG2 cells import NCG (Figure 28), and therefore the HepG2 line will be used in initial experiments to identify the putative NCG transporter(s).

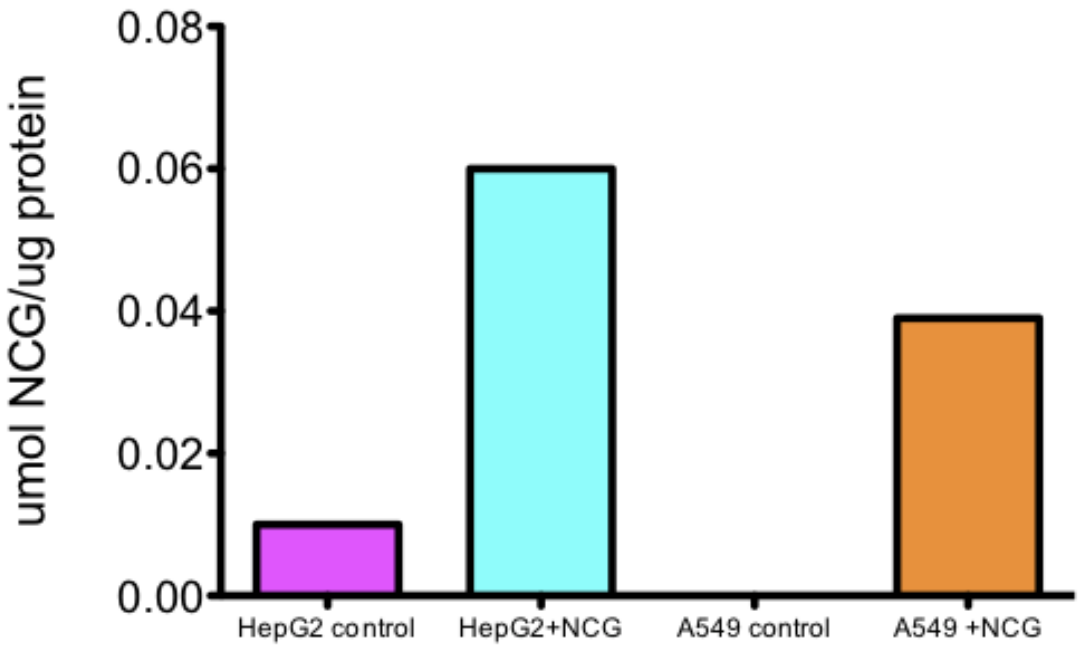

Figure 28. HepG2 and A549 cell lines take up NCG.
HepG2 and A549 (a lung cell line) were exposed to NCG for 3 hours. Cells were lysed, and analyzed for NCG content. Since A549 cells take up NCG, the transporter is likely to be common to various types of cells.

Identification of the plasma membrane and mitochondrial transporters for NCG by affinity labeling

The first approach uses affinity labeling followed by proteomic mass spectrometric analysis of membrane proteins. 1-ethyl-3-[3-(dimethylamino)propyl]carbodiimide (EDC) is a crosslinker that reacts with the epsilon amino group of lysine residues in proteins. EDC-activated NAG was used to identify the NAG binding site of CPS1 [150]. We believe that we could activate NCG with EDC, and then add it to cells, resulting in EDC-NCG binding to and cross-linking with its plasma membrane transporter. Then, plasma membrane proteins will be isolated via SDS-PAGE gel, subjected to trypsin digestion, and then fragments will be analyzed by mass spectrometry in the proteomics core facility. Modifications of lysine residues from cross-linking with EDC-NCG will result in a loss of a tryptic digestion site and a shift in the mass of the peptide with the attached NCG. These experiments will be repeated with mouse intestinal epithelial cells to determine if the NCG transporter is the same in the intestine. Additionally, we will use a similar approach using isolated liver and intestinal mitochondria to identify the mitochondrial transporters.

Using siRNA knockdown to identify the NCG transporters

We also plan to use siRNA knockdown experiments to demonstrate that putative transporters identified in the proteomics experiments are successful in transporting NCG. For this experiment, we will use hepatocytes isolated from *Nags*$^{-/-}$ mice, which will allow testing if NCG uptake is reduced and ureagenesis inhibited when the transporter is silenced.

If we are unable to identify the transporter using the proteomics methods outlined above, we will use a siRNA knockdown screen. Primary hepatocytes from *Nags-/-* mice will be isolated and cultured under conditions that maintain hepatocyte metabolism, apical/basal polarization and expression of transporters [151,152]. We will use methods that have been shown to silence organic anion transporters in hepatocytes [153,154]. After transporters have been silenced, hepatocytes will be cultured in media containing NCG. Cells in which NCG transport has not been compromised will produce urea, which can be visualized using a colorimetric assay. If the NCG transporter has been silenced, ureagenesis will not occur. Transport or lack of transport can be confirmed using our LC-MS assay.

Chapter 6: Conclusions

Hyperammonemia is a state of metabolic disturbance characterized by an increased concentration of ammonia in the plasma. Hyperammonemia can occur in patients with untreated or undiagnosed urea cycle disorders, as well as in patients with defects in fatty acid oxidation, cirrhosis, acute liver failure, Reye syndrome, and as a complication from certain surgeries and chemotherapy. Though hyperammonemia occurs when the urea cycle, a liver pathway, is compromised, hyperammonemia negatively affects the brain. Elevated plasma ammonia compromises astrocyte and neuronal function, causing cerebral edema and neuronal damage, which results in patient symptoms including lethargy, vomiting, seizures, coma, and death. Currently, treatment for hyperammonemia is focused on the liver, by decreasing protein load, using ammonia scavenging drugs (which are not 100% effective), dialysis, or liver transplant. A thorough understanding of how ammonia affects pathways in the central nervous system and treatments that protect the brain from ammonia are desperately needed.

One step in understanding the pathophysiology of hyperammonemia is the development of a clean, inducible rodent model of hyperammonemia. Current models of hyperammonemia involve procedures with confounding factors or urea cycle deficient mouse models that do not survive into adulthood. Here we describe the first clean, inducible, rescuable animal model of hyperammonemia: a mouse model of N-acetylglutamate synthase (NAGS) deficiency that can be rescued with a combination of N-carbamylglutamate (NCG) and citrulline. This model recapitulates the human disease, as *Nags*$^{-/-}$ mice become lethargic, ataxic, comatose, and hyperammonemic and develop abnormal amino acid profiles within 24 hours of NCG/cit withdrawal. Using this mouse

model and methods to quantitate behavior, we showed that following NCG/cit withdrawal, *Nags*$^{-/-}$ mice decrease all behaviors and become severely lethargic within 22 hours.

The development and usefulness of this mouse model extends far beyond NAGS deficiency. Since this mouse develops hyperammonemia solely due to one factor, the blockage of ureagenesis, we can use this mouse to study hyperammonemia and be confident there are no other confounding factors contributing to the development of the disease state. Using the behavioral chronology, we plan to use this model to identify novel compounds that may offer neuro-protection from hyperammonemia. These drugs would transform the treatments of both urea cycle disorders and acute or chronic liver failure.

Additionally, the *Nags*$^{-/-}$ mice will be used as a model to understand the pharmacology of the drug NCG. NCG is sold under the name Carbaglu and approved by the FDA for the treatment of NAGS deficiency. However, this drug is now being prescribed off label for the treatment of CPS1 and organic academia disorders, and used as a performance-enhancing supplement in athletes. The increasing use of this drug means that physicians now need to be aware of any other drugs that may interact with or inhibit NCG. The development of an LCMS method to analyze concentrations of NCG in liver, intestine, plasma, urine, or feces will aid in the enhanced understanding of NCG pharmacology. This method can be used by clinicians to analyze the efficacy of NCG in patients, simply by collecting plasma or urine. We plan to use the *Nags*$^{-/-}$ mice and the LCMS method to identify the NCG transporter, which will enhance our understanding of NCG pharmacology.

In conclusion, we have developed a novel, improved animal model of hyperammonemia, which we plan to use to increase the understanding of the

pathophysiology of this disease. By understanding how ammonia affects the brain, we hope to develop novel drug treatments to improve the health and quality of life of patients suffering from hyperammonemia.

Appendix: Urea Cycle Enzyme expression in HepG2 and IEC-6 cell lines

Methods and Materials

Total RNA was extracted from cells using the TRIzol reagent (Invitrogen). cDNA was generated using the Superscript III First strand synthesis kit (Invitrogen). Primers for human HepG2 cells and rat IEC-6 cells are listed in Table 3. Real-time PCR analysis was carried out using the 7900 HT Fast Real Time PCR System (Applied Biosciences) and SDS version 2.3 software using iQ SYBR green supermix (Bio-Rad). PCR reactions were carried out as follows: one cycle of 95°C for 2 minutes, followed by 40 cycles of 95°C 30 seconds, 60°C 30 seconds, 72°C seconds, and a dissociation step of 95°C 15 seconds, 50°C 15 seconds, and 95°C 15 seconds.

Gene	Species	Orientation	Sequence
NAGS	Human	FWD	5’-CCGCGGCCTACGGCTCCCTCGGGCTGTCT-3’
		REV	5’-GCGGGCAGGTTCACGTTACTCAGGACCTT-3’
	Rat	FWD	5’-CCTACCCCCACGGCACCTTCTGGCTG -3’
		REV	5’-GCGGGCAGGTTCACGTTGCTCAGGA -3’
CPS1	Human	FWD	5’-TCCTGATACTACTGCTCTGGATGAACT-3’
		REV	5’-CCCGGTCCTCCCGCGATCAAAATCCCATCAT-3’
	Rat	FWD	5’-ATCTGAGGAAGGAGCTGTCT-3’
		REV	5’-AAAACCACTTCTCAATGGAT-3’
OTC	Human	FWD	5’-GCGAAATTCGGAATGCACCTTCAGGCAGCTACT-3’
		REV	5’-TCTGCCTCTGGGAACACTAGTGATCGAGGAGAA-3’
	Rat	FWD	5’-ATGACAGATGCAGTGTTAGC-3’
		REV	5’-CAGGATCTGGATAGGATGAT-3’
ASS	Human	FWD	5’-TCGTGCATCCTCGTCGTGTGGCTGAA-3’
	Rat	REV	5’-CCACAAACTCCCTGCTGACATCC-3’
ASL	Human	FWD	5’-GAGGTGCGGAAGGCCATCAATGT-3’
		REV	5’-TTGGTGCAGTAGAGGATGAGGTCC-3’
	Rat	FWD	5’-GGAATTCAACTTTGTGCAGCTCTCCG-3’
		REV	5’-AACACAGCCTCCTTGTCTTCCTGT-3’
ARG1	Human	FWD	5’-GCAGAAGTCAAGAAGAACGG-3’
		REV	5’-GGTTGTCAGTGGAGTGTTG-3’
	Rat	FWD	5’-TCACACTGACATCAACACTCCGCT-3’
		REV	5’-TTCCCAGCTTGTCCACTTCAGTCA-3’
GAPDH	Human	FWD	5’-CGCGGGGCTCTCGAGAACATCATC-3’
		REV	5’-CAGGTCCACCACTGACACGTTGGCA-3’
	Rat	REV	5’-GGCTGCCCAGAACATCATCCCTGCAT-3’
		FWD	5’-ACGTCAGATCCACGACGGACACATTG-3’
ACT	Human	FWD	5’-GGCTGGCCGGGACCTGACTGACTA-3’
		REV	5’-AGCCGTGGCCATCTCTTGCTCGAAG-3’
	Rat	FWD	5’-GGCTGGCCGGGACCTGACAGACTAC-3’
		REV	5’-GCAGTGGCCATCTCCTGCTCGAAGTC-3’

Table 4. Primers for Urea Cycle enzymes used for HepG2 (Human) and IEC-6 (Rat) cell lines.

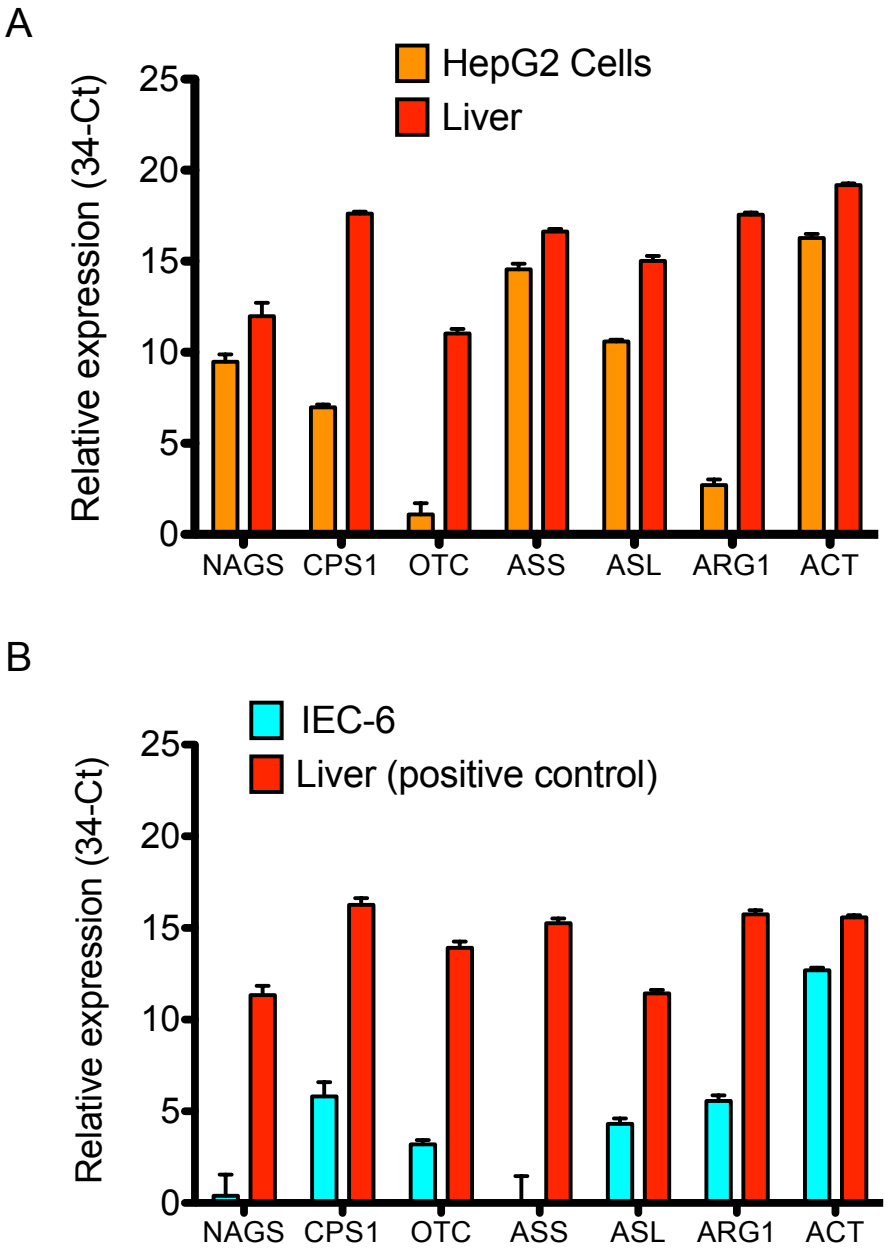

Figure 29. Expression of urea cycle enzymes in HepG2 liver carcinoma cells (A) and IEC-6 intestinal epithelial cells (B).
Expression was quantitated via RT-PCR. Ct (cycle threshold) values for transcripts are expressed as (34-Ct) using 34 as a theoretical "no expression" value for RT-PCR.

Bibliography

[1] A. Auron, P.D. Brophy, Hyperammonemia in review: pathophysiology, diagnosis, and treatment, Pediatr Nephrol. (2011).

[2] H. Krebs, K. Hanseleit, Studies on urea formation in the animal organism, Hoppe-Seylers Z. Physiol. Chem. 210 (1932) 33–66.

[3] A.J. Cooper, F. Plum, Biochemistry and physiology of brain ammonia, Physiol. Rev. 67 (1987) 440–519.

[4] G.N. Breningstall, Neurologic syndromes in hyperammonemic disorders, Pediatr. Neurol. 2 (1986) 253–262.

[5] P.P. Cohen, S. Grisolía, The mechanism of enzymatic synthesis of citrulline from ornithine, Fed. Proc. 7 (1948) 150.

[6] K. Shigesada, M. Tatibana, Enzymatic synthesis of acetylglutamate by mammalian liver preparations and its stimulation by arginine, Biochem. Biophys. Res. Commun. 44 (1971) 1117–1124.

[7] L. Begum, M. Jalil, K. Kobayashi, M. Iijima, Expression of three mitochondrial solute carriers, citrin, aralar1 and ornithine transporter, in relation to urea cycle in mice, Biochim. Biophys. Acta. 1574 (2002) 238–292.

[8] S.M. Morris, D. Kepka-Lenhart, Hormonal induction of hepatic mitochondrial ornithine/citrulline transporter mRNA, Biochem. Biophys. Res. Commun. 294 (2002) 749–752.

[9] L. Caldovic, M. Tuchman, N-acetylglutamate and its changing role through evolution, Biochem. J. 372 (2003) 279–290.

[10] V. Walker, Ammonia toxicity and its prevention in inherited defects of the urea

cycle, Diabetes, Obesity and Metabolism. 11 (2009) 823–835.

[11] A.L. Gropman, M. Summar, J.V. Leonard, Neurological implications of urea cycle disorders, J Inherit Metab Dis. 30 (2007) 865–879.

[12] R.F. Butterworth, Effects of hyperammonaemia on brain function, J Inherit Metab Dis. 21 Suppl 1 (1998) 6–20.

[13] V. Felipo, R.F. Butterworth, Neurobiology of ammonia, Prog. Neurobiol. 67 (2002) 259–279.

[14] S.W. Brusilow, N.E. Maestri, Urea cycle disorders: diagnosis, pathophysiology, and therapy, Adv Pediatr. 43 (1996) 127–170.

[15] J. Albrecht, M.D. Norenberg, Glutamine: a Trojan horse in ammonia neurotoxicity, Hepatology. 44 (2006) 788–794.

[16] G. Wright, R. Soper, H.F. Brooks, V. Stadlbauer, B. Vairappan, N.A. Davies, et al., Role of aquaporin-4 in the development of brain oedema in liver failure, J. Hepatol. 53 (2010) 91–97.

[17] U. Lichter-Konecki, J.M. Mangin, H. Gordish-Dressman, E.P. Hoffman, V. Gallo, Gene expression profiling of astrocytes from hyperammonemic mice reveals altered pathways for water and potassium homeostasis in vivo, Glia. 56 (2008) 365–377.

[18] Olivier Braissant, Current concepts in the pathogenesis of urea cycle disorders, Molecular Genetics and Metabolism. 100 (2010) S3–S12.

[19] B.A. Vogels, M.A. Maas, J. Daalhuisen, G. Quack, R.A. Chamuleau, Memantine, a noncompetitive NMDA receptor antagonist improves hyperammonemia-induced encephalopathy and acute hepatic encephalopathy in

rats, Hepatology. 25 (1997) 820–827.

[20] O. Cauli, R. Rodrigo, J. Boix, B. Piedrafita, A. Agusti, V. Felipo, Acute liver failure-induced death of rats is delayed or prevented by blocking NMDA receptors in brain, Am. J. Physiol. Gastrointest. Liver Physiol. 295 (2008) G503–G511.

[21] H.G. Windmueller, Glutamine utilization by the small intestine, Advances in Enzymology and Related Areas of Molecular Biology. (1982) 201–237.

[22] R. Hurwitz, N. Kretchmer, Development of arginine-synthesizing enzymes in mouse intestine, Am. J. Physiol. 251 (1986) G103–10.

[23] Y. Wakabayashi, M.E. Jones, Pyrroline-5-carboxylate synthesis from glutamate by rat intestinal mucosa, J. Biol. Chem. 258 (1983) 3865–3872.

[24] C. Wraight, K. Lingelbach, N. Hoogenraad, Comparison of ornithine transcarbamylase from rat liver and intestine, Eur. J. Biochem. 153 (1985) 239–242.

[25] G. Ross, D. Dunn, M.E. Jones, Ornithine synthesis from glutamate in rat intestinal mucosa homogenates: evidence for the reduction of glutamate to gamma-glutamyl semialdehyde, Biochem. Biophys. Res. Commun. 85 (1978) 140–147.

[26] S. Morris Jr, Enzymes of Arginine Metabolism, J. Nutr. (2004).

[27] H.G. Windmueller, A.E. Spaeth, Source and fate of circulating citrulline, Am. J. Physiol. 241 (1981) E473–80.

[28] S. Morris Jr, Regulation of enzymes of the urea cycle and arginine metabolism, Annu. Rev. Nutr. (2002).

[29] M.E. Brosnan, J.T. Brosnan, Renal arginine metabolism, J. Nutr. 134 (2004) 2791S–2795S; discussion 2796S–2797S.

[30] C. Bachmann, J.P. Colombo, K. Jaggi, N-acetylglutamate synthetase (NAGS) deficiency: diagnosis, clinical observations and treatment, Adv. Exp. Med. Biol. 153 (1982) 39–45.

[31] M. Tuchman, B. Lee, U. Lichter-Konecki, M.L. Summar, M. Yudkoff, S.D. Cederbaum, et al., Cross-sectional multicenter study of patients with urea cycle disorders in the United States, Mol. Genet. Metab. 94 (2008) 397–402.

[32] A. Mew, N-acetylglutamate synthase deficiency: an insight into the genetics, epidemiology, pathophysiology, and treatment, The Application of Clinical Genetics. (2011).

[33] L. Caldovic, H. Morizono, X. Yu, M. Thompson, D. Shi, R. Gallegos, et al., Identification, cloning and expression of the mouse N-acetylglutamate synthase gene, Biochem. J. 364 (2002) 825–831.

[34] L. Caldovic, H. Morizono, M. Gracia Panglao, R. Gallegos, X. Yu, D. Shi, et al., Cloning and expression of the human N-acetylglutamate synthase gene, Biochem. Biophys. Res. Commun. 299 (2002) 581–586.

[35] L. Caldovic, N. Ah Mew, D. Shi, H. Morizono, M. Yudkoff, M. Tuchman, N-acetylglutamate synthase: structure, function and defects, Mol. Genet. Metab. 100 Suppl 1 (2010) S13–9.

[36] O.N. Elpeleg, J.P. Colombo, N. Amir, C. Bachmann, H. Hurvitz, Late-onset form of partial N-acetylglutamate synthetase deficiency, Eur. J. Pediatr. 149 (1990) 634–636.

[37] O. Elpeleg, A. Shaag, E. Ben-Shalom, T. Schmid, C. Bachmann, N-acetylglutamate synthase deficiency and the treatment of hyperammonemic encephalopathy, Ann. Neurol. 52 (2002) 845–849.

[38] J. Hinnie, J.P. Colombo, B. Wermuth, F.J. Dryburgh, N-Acetylglutamate synthetase deficiency responding to carbamylglutamate, J Inherit Metab Dis. 20 (1997) 839–840.

[39] P. Gessler, P. Buchal, H.U. Schwenk, B. Wermuth, Favourable long-term outcome after immediate treatment of neonatal hyperammonemia due to N-acetylglutamate synthase deficiency, Eur. J. Pediatr. 169 (2009) 197–199.

[40] P.P. Forget, M. van Oosterhout, J.A. Bakker, B. Wermuth, J.S. Vles, L.J. Spaapen, Partial N-acetyl-glutamate synthetase deficiency masquerading as a valproic acid-induced Reye-like syndrome, Acta Paediatr. 88 (1999) 1409–1411.

[41] J. Häberle, E. Schmidt, S. Pauli, J.G. Kreuder, B. Plecko, A. Galler, et al., Mutation analysis in patients with N-acetylglutamate synthase deficiency, Hum. Mutat. 21 (2003) 593–597.

[42] L. Caldovic, H. Morizono, M.G. Panglao, G.Y. Lopez, D. Shi, M.L. Summar, et al., Late onset N-acetylglutamate synthase deficiency caused by hypomorphic alleles, Hum. Mutat. 25 (2005) 293–298.

[43] J.L. Deignan, S.D. Cederbaum, W.W. Grody, Contrasting features of urea cycle disorders in human patients and knockout mouse models, Mol. Genet. Metab. 93 (2008) 7–14.

[44] R.H. Singh, Nutritional management of patients with urea cycle disorders, J

Inherit Metab Dis. 30 (2007) 880–887.

[45] M.L. Batshaw, Alternative pathway therapy for urea cycle disorders: Twenty years later, J. Pediatr. 138 (2001) S46–S55.

[46] B.A. Barshop, J. Breuer, J. Holm, J. Leslie, Excretion of hippuric acid during sodium benzoate therapy in patients with hyperglycinaemia or hyperammonaemia, J Inherit Metab Dis. (1989).

[47] L. Zimmerman, H. Jörnvall, J. Bergström, Phenylacetylglutamine and hippuric acid in uremic and healthy subjects, Nephron. 55 (1990) 265–271.

[48] J.E. O'Connor, A. Jordá, S. Grisolía, Acute and chronic effects of carbamyl glutamate on blood urea and ammonia, Eur. J. Pediatr. 143 (1985) 196–197.

[49] P.P. Cohen, S. Grisolía, The intermediate role of carbamyl-L-glutamic acid in citrulline synthesis, J. Biol. Chem. 174 (1948) 389.

[50] S. Grisolía, P.P. Cohen, The catalytic rôle of carbamyl glutamate in citrulline biosynthesis, J. Biol. Chem. 198 (1952) 561–571.

[51] L.M. Hall, R. Metzenberg, P.P. Cohen, Isolation and characterization of a naturally occurring cofactor of carbamyl phosphate biosynthesis, J. Biol. Chem. 230 (1958) 1013–1021.

[52] S. Kim, W.K. Paik, P.P. Cohen, Ammonia intoxication in rats: protection by N-carbamoyl-L-glutamate plus L-arginine, Proc. Natl. Acad. Sci. U.S.a. 69 (1972) 3530–3533.

[53] N. Guffon, C. Vianey-Saban, J. Bourgeois, D. Rabier, J.P. Colombo, P. Guibaud, A new neonatal case of N-acetylglutamate synthase deficiency treated by carbamylglutamate, J Inherit Metab Dis. 18 (1995) 61–65.

[54] L. Caldovic, H. Morizono, Y. Daikhin, I. Nissim, R.J. McCarter, M. Yudkoff, et al., Restoration of ureagenesis in N-acetylglutamate synthase deficiency by N-carbamylglutamate, J. Pediatr. 145 (2004) 552–554.

[55] N. Guffon, M. Schiff, D. Cheillan, B. Wermuth, J. Häberle, C. Vianey-Saban, Neonatal hyperammonemia: the N-carbamoyl-L-glutamic acid test, J. Pediatr. 147 (2005) 260–262.

[56] G. Kuchler, D. Rabier, F. Poggi-Travert, D. Meyer-Gast, J. Bardet, V. Drouin, et al., Therapeutic use of carbamylglutamate in the case of carbamoyl-phosphate synthetase deficiency, J Inherit Metab Dis. 19 (1996) 220–222.

[57] M. Tuchman, L. Caldovic, Y. Daikhin, O. Horyn, I. Nissim, I. Nissim, et al., N-carbamylglutamate markedly enhances ureagenesis in N-acetylglutamate deficiency and propionic acidemia as measured by isotopic incorporation and blood biomarkers, Pediatr. Res. 64 (2008) 213–217.

[58] N.A. Mew, R. McCarter, Y. Daikhin, I. Nissim, M. Yudkoff, M. Tuchman, N-carbamylglutamate Augments Ureagenesis and Reduces Ammonia and Glutamine in Propionic Acidemia, Pediatrics. 126 (2010) e208–e214.

[59] C.S. Kasapkara, F.S. Ezgu, I. Okur, L. Tumer, G. Biberoglu, A. Hasanoglu, N-carbamylglutamate treatment for acute neonatal hyperammonemia in isovaleric acidemia, Eur. J. Pediatr. 170 (2011) 799–801.

[60] N.B. Javitt, Hep G2 cells as a resource for metabolic studies: lipoprotein, cholesterol, and bile acids, Faseb J. 4 (1990) 161–168.

[61] D. Mavri-Damelin, S. Eaton, L.H. Damelin, M. Rees, H.J.F. Hodgson, C. Selden, Ornithine transcarbamylase and arginase I deficiency are responsible for

diminished urea cycle function in the human hepatoblastoma cell line HepG2, Int. J. Biochem. Cell Biol. 39 (2007) 555–564.

[62] D. Mavri-Damelin, L.H. Damelin, S. Eaton, M. Rees, C. Selden, H.J.F. Hodgson, Cells for bioartificial liver devices: the human hepatoma-derived cell line C3A produces urea but does not detoxify ammonia, Biotechnol. Bioeng. 99 (2008) 644–651.

[63] A. Monks, C.A. Chisena, R.L. Cysyk, Influence of ammonium ions on hepatic de novo pyrimidine biosynthesis, Arch. Biochem. Biophys. 236 (1985) 1–10.

[64] A.E. Pegg, Regulation of Ornithine Decarboxylase, Journal of Biological Chemistry. (2006).

[65] H. Wallace, A.V. Fraser, A. Hughes, A perspective of polyamine metabolism, Biochem. J. 376 (2003) 1.

[66] N. Tang, Y. Wang, X. Wang, L. Zhou, F. Zhang, X. Li, et al., Stable overexpression of arginase I and ornithine transcarbamylase in HepG2 cells improves its ammonia detoxification, J. Cell. Biochem. 113 (2012) 518–527.

[67] H. Liu, H. Dong, K. Robertson, C. Liu, DNA Methylation Suppresses Expression of the Urea Cycle Enzyme Carbamoyl Phosphate Synthetase 1 (CPS1) in Human Hepatocellular Carcinoma, Ajpa. 178 (2011) 652–661.

[68] A. Quaroni, J. Wands, R.L. Trelstad, K.J. Isselbacher, Epithelioid cell cultures from rat small intestine. Characterization by morphologic and immunologic criteria, J. Cell Biol. 80 (1979) 248–265.

[69] R. DeMars, S.L. LeVan, B.L. Trend, L.B. Russell, Abnormal ornithine carbamoyltransferase in mice having the sparse-fur mutation, Proc. Natl. Acad.

Sci. U.S.a. 73 (1976) 1693–1697.

[70] G. Veres, R.A. Gibbs, S.E. Scherer, C.T. Caskey, The molecular basis of the sparse fur mouse mutation, Science. 237 (1987) 415–417.

[71] D.P. Doolittle, L.L. Hulbert, C. Cordy, A new allele of the sparse fur gene in the mouse, J. Hered. 65 (1974) 194–195.

[72] P.E. Hodges, L.E. Rosenberg, The spfash mouse: a missense mutation in the ornithine transcarbamylase gene also causes aberrant mRNA splicing, Proc. Natl. Acad. Sci. U.S.a. 86 (1989) 4142–4146.

[73] M.L. Batshaw, M. Yudkoff, B.A. McLaughlin, E. Gorry, N.J. Anegawa, I.A. Smith, et al., The sparse fur mouse as a model for gene therapy in ornithine carbamoyltransferase deficiency, Gene Ther. 2 (1995) 743–749.

[74] L. Wang, H. Morizono, J. Lin, P. Bell, D. Jones, D. McMenamin, et al., Preclinical evaluation of a clinical candidate AAV8 vector for ornithine transcarbamylase (OTC) deficiency reveals functional enzyme from each persisting vector genome, Molecular Genetics and Metabolism. 105 (2012) 203–211.

[75] J.P. Schofield, J.P. Schofield, T.M. Cox, C.T. Caskey, M. Wakamiya, Mice deficient in the urea-cycle enzyme, carbamoyl phosphate synthetase 1, die during the early neonatal period from hyperammonemia, Hepatology. 29 (1999) 181–185.

[76] G. Patejunas, A. Bradley, A.L. Beaudet, W.E. O'Brien, Generation of a mouse model for citrullinemia by targeted disruption of the argininosuccinate synthetase gene, Somat. Cell Mol. Genet. 20 (1994) 55–60.

[77] X. Ye, X. Ye, B. Whiteman, B. Whiteman, M. Jerebtsova, M. Jerebtsova, et al., Correction of argininosuccinate synthetase (AS) deficiency in a murine model of citrullinemia with recombinant adenovirus carrying human AS cDNA, Gene Ther. 7 (2000) 1777–1782.

[78] C.J. Perez, J. Jaubert, J.-L. Guénet, K.F. Barnhart, C.M. Ross-Inta, V.C. Quintanilla, et al., Two Hypomorphic Alleles of Mouse Ass1 as a New Animal Model of Citrullinemia Type I and Other Hyperammonemic Syndromes, Am. J. Pathol. 177 (2010) 1958–1968.

[79] V.R. Sutton, Y. Pan, E.C. Davis, W.J. Craigen, A mouse model of argininosuccinic aciduria: biochemical characterization, Mol. Genet. Metab. 78 (2003) 11–16.

[80] R.K. Iyer, P.K. Yoo, R.M. Kern, N. Rozengurt, R. Tsoa, W.E. O'Brien, et al., Mouse model for human arginase deficiency, Mol Cell Biol. 22 (2002) 4491–4498.

[81] I. Azorín, M. Minana, V. Felipo, S. Grisolía, A simple animal model of hyperammonemia, Hepatology. 10 (1989) 311–314.

[82] V. Felipo, M. Minana, S. Grisolía, Long-term ingestion of ammonium increases acetylglutamate and urea levels without affecting the amount of carbamoyl-phosphate synthase, Eur. J. Biochem. 176 (1988) 567–571.

[83] R.F. Butterworth, M.D. Norenberg, V. Felipo, P. Ferenci, J. Albrecht, A.T. Blei, et al., Experimental models of hepatic encephalopathy: ISHEN guidelines, Liver Int. 29 (2009) 783–788.

[84] C. Beaubernard, F. Salomon, D. Grange, Experimental hepatic encephalopathy.

Changes of the level of wakefulness in the rat with portacaval shunt, Biomedicine. 27 (1977) 169–171.

[85] J.F. Giguère, R.F. Butterworth, Amino acid changes in regions of the CNS in relation to function in experimental portal-systemic encephalopathy, Neurochem. Res. 9 (1984) 1309–1321.

[86] A. Gjedde, A.H. Lockwood, T.E. Duffy, F. Plum, Cerebral blood flow and metabolism in chronically hyperammonemic rats: effect of an acute ammonia challenge, Ann. Neurol. 3 (1978) 325–330.

[87] B. Hindfelt, F. Plum, Effect of acute ammonia intoxication on cerebral metabolism in rats with portacaval shunts, J. Clin. Invest. (1977).

[88] A.J. Cooper, Ammonia metabolism in normal and portacaval-shunted rats, Adv. Exp. Med. Biol. 272 (1990) 23–46.

[89] R. Jover, R. Rodrigo, V. Felipo, R. Insausti, J. Sáez-Valero, M.S. García-Ayllón, et al., Brain edema and inflammatory activation in bile duct ligated rats with diet-induced hyperammonemia: A model of hepatic encephalopathy in cirrhosis, Hepatology. 43 (2006) 1257–1266.

[90] C.-Y. Chan, S.-W. Huang, T.-F. Wang, R.-H. Lu, F.-Y. Lee, F.-Y. Chang, et al., Lack of detrimental effects of nitric oxide inhibition in bile duct-ligated rats with hepatic encephalopathy, Eur. J. Clin. Invest. 34 (2004) 122–128.

[91] R. Rodrigo, R. Jover, A. Candela, A. Compañ, J. Sáez-Valero, S. Erceg, et al., Bile duct ligation plus hyperammonemia in rats reproduces the alterations in the modulation of soluble guanylate cyclase by nitric oxide in brain of cirrhotic patients, Neuroscience. 130 (2005) 435–443.

[92] C. Bachmann, S. Krähenbühl, J.P. Colombo, G. Schubiger, K.H. Jaggi, O. Tönz, N-acetylglutamate synthetase deficiency: a disorder of ammonia detoxication, N. Engl. J. Med. 304 (1981) 543.

[93] L. Hulbert, Abnormal skin and hair: a sex-linked mutation in the house mouse, Genetics. 68 (1971) S29.

[94] G. Patejunas, A. Bradley, A.L. Beaudet, W.E. O'Brien, Generation of a mouse model for citrullinemia by targeted disruption of the argininosuccinate synthetase gene, Somat. Cell Mol. Genet. 20 (1994) 55–60.

[95] O. Shi, S.M. Morris, H. Zoghbi, C.W. Porter, W.E. O'Brien, Generation of a Mouse Model for Arginase II Deficiency by Targeted Disruption of the Arginase II Gene, Mol Cell Bio. 21 (2001) 811–813.

[96] D.M. Valenzuela, A.J. Murphy, D. Frendewey, N.W. Gale, A.N. Economides, W. Auerbach, et al., High-throughput engineering of the mouse genome coupled with high-resolution expression analysis, Nat. Biotechnol. 21 (2003) 652–659.

[97] G.S. Evans, N. Flint, A.S. Somers, B. Eyden, C.S. Potten, The development of a method for the preparation of rat intestinal epithelial cell primary cultures, J. Cell. Sci. 101 (Pt 1) (1992) 219–231.

[98] H.C. van Anken, M.E. Schiphorst, A kinetic determination of ammonia in plasma, Clin. Chim. Acta. 56 (1974) 151–157.

[99] T. Wang, T. Wang, A.M. Lawler, A.M. Lawler, G. Steel, G. Steel, et al., Mice lacking ornithine–δ–amino–transferase have paradoxical neonatal hypoornithinaemia and retinal degeneration, Nat Genet. 11 (1995) 185–190.

[100] T. Shimada, M. Tashiro, T. Kanzaki, T. Noda, T. Murakami, M. Takiguchi, et

al., Normalization of hair growth in sparse fur-abnormal skin and hair (SPF-ASH) mice by introduction of the rat ornithine transcarbamylase (OTC) gene, J Dermatol Sci. 7 Suppl (1994) S27–32.

[101] X. Ye, M.B. Robinson, C. Pabin, T. Quinn, A. Jawad, J.M. Wilson, et al., Adenovirus-mediated in vivo gene transfer rapidly protects ornithine transcarbamylase-deficient mice from an ammonium challenge, Pediatr. Res. 41 (1997) 527–534.

[102] M.J. Mihatsch, U.N. Riede, H. Ohnacker, H. Wick, C. Bachmann, Liver morphology in a case of citrullinemia (a light and electron microscopic study), Beitr Pathol. 151 (1974) 200–207.

[103] J.M. Shapiro, F. Schaffner, H.H. Tallan, G.E. Gaull, Mitochondrial Abnormalities of Liver in Primary Ornithine Transcarbamylase Deficiency, Pediatr. Res. 14 (1980) 735–739.

[104] A. Zimmermann, C. Bachmann, J.P. Colombo, Ultrastructural pathology in congenital defects of the urea cycle: Ornithine transcarbamylase and carbamylphosphate synthetase deficiency, Virchows Arch. a Path. Anat. and Histol. 393 (1981) 321–331.

[105] J.C. Marini, B. Lee, P.J. Garlick, Ornithine restores ureagenesis capacity and mitigates hyperammonemia in Otc(spf-ash) mice, J. Nutr. 136 (2006) 1834–1838.

[106] I. Nissim, M.E. Brosnan, M. Yudkoff, J.T. Brosnan, Studies of hepatic glutamine metabolism in the perfused rat liver with (15)N-labeled glutamine, J. Biol. Chem. 274 (1999) 28958–28965.

[107] I. Nissim, M. Yudkoff, J.T. Brosnan, Regulation of [15N]urea synthesis from [5-15N]glutamine. Role of pH, hormones, and pyruvate, J. Biol. Chem. 271 (1996) 31234–31242.

[108] G. Wu, S.M. Morris, Arginine metabolism: nitric oxide and beyond, Biochem. J. 336 (Pt 1) (1998) 1–17.

[109] E. Seifter, G. Rettura, A. Barbul, S.M. Levenson, Arginine: an essential amino acid for injured rats, Surgery. 84 (1978) 224–230.

[110] A. Barbul, G. Rettura, S.M. Levenson, E. Seifter, Arginine: a thymotropic and wound-healing promoting agent, Surg Forum. 28 (1977) 101–103.

[111] P.J. Popovic, H.J. Zeh, J.B. Ochoa, Arginine and immunity, J. Nutr. 137 (2007) 1681S–1686S.

[112] V. Bronte, P. Zanovello, Regulation of immune responses by L-arginine metabolism, Nat. Rev. Immunol. 5 (2005) 641–654.

[113] A. Nordenström, M. Halldin, B. Hallberg, A trial with N-carbamylglutamate may not detect all patients with NAGS deficiency and neonatal onset, J Inherit Metab Dis. 30 (2007) 400.

[114] C. Bachmann, Mechanisms of hyperammonemia, Clin. Chem. Lab. Med. 40 (2002) 653–662.

[115] M. Summar, Proceedings of Management of Patients with Urea Cycle Disorders, (2001).

[116] F.S. Larsen, J. Wendon, Alternative pathway therapy for hyperammonemia in liver failure, Hepatology. 50 (2009) 3–5.

[117] E. Senkevitch, J. Cabrera-Luque, H. Morizono, L. Caldovic, M. Tuchman, A

novel biochemically salvageable animal model of hyperammonemia devoid of N-acetylglutamate synthase, Mol. Genet. Metab. 106 (2012) 160–168.

[118] C.A. Hundahl, J. Fahrenkrug, A. Hay-Schmidt, B. Georg, B. Faltoft, J. Hannibal, Circadian Behaviour in Neuroglobin Deficient Mice, PLoS ONE. 7 (2012) e34462.

[119] J. Hannibal, F. Jamen, H.S. Nielsen, L. Journot, P. Brabet, J. Fahrenkrug, Dissociation between light-induced phase shift of the circadian rhythm and clock gene expression in mice lacking the pituitary adenylate cyclase activating polypeptide type 1 receptor, Journal of Neuroscience. 21 (2001) 4883–4890.

[120] B.N. Greenwood, A.B. Loughridge, N. Sadaoui, J.P. Christianson, M. Fleshner, The protective effects of voluntary exercise against the behavioral consequences of uncontrollable stress persist despite an increase in anxiety following forced cessation of exercise, Behav. Brain Res. 233 (2012) 314–321.

[121] L.P. Bogdanik, H.D. Chapman, K.E. Miers, D.V. Serreze, R.W. Burgess, A MusD Retrotransposon Insertion in the Mouse Slc6a5 Gene Causes Alterations in Neuromuscular Junction Maturation and Behavioral Phenotypes, PLoS ONE. 7 (2012) e30217.

[122] A.D. Steele, W.S. Jackson, O.D. King, S. Lindquist, The power of automated high-resolution behavior analysis revealed by its application to mouse models of Huntington's and prion diseases, Proc. Natl. Acad. Sci. U.S.a. 104 (2007) 1983.

[123] E. Kyzar, S. Gaikwad, A. Roth, J. Green, M. Pham, A. Stewart, et al., Towards high-throughput phenotyping of complex patterned behaviors in rodents: Focus on mouse self-grooming and its sequencing, Behav. Brain Res. 225 (2011) 426–

431.

[124] A. Langford-Smith, M. Malinowska, K.J. Langford-Smith, G. Wegrzyn, S. Jones, R. Wynn, et al., Hyperactive behaviour in the mouse model of mucopolysaccharidosis IIIB in the open field and home cage environments, Genes Brain Behav. 10 (2011) 673–682.

[125] K. Martinowich, R.J. Schloesser, D.V. Jimenez, D.R. Weinberger, B. Lu, Activity-dependent brain-derived neurotrophic factor expression regulates cortistatin-interneurons and sleep behavior, Mol Brain. 4 (2011) 11.

[126] V.M. Afonso, R. Eikelboom, Relationship between wheel running, feeding, drinking, and body weight in male rats, Physiol. Behav. 80 (2003) 19–26.

[127] K. Takeda, M. Machida, A. Kohara, N. Omi, T. Takemasa, Effects of citrulline supplementation on fatigue and exercise performance in mice, J. Nutr. Sci. Vitaminol. 57 (2011) 246–250.

[128] S.W. Brusilow, R.C. Koehler, R.J. Traystman, A.J.L. Cooper, Astrocyte glutamine synthetase: importance in hyperammonemic syndromes and potential target for therapy, Neurotherapeutics. 7 (2010) 452–470.

[129] N. ElMlili, J. Boix, H. Ahabrach, R. Rodrigo, M. Errami, V. Felipo, Chronic hyperammonemia induces tonic activation of NMDA receptors in cerebellum, Journal of Neurochemistry. 112 (2010) 1005–1014.

[130] R.F. Butterworth, Hepatic encephalopathy: a neuropsychiatric disorder involving multiple neurotransmitter systems, Current Opinion in Neurology. (2000).

[131] F. Ghoddoussi, M.P. Galloway, A. Jambekar, M. Bame, R. Needleman, W.S.A.

Brusilow, Methionine sulfoximine, an inhibitor of glutamine synthetase, lowers brain glutamine and glutamate in a mouse model of ALS, J. Neurol. Sci. 290 (2010) 41–47.

[132] M. Tuchman, Persistent acitrullinemia after liver transplantation for carbamylphosphate synthetase deficiency, N. Engl. J. Med. 320 (1989) 1498–1499.

[133] M. Tuchman, Human hepatic N-acetylglutamate content and N-acetylglutamate synthase activity. Determination by stable isotope dilution, Biochem. J. (1990).

[134] H. Morizono, L. Caldovic, D. Shi, M. Tuchman, Mammalian N-acetylglutamate synthase, Molecular Genetics and Metabolism. 81 Suppl 1 (2004) S4–11.

[135] A. Barbul, G. Rettura, S.M. Levenson, E. Seifter, Arginine: a thymotropic and wound-healing promoting agent, Surg Forum. 28 (1977) 101–103.

[136] J. Nirgiotis, P. Hennessey, The effects of an arginine-free enteral diet on wound healing and immune function in the postsurgical rat, Journal of Pediatric Surgery. (1991).

[137] J.B. Ochoa, A.C. Bernard, S.K. Mistry, S.M. Morris, P.L. Figert, M.E. Maley, et al., Trauma increases extrahepatic arginase activity, Surgery. 127 (2000) 419–426.

[138] A. Barbul, D.A. Sisto, H.L. Wasserkrug, G. Efron, Arginine stimulates lymphocyte immune response in healthy human beings, Surgery. 90 (1981) 244–251.

[139] G.Y. Wu, J.T. Brosnan, Macrophages can convert citrulline into arginine, Biochem. J. 281 (Pt 1) (1992) 45–48.

[140] V. Bronte, P. Serafini, A. Mazzoni, D.M. Segal, P. Zanovello, L-arginine metabolism in myeloid cells controls T-lymphocyte functions, Trends Immunol. 24 (2003) 302–306.

[141] A.B. Levine, D. Punihaole, T.B. Levine, Characterization of the Role of Nitric Oxide and Its Clinical Applications, Cardiology. 122 (2012) 55–68.

[142] L. Milakofsky, N. Harris, W.H. Vogel, Effects of repeated stress on plasma arginine levels in young and old rats, Physiol. Behav. 54 (1993) 725–728.

[143] FDA, Carglumic Acid Briefing Document, Orphan Europe. (2009) 1–91.

[144] A.A. Jambekar, E. Palma, L. Nicolosi, A. Rasola, V. Petronilli, F. Chiara, et al., A glutamine synthetase inhibitor increases survival and decreases cytokine response in a mouse model of acute liver failure, Liver Int. (2011).

[145] C.L. Willard-Mack, R.C. Koehler, T. Hirata, L.C. Cork, H. Takahashi, R.J. Traystman, et al., Inhibition of glutamine synthetase reduces ammonia-induced astrocyte swelling in rat, Neuroscience. 71 (1996) 589–599.

[146] H. Tanigami, A. Rebel, L.J. Martin, T.-Y. Chen, S.W. Brusilow, R.J. Traystman, et al., Effect of glutamine synthetase inhibition on astrocyte swelling and altered astroglial protein expression during hyperammonemia in rats, Neuroscience. 131 (2005) 437–449.

[147] P. Desjardins, M. Bélanger, R.F. Butterworth, Alterations in expression of genes coding for key astrocytic proteins in acute liver failure, J. Neurosci. Res. 66 (2001) 967–971.

[148] H. Chan, A.S. Hazell, P. Desjardins, R.F. Butterworth, Effects of ammonia on glutamate transporter (GLAST) protein and mRNA in cultured rat cortical

astrocytes, Neurochemistry International. 37 (2000) 243–248.

[149] I. Suárez, G. Bodega, B. Fernández, Glutamine synthetase in brain: effect of ammonia, Neurochemistry International. 41 (2002) 123–142.

[150] C.R. McCudden, S.G. Powers-Lee, Required allosteric effector site for N-acetylglutamate on carbamoyl-phosphate synthetase I, J. Biol. Chem. 271 (1996) 18285–18294.

[151] K. Mathijs, A.S. Kienhuis, K.J.J. Brauers, D.G.J. Jennen, A. Lahoz, J.C.S. Kleinjans, et al., Assessing the metabolic competence of sandwich-cultured mouse primary hepatocytes, Drug Metab. Dispos. 37 (2009) 1305–1311.

[152] K.A. Hoffmaster, M.J. Zamek-Gliszczynski, G.M. Pollack, K.L.R. Brouwer, Hepatobiliary disposition of the metabolically stable opioid peptide [D-Pen2, D-Pen5]-enkephalin (DPDPE): pharmacokinetic consequences of the interplay between multiple transport systems, J. Pharmacol. Exp. Ther. 311 (2004) 1203–1210.

[153] M. Liao, A.R. Raczynski, M. Chen, B.C. Chuang, Q. Zhu, R. Shipman, et al., Inhibition of Hepatic Organic Anion-Transporting Polypeptide by RNA Interference in Sandwich-Cultured Human Hepatocytes: An In Vitro Model to Assess Transporter-Mediated Drug-Drug Interactions, Drug Metabolism and Disposition. 38 (2010) 1612–1622.

[154] V. Laurent, A. Fraix, T. Montier, S. Cammas-Marion, C. Ribault, T. Benvegnu, et al., Highly efficient gene transfer into hepatocyte-like HepaRG cells: New means for drug metabolism and toxicity studies, Biotechnology Journal. 5 (2010) 314–320.